Reversible Photocontrol of Biological Systems by the Incorporation of Molecular Photoswitches

Szymanski, Wiktor; Beierle, John M.; Kistemaker, Hans A. V.; Velema, Willem A.; Feringa, Ben L.; Szymański, Wiktor

Published in:
Chemical reviews

DOI:
10.1021/cr300179f

CHEMICAL REVIEWS

Review

pubs.acs.org/CR

Reversible Photocontrol of Biological Systems by the Incorporation of Molecular Photoswitches

Wiktor Szymański, John M. Beierle,[†] Hans A. V. Kistemaker,[‡] Willem A. Velema, and Ben L. Feringa*

Stratingh Institute for Chemistry, University of Groningen, Nijenborgh 4, 9747 AG, Groningen, The Netherlands

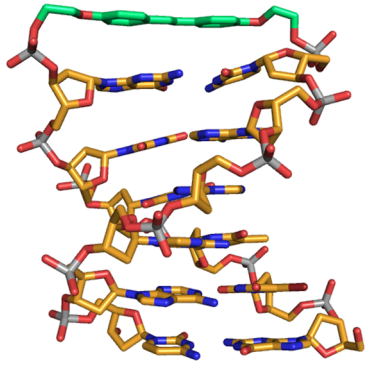

CONTENTS

Received: May 3, 2012
Published: April 25, 2013

   dx.doi.org/10.1021/cr300179f | *Chem. Rev.* 2013, 113, 6114–6178

1. INTRODUCTION

1.1. General

Controlling the conformation and activity of biomolecules in a reversible manner is a fascinating challenge[1−3] that has an outstanding potential for the study of and interference with complex processes in living cells.[4,5] Spatial and temporal control of cellular processes could provide unparalleled opportunities for studying organism development or disease progression.[6] As stated recently by Woolley and co-workers,[7] an ideal mode for reversibly controlling living systems would combine in itself high spatial resolution and high temporal resolution using a mode of control orthogonal to most cellular processes.

Light seems to be an ideal external control element for *in situ* chemical and biological manipulation because it offers a high level of spatiotemporal resolution, is generally noninvasive (at a range of wavelengths), is orthogonal toward most elements of living systems, and does not cause the contamination of the sample.[2] Furthermore, its wavelength and intensity can be precisely regulated. These unique properties have led to the use of light in the study of fluorescently labeled small molecules[8] and proteins (such as GFP[9]) in cells and to recent inspiring developments in the area of bioorthogonal introduction of photoactive compounds into biomolecules.[10]

One of the most widely used methods for the introduction of light-sensitivity into biological molecules is through functionalization with bistable molecular photoswitches. This approach has been used to photoregulate a multitude of important biological processes (Figure 1), such as nucleic acid structure and function, transcription and translation, protein folding, enzyme activity, protein−ligand interactions, peptide structure and function, membrane transport, and receptor modulation, including signaling.

This review aims at providing a comprehensive and critical literature review on reversible photocontrol of biomolecules' structure and function with molecular photoswitches. For the information on photocaged, i.e. irreversibly controlled, systems, the reader is referred to other recent reviews.[2,6,11−13] Information on photocontrolled cell adhesion to surfaces can be found in recent reviews by Mendes[14] and Feringa et al.[15]

1.2. Introduction to Molecular Photoswitches

Several essential biological processes, such as vision[16] and photosynthesis,[17] are fueled by light. A chromophore in the protein structure absorbs a photon, which results in a chemical transformation that may induce a change in the conformation of the attached protein. These light-activated processes are usually completely reversible, and the chromophores can switch between two or more isomeric forms, hence the commonly used term "photoswitches".[3]

A variety of synthetic photoswitches, that can undergo a reversible change in their structure upon irradiation with light, have been designed (Table 1). They are commonly characterized by the absorption maxima of their isomeric forms, as well as by the photostationary state (PSS), defined as the equilibrium composition during irradiation. For biological applications, these compounds require a fast switching process and large extinction coefficient with high quantum yield at wavelengths that are nondestructive for a living cell. In selected cases, high fatigue resistance in an aqueous environment is an important prerequisite.

Table 1. Selected Molecular Structures of Photoswitches Introduced into Biomolecules

	Photoswitches	Isomerization	λ_1/λ_2	polarity change
A	Azobenzenes	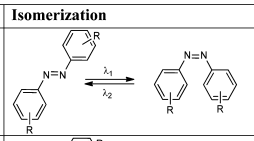	UV/VIS (ΔT)	medium (Δμ = ~3 D)
B	Stilbenes	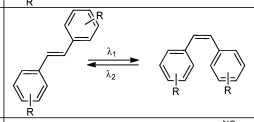	UV/UV	small
C	Spiropyrans	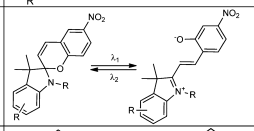	UV/VIS (ΔT) or VIS/UV	large (Δμ = 8-15 D)
D	Diarylethenes	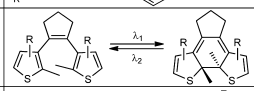	UV/VIS	small
E	Thiophenefulgides	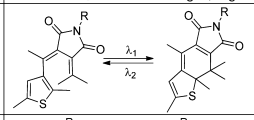	UV/VIS	small
F	Hemithioindigos	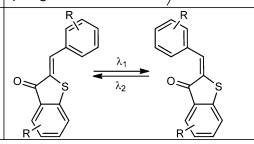	VIS/VIS (ΔT)	medium (Δμ = ~1.6 D)

1.3. Overview of the Most Commonly Used Photoswitches and Their Properties

Many strategies for the reversible photocontrol of biomolecules have been explored with a wide variety of chromophores (Table 1). The chromophores switch upon irradiation between the *cis* and *trans* isomers (azobenzenes, stilbenes, and hemithioindigos) or interconvert between closed and open forms (spiropyrans, diarylethenes, and fulgides). This results in a change in geometry, which can be especially large in the cases of azobenzenes and hemithioindigos or small as in diarylethenes. Besides this change, photoisomerization may also alter the polarity and charge distribution of the compound.

1.3.1. Azobenzenes. Azobenzenes form one of the largest and most studied classes of photochromic molecules.[18,19] They exist in two isomeric states, *trans* and *cis*, with the former being ~10 kcal/mol more stable than the latter (Table 1A). The planar conformation of the *trans* isomer, although its actual geometry is still actively disputed and substituent-dependent,[18,20,21] places it in the C_{2h} point symmetry group and results in a zero dipole moment. The UV−vis spectrum of unsubstituted *trans*-azobenzene shows two absorption maxima: a strong one around 320 nm resulting from the symmetry-allowed $\pi-\pi^*$ transition and a weaker one around 430 nm indicative of the symmetry forbidden $n-\pi^*$ transition. The absorption at about 320 nm leads to rotation around the N−N bond and the formation of the *cis* isomer. The transition associated with the signal at 430 nm is related to the *trans* to *cis* isomerization *via* one of several possible pathways.[22] The *trans* to *cis* isomerization is accompanied by a considerable change in polarity (the dipole moment of the *cis* form is ~3 D) (Table 1). The reverse, *cis* to *trans*, isomerization occurs thermally or can be achieved by irradiation with visible light (>460 nm).

dx.doi.org/10.1021/cr300179f | *Chem. Rev.* 2013, 113, 6114−6178

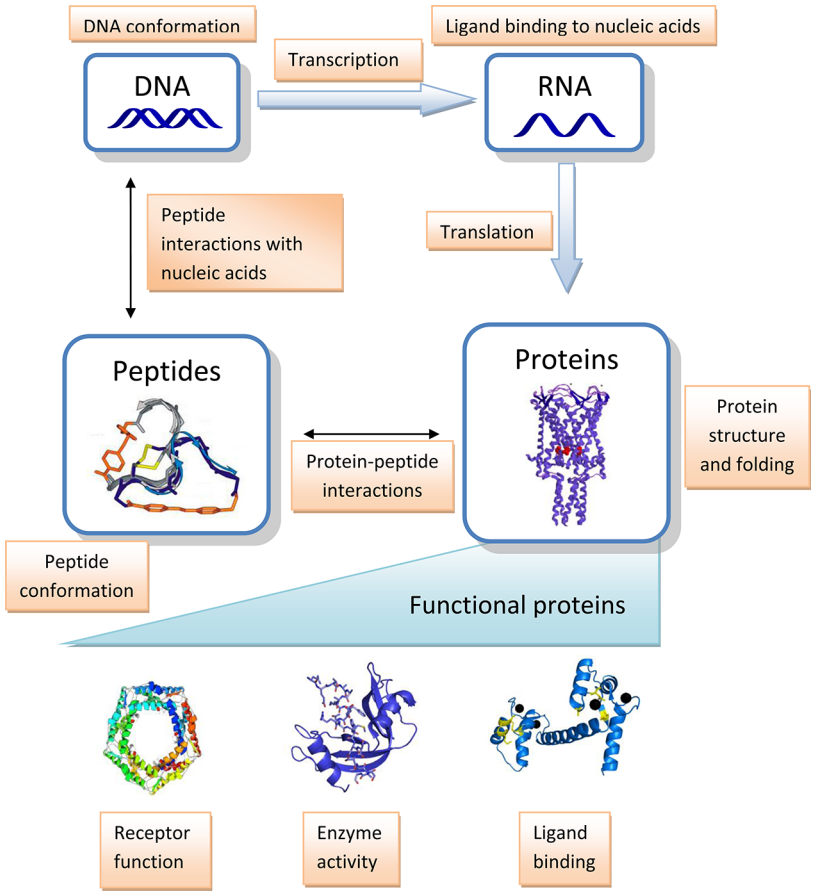

Figure 1. Overview of the main biological processes (highlighted in orange), which can be photoregulated by the incorporation of molecular photoswitches into biomolecules (shown in blue boxes).

Azobenzenes remain the most widely used photoswitches in biological applications.[7] The reasons behind this include[23] their easy synthesis, relatively high photostationary states and quantum yields, fast photoisomerization, and low rate of photobleaching. While the medium has a rather small influence on the photochemistry, it has been shown that the kinetics of the thermal step is strongly influenced by the secondary interactions with proteins.[24] Recent reports suggest that the difference in energy of the photostates and the height of the thermal barrier for *cis* to *trans* isomerization (∼18 kcal/mol) are sufficient to drive conformational changes in proteins, allowing for the photochemical control of protein folding and unfolding.[25] Furthermore, a new classes of azobenzene molecules were recently reported from the groups of Temps[26] and Woolley,[27] which can be switched between *trans* and *cis* forms using visible light. This allows avoiding the use of UV light, which is unable to penetrate into tissues and can cause severe damage to living cells.

The isomerization rate and the photostationary state are heavily affected by solvent and substituents present in the azobenzene unit.[28] For example, compounds with a *para*-EWG substituent and a *para*′-EDG substituent (so-called "push−pull azobenzenes") have an increased rate of thermal *cis* to *trans* isomerization in more polar solvents,[29] while the quantum yields for the *cis* to *trans* photoisomerization of azobenzene are increased in apolar solvents.[30] Azobenzenes can also undergo reduction under physiological conditions, which may be a limitation to their application *in vivo*.[31] Recently it has been shown, however, that peptides modified with azobenzenes are not reduced by glutathione *in vivo*[7] or *in vitro*[32] and their photoswitching behavior has been confirmed in living zebrafish.[33,34] For more information on the tailoring of azobenzene properties for the applications in biological systems, the reader is referred to section 3 of this paper and to other reviews.[7,35]

1.3.2. Stilbenes. The stilbene system (Table 1, B), which is a special case of the general class of diarylethene chromophore (see section 1.3.4), is isoelectronic to azobenzene, and it undergoes an analogous $E-Z$ isomerization.[36] The mechanism of stilbene photoisomerization has been extensively studied.[37] It differs slightly from the one of azobenzene, as the excited state of the E form, obtained *via* the $\pi-\pi^*$ transition, is metastable.[36,37] The isomerization, induced by the irradiation at the absorption maximum of 313 nm (for unsubstituted stilbene) results in the formation of a *cis* form, in which the angle between the planes of the phenyl rings is 43°.[37] Importantly, the barrier of the thermal $Z-E$ reisomerization is 41−46 kcal/mol; that is, thermal isomerization is negligible at room temperature.[37] From the point of view of photocontrol of biological systems, a major drawback of stilbenes is their tendency to undergo irreversible, cyclization/oxidation in the *cis* form.[38]

1.3.3. Spiropyrans.[39] The photochromic behavior of spiropyrans stems from the fact that the $C_{spiro}-O$ bond undergoes heterolytic cleavage upon UV irradiation (360−370 nm), resulting in the formation of a zwitterionic conjugated system, known as the merocyanine form (Table 1, C).[40,41] This isomerization is accompanied by a very large (8−15 D)[42,43] change in polarity and is reversible both thermally and

dx.doi.org/10.1021/cr300179f | *Chem. Rev.* 2013, 113, 6114−6178

photochemically, by irradiation with visible (>460 nm) light. The equilibrium between the merocyanine state and the spiropyran state is shifted toward the former for compounds with a nitro substituent in the phenyl ring.[44,45] The same effect is observed with increased polarity of the local environment.[44,46] In rare cases the reverse photochromism is observed; that is, irradiation with visible light shifts the equilibrium toward the open state and UV irradiation restores the closed form.[47,48] The importance of spiropyrans as regulatory elements stems mainly from the large change in polarity upon photoiomerization, which is reflected by changes in hydrophilicity/hydrophobicity. In biological context, the merocyanine form of the spiropyran switch has been found to interact strongly with model proteins.[49]

1.3.4. Diarylethenes.[50,51] The photochromism of diarylethenes is caused by reversible, photochemically induced cyclization, due to the presence of a hexatriene moiety in the open form. The first examples of thermally irreversible photochromic diarylethenes (Table 1, D, shown with thiophenes) were reported in the 1960s.[52] Theoretical studies[53] attribute the thermal stability of both isomers to the low aromatic stabilization energies of the heterocyclic acryl groups, such as furyl or thiophenyl, introduced on both sides of the bridging *Z*-alkene moiety. Electron-withdrawing groups on the aromatic rings decrease the thermal stability of the closed state.[54] Diarylethenes show very high fatigue resistance, as the switching cycles can usually be repeated up to 10^4 times.[50] The effects of substitution on the absorption wavelengths and quantum yields of ditheinylethenes were studied in detail and resulted in important guidelines for tailoring the properties of these molecular switches.[50]

1.3.5. Thiophenefulgides.[55] As in the case of diarylethenes, the photochromic behavior of fulgides stems from their reversible photochemical cyclization of the hexatriene moiety, which results in the formation of a cyclohexadiene ring (Table 1, E).[56,57] When the carbon atoms that make up the C−C-double bond are substituted, and when there is a heteroaromatic ring present in the structure of the compound, this reaction is thermally irreversible.[58,59] Quantum yields depend on the steric bulk of the substituents around the cyclohexatriene, as these substituents influence the conformation of the fulgides in the ground state.[60,61] By changing the electronic properties of the substituents, it is possible to adjust maximum absorption wavelengths over a wide range.[57]

1.3.6. Hemithioindigos. The photoisomerization of hemithioindigos (Table 1, F) involves the *Z* to *E* isomerization of the olefinic bond and results in a considerable change in the orientation of the dipole moment.[62] Hemithioindigos show little fatigue over many switching cycles.[62] The photoswitching is induced by irradiation at 400−410 nm (*Z* to *E*) and 480−490 nm (*E* to *Z*),[63] and it takes place on a picosecond time scale.[64] The thermal *E*−*Z* reisomerization is very slow, especially in organic solvents.[63] A strong influence of substituents on the dynamics of photoisomerization has been reported.[65] Model studies on hemithioindigo-modified chromopeptides have shown that they can exert forces strong enough to drive structural changes in the peptides.[64]

2. INTRODUCTION OF MOLECULAR PHOTOSWITCHES INTO NUCLEIC ACIDS

The prospect of reversible spatial and temporal control of replication, transcription, and translation processes using light makes photoswitchable nucleic acids and their analogs attractive targets. Various groups have used light to alter the structure and binding properties of nucleic acids and nucleic acid analogs by employing photochromic molecules introduced in diverse structural positions, including the phosphate backbone, the nucleobase, and ribose moiety in native nucleic acids. The resulting photosensitive oligomers have allowed the initiation or inhibition of nucleic acid hybridization simply by using the proper wavelength of light. The modular introduction of these switchable units into DNA strands using automated nucleic acid synthesizers has allowed diverse applications ranging from photoswitchable RNA silencing, reversible control of gene transcription, reversible aptamer recognition, and the reversible photocontrol of DNAzymes. The following section details the introduction of photoresponsive moieties into nucleic acid and nucleic acid analog structures. Approaches of photocaged nucleic acids, that is oligomers with photolabile protecting groups, and light initiated nucleic acid cross-linking have been recently reviewed[2,66,67] and are often restricted to low or nonexistent reversibility and, therefore, lie outside the scope of this review.

2.1. Molecular Switches as Phosphate Backbone Linkers in Hairpin Structures

The photochromic molecules stilbene and azobenzene have both been derivatized toward incorporation into the phosphate backbone of DNA oligomers.[68−76] These approaches can be summarized as follows: the *trans* form of the switches act to form unusually stable hairpins in self-pairing sequences, and the *cis* forms act to destabilize the hairpin structure (Figure 2). The overall effects of switching on duplex structure are limited compared to the examples discussed later (*vide infra*). The stability of the *trans* form may seem counterintuitive, as the *cis* form could hypothetically juxtapose the neighboring strands in a hairpin-like backbone configuration predisposing the strands

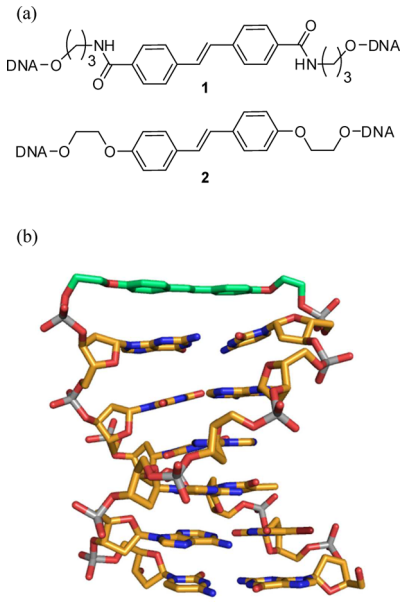

Figure 2. Stilbene as a nucleic acid linker in hairpins. (a) Stilbene derivatives from Letsinger and co-workers (**1**)[69] and Lewis and co-workers (**2**)[70,71] differ by their spacer units. (b) Crystal structure of a stilbene-linked DNA hairpin. C is gold, N is blue, O is red, and P is gray. Stilbene carbons are highlighted in green, and H is omitted for clarity. Adapted from coordinate data (1CS7)[77] from the protein databank, using PyMOL software.

dx.doi.org/10.1021/cr300179f | *Chem. Rev.* 2013, 113, 6114−6178

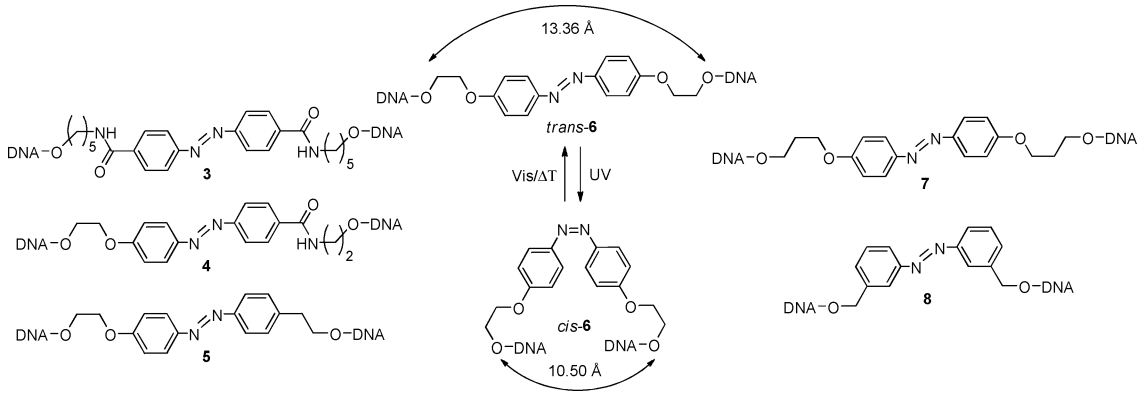

Figure 3. Azobenzenes that have been derivatized for linking two nucleic acid strands.[72−76] Compound **6** is highlighted in the center, along with the distances between the external oxygen atoms in the *trans* and *cis* forms. The change in hairpin stability for this compound is attributed to the 2.86 Å change in distance between the ends of the two isomers.

to hybridize. However, the system is better defined as *trans*-stilbene and *trans*-azobenzene linker units acting as efficient $\pi-\pi$ stacking hydrophobic caps (Figure 2b). The *cis* forms of these switches are less efficient at $\pi-\pi$ stacking due to their shape, and in some of the cases described, the *cis* geometry is too short a linker to properly stack with the underlying helix. Thus, the term "backbone linkers" is used here, as the incorporation of these switchable units does not carry much similarity to native phosphate backbone structure, nor are they similar in internucleobase distance. Instead, these switches act as linkers between two nucleic acid oligomer strands.

Letsinger and Wu were the first to incorporate a photoswitchable unit into nucleic acid structure in the form of stilbene as a backbone linker of two DNA oligonucleotides (Figure 2, **1**).[69] An initial publication using a non-self-complementary strand showed heteroduplex formation was energetically disfavored by the linker to a slight degree (a T_m shift of ∼−4 °C).[68] When self-complementary strands were employed, such as GCG-[ST]-CGC (where [ST] is **1**), melting temperature (T_m) values were uncharacteristically high (>80 °C). Furthermore, the T_m values calculated were significantly higher than those of the native duplex structures in equimolar salt concentrations. Combining these factors with previously published photochemical analyses[68] indicated that hairpin structures, stabilized by the switchable unit, were likely the cause of the high stability. This premise was also applied to explain the unusual stability of (TTTTTT-[ST])$_2$-AAAAAA as a doubly stabilized triplex structure, and the observation of an increased affinity for DNA intercalators, even for strands as short as trimers. Photoreversibility of the hairpin switch was also observed. Following irradiation, the *cis* form of the stilbene unit was found to destabilize hairpin structures, for instance in the strand T$_6$-[ST]-A$_6$, a shift of 10 °C was observed (T_m(*trans*) = 59 °C and T_m(*cis*) = 49 °C, 100 mM NaCl). Interestingly, when a G-C base pair was next to the switch, the stilbene unit became nonresponsive to light, probably due to quenching.[69]

Follow-up work from Lewis and co-workers, using a similar stilbene switch with a modified spacer, served to clarify the unusual thermal stability (Figure 2, **2**).[70,71] Photocontrol of hairpin formation was achieved using a diether-linked switch. When comparing the quantum yields of the random coil form of a dT$_4$[ST]dA$_4$ in methanol to a hairpin-folded structure in 1 M NaCl aqueous buffered solution, it was found that the *trans* to *cis* isomerization disappeared (0.37 in methanol versus <0.001 in aqueous media), while the *cis* to *trans* isomerization was diminished but still high (0.36 versus 0.17, respectively). Similar to Letsinger and Wu's approach, the diether-linked stilbene derivative gave unusually large T_m values (61−50 °C in aqueous systems) when in the *trans* form. Those values dropped significantly (33−26 °C) with the *cis*-isomer of the switch. In some cases, side reactions dominated the photoreaction (λ = 340 nm), depending on solvent pH or composition, such as ethanol/water mixtures. When Lewis and Liu tested the photoreversibilty of hairpin formation, they made two interesting observations. First, when the transition from *cis* to *trans* takes place, it occurs readily and gives quantitative *trans* formation, indicating the DNA may act as template. Second, *trans* to *cis* isomerization in the folded state was not observed. The authors gave two explanations: extremely stable *trans*-hairpin association and/or photoquenching from the neighboring base pairs. In a later study, a number of hairpins and their respective crystal structures helped to clarify the quenching effect (Figure 2b).[71] Neighboring pyrimidine nucleobases were capable of acting as electron acceptors. If the neighboring bases to the switch were G:G (noncanonical pairing), efficient photoisomerization was restored.

Yamana and co-workers synthesized an azobenzene DNA oligomer linker with spacer units of differing functionality and length between the switch and the nucleic acids (Figure 3, **3**−**5**).[72−74] The results mirror the studies described above; that is, very stable hairpin formation was found in the *trans* state of the azobenzene. In organic solvents and with unfolded strands, isomerizations were fully reversible. However, in the folded state the isomerization efficiency from *trans* to *cis* was reduced.

An adapted design, using ether-linked azobenzenes, showed the potential effects of subtle changes in spacer length between the DNA and the switch (Figure 3, **6** and **7**).[76] Sugimoto and co-workers, based on a crystal structure from the studies described above,[71] designed and synthesized two azobenzene derivatives differing in length by two methylene units in the spacer region between the DNA and the switch (**6** versus **7**). The aim was to provoke the most dramatic change in hairpin stability based on the conformation of the azobenzene switch by limiting degrees of freedom in the spacer units. Preliminary irradiation experiments monitored by HPLC indicated *cis* to *trans* isomerization of the two azobenzene linkers proceeded efficiently in the folded state of linked pentamers with comparable values (95.8% for **6** and 97.1% for **7**). Unlike the previous reports using stilbene, *trans* to *cis* isomerization also

dx.doi.org/10.1021/cr300179f | *Chem. Rev.* 2013, 113, 6114−6178

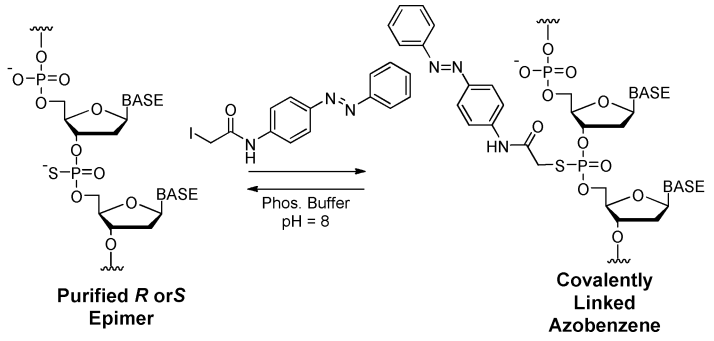

Figure 4. Postsynthetic modification of DNA by alkylation of a thiophosphate with an iodine derived azobenzene switch.[78] Beginning with the epimerically pure thiophosphate allowed for access to a covalently linked switch in epimerically pure form.

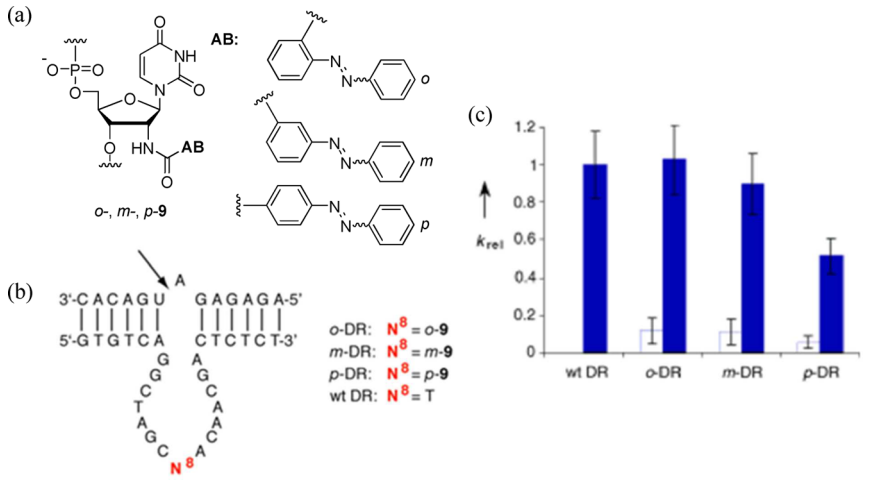

Figure 5. Sugar-linked azobenzenes for light controlled DNAzymes. (a) 2-Aminodeoxyuridylate is covalently modified *via* amide bond formation with three different azobenzenes (**AB**): *ortho*- (*o*-**9**), *meta*- (*m*-**9**), and *para*-azobenznene (*p*-**9**). (b) Introduction of azobenzene-modified uracil derivatizes to 10−23 DNAzyme at position N^8 (red). T is unmodified DNAzyme. The arrow indicates the cleavage site of bound RNA. (c) k_{rel} values for dark-adapted (*trans* azobenzene, open bars) and UV irradiated deoxyribozymes (*cis* azobenzene, blue bars) normalized to the wild-type DNAzyme (first bar). Reproduced with permission from ref 79. Copyright 2006 Wiley-VCH Verlag GmbH & Co. KGaA.

proceeded efficiently in the folded state, again with comparable values (81.7% for **6** and 86.1% for **7**). Azobenzene has added reactivity of thermal isomerization from the *cis* to the *trans* state, and it was determined that the *cis* form remained stable up to 60 °C for both **6** and **7**. After subjecting the two alternatively substituted strands to thermal denaturation experiments, the difference between the two linker units was clear. Photoinduced isomerization of **6** from *trans* to *cis* resulted in a T_m shift of 20 °C (57.5 to 37.5 °C), while similar photoinduced isomerization of **7** resulted in a shift of less than 2 °C (49.7 to 47.9 °C). This large discrepancy was explained by the different relative changes in loop size between the two switches (see distance labeled in Figure 3). Namely, the additional methylene units in **7** allowed more conformational freedom before and after irradiation while *cis*-**6** forced the DNA hairpin to become conformationally strained. Reversibility was confirmed by successive irradiations using UV monitored thermal denaturation experiments over five cycles.

Xi and co-workers investigated a *meta*-substituted azobenzene linker (**8**) for on/off regulation of *in vitro* DNA polymerization.[75] The authors presented data showing that UV irradiation of three different strands of switch-modified DNA reduced polymerization activity of *E. coli* Pol I. Gel electrophoresis patterns supported UV irradiation inhibiting polymerization. However, no data were given showing the isomerization efficiencies of the switch, nor was any stability information (melting curves, CD, etc.) reported in order to correlate DNA structure with the state of the switch. Furthermore, the authors provided a structural explanation that disagrees with that of the previously described systems. They proposed the *cis* form of the switch favored hairpin formation and the *trans* form promoted duplex formation impacting the polymerization rate of the enzyme. Though it is possible that the *meta*-substituted switch had different structural propensities than the previously reported *para*-substituted systems **3**−**7**, the research could benefit from UV and CD measurements of the switch incorporated to DNA to support the proposed hypothesis.[75]

A prevalence of literature[68−76] shows the interesting structural, functional, and photophysical properties of stilbene- and azobenzene-linked nucleic acid strands. From a fundamental perspective, the data gleaned from these experiments is invaluable in the design of future switchable oligomers. The far-reaching effects of the stilbene-linked approaches may be limited by the unusual stability of the hairpins themselves. As the switch capped hairpins are so stable, on−off reversibility is difficult to achieve for longer strands at reasonable temperatures. Furthermore, the propensity for quenching effects from pyrimidines could also be a limitation. The work by Sugimoto and co-workers[76] shows, on the other hand, that employing

dx.doi.org/10.1021/cr300179f | *Chem. Rev.* 2013, 113, 6114−6178

azobenzene with a proper linker length may remedy the quenching effects as well as increase reversible behavior even at moderate temperatures.

2.2. Molecular Switches Ligated to Nucleotides

Photoswitchable units have been introduced to nucleotide monophosphates in nucleic acid oligomers *via* two methods: alkylation of a thiophosphate-modified backbone and amidation of the ribose moiety on a 2′-aminodeoxyuridylate analog (Figures 4 and 5, respectively). In both cases, azobenzene was employed for similar reasons as in other approaches discussed here: highly efficient light-induced and thermal isomerization rates as well as facile introduction of the switchable unit, as synthetic anchoring methods are well-known for azobenzenes.

Alkylation of the thiophosphate-modified backbone of nucleic acid oligomers allowed for introduction of an azobenzene switch after oligonucleotide synthesis, a unique attribute in the discussed approaches.[78] Gupta and co-workers introduced a thiophosphate group at a single position in a series of nucleic acid strands, and separation of the *R* and *S* thiophosphate analogs was achieved using RP-HPLC. When an excess of iodoacetic amide-modified azobenzene was used (Figure 4), alkylation took place at the thiophosphate positions. Switching of the azobenzene unit was achieved with 365 nm light ($E \rightarrow Z$ isomerization) to a photostationary state of 17% *cis* isomer (beginning with 8% *Z*). Reversibility was achieved by irradiating with 430 nm light to a photostationary state of 89% *trans* isomer. Both isomerization processes could be followed by RP-HPLC. Following alkylation of a poly-T_8 strand of DNA between T_7 and T_8 with azobenzene, the melting temperature with a poly-A_8 strand was shown to increase significantly (pH = 7 and 1.0 M NaCl): +12.9 °C from the native strand and +9.8 °C from the thiophosphate analog. Modification of native nucleic acids to contain a single thiophosphate position has been known to increase stability slightly [∼1−3 °C].[78] Following irradiation with 365 nm wavelength light, the melting temperature shifted from 35.2 to 28.2 °C (a total change of −7.0 °C). The same trend was seen when azobenzene was introduced to a poly-A_8 strand between A_7 and A_8 following incubation with a poly-T_8, though these shifts were slightly less pronounced. That is, introduction of the azobenzene unit increased stability relative to the native oligomer (+6.0 °C) and the thiophosphate analog (+5.1 °C), and irradiation to achieve the *cis* isomer destabilized the duplex (a T_m shift of −5.0 °C). Moving the azobenzene modification toward the center of the nucleic acid oligomers led to lower T_m values than azobenzene introduction near the ends. However, the T_m values still indicated higher stability than the unmodified oligomers in most cases, and in all cases photocatalyzed $E \rightarrow Z$ isomerization destabilized the duplex. The *R* thiophosphate analogs generally gave higher T_m values with larger changes in T_m than the *S* thiophosphate analogs. The isomerization processes were also shown to be reversible following irradiation with λ = 430 nm light, yielding superimposable melting curves with the starting oligomer. Circular dichroism studies were performed that gave some evidence of intercalation effects from the azobenzene. Further studies need to be performed using this approach, as the temperatures at which the T_m data were obtained in many cases seem to not be low enough to establish sigmoidal melting transitions. Because of this, the results shown could vary, as T_m values are generally reported as the temperature at 50% transition, and this is only estimated in this study. Molecular modeling and/or further structural characterization studies would also greatly enhance the understanding of this unique approach as well as offer a firmer foundation for further functionalization.

Keiper and Vyle used photoswitchable nucleotide derivatives to gain spatiotemporal control of 10−23 deoxyribozyme, a well-known biocatalyst for RNA cleavage.[79] Introduction of *ortho*-, *meta*-, and *para*-carboxyl-substituted azobenzene units onto a 2′-amino derived deoxyuridylate unit was achieved *via* succinimide ester activation (Figure 5). The resulting uracil-azobenzene derivatives: *o*-**9**, *m*-**9**, and *p*-**9** were introduced to 10−23 deoxyribozyme sequences at a specified position (Figure 5a and b) and were tested for *trans* → *cis* isomerization efficiency showing PSS of 86%, 75%, and 61%, respectively. Thermally reversed isomerization took place rapidly for *p*-**9**, while *o*-**9** and *m*-**9** were highly stable to thermal isomerization. Irradiation with 435 nm of light provoked complete isomerization back to the *trans* state in 2 min.

It was subsequently shown that 10−23 deoxyribozyme (DR) activity could be controlled by light (Figure 5c) under multiple-turnover conditions using these modified nucleotides with efficiencies differing nearly an order of magnitude in response to light.[79] The RNA cleavage rates of the three deoxyribozymes *o*-DR, *m*-DR, and *p*-DR were compared to those of wild-type 10−23 deoxyribozyme both during irradiation with 366 nm light and under dark-conditions (Figure 5b and c). In all three cases, RNA cleavage rates were comparable to those of wild-type 10−23 deoxyribozyme while the samples were under UV irradiation with *o*-DR operating at 100%, *m*-DR operating at 90%, and *p*-DR operating at 50% wild-type activity. These rates were significantly different under dark-adapted conditions, with *o*-DR and *p*-DR giving $k_{irr}/k_{d\text{-}a}$ of 9:1 and *m*-DR of 8:1 (Figure 5c). The results were derived from analysis by PAGE and RP-HPLC. Reversible control of catalytic activity under multiple turnover conditions *in situ* was shown by irradiating light of 366 nm wavelength to turn on the catalyst (*trans* → *cis* isomerization, irradiated DR) and irradiating with 435 nm light to turn off the catalyst (*cis* → *trans* isomerization, analogous to dark-adapted DR). Though the differences in activity were lower, they were still significant with all three $k_{irr}/k_{d\text{-}a}$ = ∼4. Diminished rates of reaction were hypothesized to be due to reduced photoisomerization of *cis* → *trans*, possibly brought about by the RNA substrate or kinetic folding traps. It should be noted, however, that upon further irradiation at 366 nm the biocatalysts all returned to initial cleavage rates, confirming reversibility.

Both of the approaches described in this section use unique methods to introduce the switchable unit to DNA oligomers. In diverging from more traditional design methods to alter nucleic acid structure, the approaches described seem to leave changes in hybridization energy or alterations to catalytic activity to chance. What is gained on the other hand is the potential to find new methods to alter the structure of nucleic acid oligomers, as the example from Keiper and Vyle shows.[79] Structural studies or *in silico* calculations to further explain the observed behaviors are eagerly awaited.

2.3. Nucleobase-Derived Molecular Switches

A relatively new method for the introduction of a photoswitchable unit into nucleic acid oligomers involves the substitution of a photoswitchable alkene unit onto a nucleobase, effectively making the π system of the nucleobase part of the switch. Though this approach has involved more complicated syntheses, the results were new diarylethenes-type

dx.doi.org/10.1021/cr300179f | *Chem. Rev.* 2013, 113, 6114−6178

switches (see e.g. Figure 6a), which may have interesting physical and photochemical properties on their own outside the

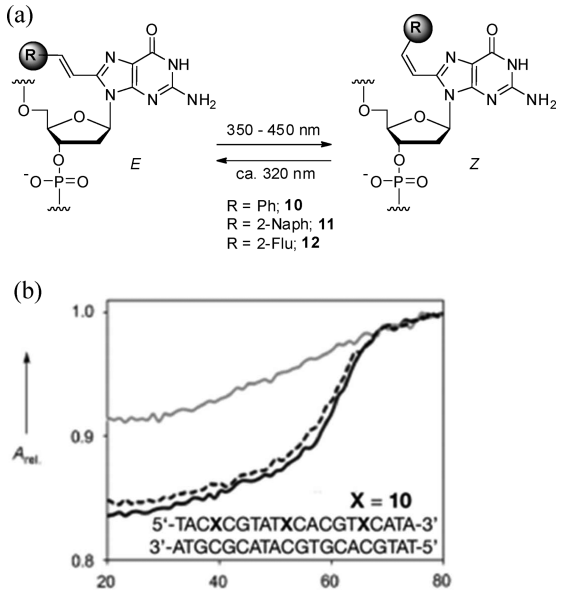

Figure 6. (a) Structure of photochromic nucleobase derivatives (**10**–**12**). (b) Comparison of UV-monitored thermal denaturation curves (260 nm) for an oligonucleotide modified with three ^{8ST}**G** (**10**) derivatives. Positions of modification are X (see inset). Conditions: 10 mM phosphate buffer (pH 7.0) and 100 mM NaCl. Solid black line: before irradiation (*E* isomer). Gray line: after 5 min of irradiation with 370 nm light (*Z* isomer). Dashed black line: after 2 additional min of irradiation at 254 nm (*E* isomer). Reproduced with permission from ref 80. Copyright 2008 Wiley-VCH Verlag GmbH & Co. KGaA.

realm of nucleic acids. Furthermore, the approach sought to discover new methods to distort or enhance nucleobase hybridization, as the effects of *Z*–*E* isomerization of these alkene units on nucleobase structure were unknown at the time of study.

Ogasawara and Maeda were the first to apply this methodology, synthesizing a phenyl- (**10**), 2-naphthyl- (**11**), and 2-fluorenyl (**12**), C8-substituted deoxyguanosine (Figure 6).[80] The three derivatives were then incorporated into DNA 12-mers *via* automated synthesis, and photoisomerization and hybridization studies were performed for comparison. The *E* forms of **10**, **11**, and **12** were irradiated for 5 min at 370, 410, and 420 nm, resulting in 86, 63, and 77% conversion to the *Z* form, respectively. Irradiating for 2 min at 254, 290, and 310 nm returned the substituted alkenes to the *E* states with photostationary states of 94, 87, and 77% *E*. In all cases the photosensitive units were shown to be thermally stable up to 80 °C, allowing for T_m calculation below this value. The incorporation of the photoswitchable deoxyguanosine unit into a single, midsequence position of a 12-mer destabilized the duplex for all three derivatives. T_m values were less than that of the native duplex. While irradiation of **10** from the *E* to the *Z* form using UV light caused a significant shift in T_m (−7.9 °C), the *E* to *Z* isomerization of **11** and **12** had less significant impact on hybridization (−1.6 and −1.4 °C, respectively). Previously performed molecular modeling and NMR studies indicated that the *Z* form of **10** forced the nucleobase to adopt a *syn* conformation relative to the sugar moiety, a conformation that inhibited duplex formation.[81] The *E* form of the switch allowed the *anti* conformation of the nucleobase (relative to the sugar) to occur, which favored duplex formation. The diminished change in T_m in the fluorenyl- (**12**) and naphthyl- (**11**) derivatives depending on *Z* or *E* isomerization is rationalized in that the large R substituents destabilized the duplex regardless of isomerization state due to steric interactions in both the *E* and *Z* states of the switch. This was supported by lower T_m values in the *E* state [39.6 °C naphthyl- (**11**) and 37.5 °C for the fluorenyl- (**12**)] as compared to the stilbene derivative (43.4 °C).

As the stilbene derivative **10** seemed the most promising for spatiotemporal control of nucleic acid hybridization, multiple incorporations of **10** into 20-mer sequences were studied.[80] Incorporation of one, two, and three units **10** into a 20-mer strand destabilized the duplex, though to less a degree than for the 12-mers described above. Furthermore, the increase in number of photoisomerizable units incorporated in the 20-mer strand resulted in increased changes in T_m upon irradiation from the *E* to the *Z* state, as one may expect. The most dramatic change occurred in the incorporation of three units, which effectively acted as an on–off switch for hybridization in that the *E* forms allowed duplex formation with a T_m of 60.2 °C while the *Z* forms resulted in no observable sigmoidal transition by UV thermal denaturation experiment (Figure 6b, 100 mM NaCl). CD measurements gave evidence of only single stranded DNA in solution in the *Z* form. This process was shown to be photoreversible, as irradiation with 254 nm light again initiated duplex formation. A serendipitous discovery arose in that the *E* form of the stilbene switch **10** was found to be six times as fluorescent as the *Z* form monitoring at 450 nm, allowing for reversible fluorescent monitoring of nucleic acid hybridization.

Spada and co-workers performed an independent study using a ribose diacetylated **10** monomer in supramolecular G architectures.[82] NMR and CD studies indicated the diacetylated **10** monomer formed ribbon-like architectures in high concentration in acetonitrile. This supramolecular assembly could be directed to form G-quadruplex-like octameric assemblies in the presence of potassium. When **10** was irradiated to the *Z* form, the octameric assembly was inhibited, while irradiation to the *E* form again allowed assembly to the G-quadruplex-like octamer. The isomerization process remained selective and highly reversible. As the studies using this switchable system were restricted to assembly in organic media and only in monomeric nucleotide form, the far reaching prospects from a biological standpoint remain to be seen.

In a later publication, Ogasawara and Maeda presented an application for the fluorenyl- (**12**) derivative in a G-quadruplex aptamer for thrombin.[83] The group substituted the switch-nucleobase into various positions and in various numbers ranging from single substitutions and up to four substitutions at selected positions in the aptamer using automated solid phase oligonucleotide synthesis. Of the 12 derivatives tested, two candidates gave the clearest on–off behavior, before and after irradiation. Prior to irradiation, the strands showed CD spectra and thermal denaturation curves indicative of quadruplex formation, and after UV irradiation, all spectroscopic evidence of quadruplex formation disappeared and the resulting spectra were indicative of unfolded single stranded oligonucleotides. Accompanying molecular modeling indicated that the fluorenyl moieties were forced into a steric clash with one another when in the *cis*, post-UV-irradiated state. A single candidate was then chosen and subjected to electrophoretic mobility shift monitored binding experiments with native thrombin. The

dx.doi.org/10.1021/cr300179f | *Chem. Rev.* 2013, 113, 6114–6178

results indicated the fluorenyl-modified oligonucleotide **12** continued to act as an aptamer when the switch was in the *E* form. Following irradiation, the thrombin-aptamer complex was disassembled. These results compared well to the affinities of the native aptamer, and the process was shown to be completely reversible.

Singer and Jaschke have taken a similar approach synthesizing a diarylethene derivative that incorporated adenosine into the photoswitch (**13**, Figure 7).[84] Unlike the previously

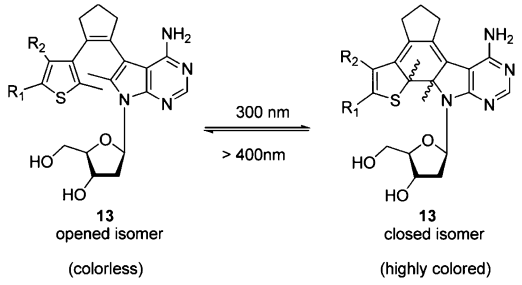

Figure 7. Diarylethene-derived deoxyadenosine.[84] Chirality is introduced to the central unit following covalent bond formation initiated by light.

described systems of Maeda and Spada,[80,82] in this approach a covalent bond is formed between the nucleobase and the switchable unit upon irradiation, introducing chirality to the normally achiral nucleobase unit. As this approach required modified substitutions at two positions on the adenosine nucleobase, the synthetic requirements were more rigorous, potentially limiting the further-reaching applications of this approach. Instead of investigating the base-pairing properties of the synthetic nucleobase-switch hybrid in oligomer form, the group opted to investigate nucleobase association in monomer form in organic solvent. Though these results cannot be extrapolated to any great degree to control properties in oligomer systems, a proof of concept that **13** can form hydrogen bonds with thymine in acetonitrile was established. The study also showed how substituent effects could be used to shift the maximum of absorbance of the switches, allowing for orthogonal triggering of cyclization by altering the wavelength of light. Though extensive evidence for the potential of this new class of switches was shown, it remains to be seen whether or not this approach will be useful in an oligomer format.

2.4. Molecular Switches as Nucleoside Surrogates

The incorporation of switches as nucleoside surrogates remains the gold standard in photoswitchable nucleic acids.[85] The approach, pioneered by Komiyama, Asanuma, and co-workers,[86] retains the facile synthetic methods of solid phase nucleic acid oligomer synthesis using a phosphoramidite-functionalized switch as nucleoside surrogate. Azobenzene has served as the best choice in terms of its ease of synthetic modification and the large impact it has on hybridization depending on the isomer. Spiropyran has also been applied, albeit with less dramatic effects.[87] As a result of the ease of the synthesis and function, this approach has seen the most applications with the furthest reaching results.

The method has been generally applied as the installation of the switch into a sequence as an additional nucleoside.[86] Azobenzene intercalates between the neighboring pairing bases in the *trans* form. Following irradiation, the *cis* form destabilized the duplex, hypothesized to be due to diminished ability to intercalate. There were two generations of the azobenzene-based nucleoside analogs. The first example described used a racemic switch (Figure 8, **14**).[88] The diastereomeric oligomers

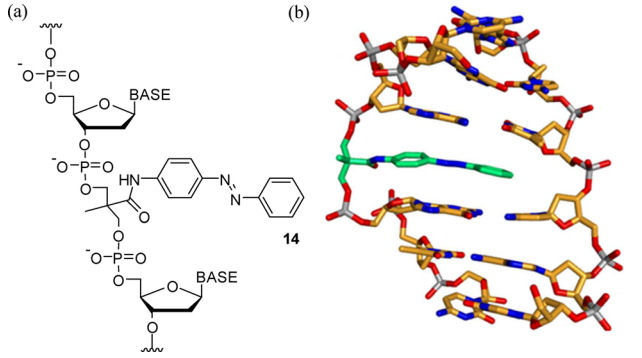

Figure 8. Komiyama, Asanuma, and co-workers' first generation azobenzene nucleoside surrogate.[88,89] (a) The switch was incorporated *via* automated solid phase methods similar to those of a standard nucleoside. The diastereomeric mixture was then purified *via* RP-HPLC. (b) Solution NMR structure of the *R* epimer nucleoside surrogate in a DNA duplex. C is gold, N is blue, O is red, and P is gray. Carbons from the synthetic azobenzene nucleoside surrogate are highlighted in green, and H is omitted for clarity.

were then separated by RP-HPLC. When incorporated into the middle of a poly-A 7mer, one diastereomeric oligomer actually induced an increase in T_m (~+1 °C) from the native strand when added to the complement in an equimolar amount. The other diastereomer reduced duplex stability (~−4 °C). Following irradiation of these two samples with UV light, a reduction in T_m values was obtained. The more stable diastereomeric duplex showed a shift of 8.9 °C (24.8 to 15.9 °C) in T_m, and the less stable diastereomeric duplex shifted 5.2 °C (19.9 to 14.7 °C) in equimolar salt concentrations. The process was also shown to be reversible with melting curves obtained following reisomerization nearly superimposable to the original. Solution-phase NMR structures of diastereomerically pure hexameric strands provided support that the *R* isomer was the more stable of the two and caused a larger change in T_m.[89] Structural evidence also supported the notion that the *trans* isomer of azobenzene readily intercalated between two pairing bases (Figure 8b). A thorough thermodynamic study on position and number of incorporated azobenzenes has been performed as well.[90]

Stretches of polypyrimidines in oligonucleotides can be used to form triplex structures.[91] This motif in nucleic acid structure is a commonly used method to prevent gene expression *in vivo*, dubbed the antigene approach.[92] Asanuma, Komiyama, and co-workers have shown that triplex formation can be regulated using azobenzene modified nucleobase surrogates.[93,94] Similar to the above-described approaches, the *trans* form of the switch stabilized triplex formation while the *cis* isomer caused a drop in T_m. The largest drops in T_m were observed when two azobenzene switches were introduced into a poly-T 13mer (ΔT_m > 48 °C). As an interesting addition to the above studies, a *meta*-azobenzene modified switch was also synthesized and studied. The largest discrepancy in T_m following *cis* to *trans* isomerization was observed when a single *para*-substituted azobenzene was employed in the center of the poly-T strand (ΔT_m > 30 °C). The *meta*-substituted azobenzene, on the other hand, offered the largest gap in T_m when placed at the end of

dx.doi.org/10.1021/cr300179f | *Chem. Rev.* 2013, 113, 6114–6178

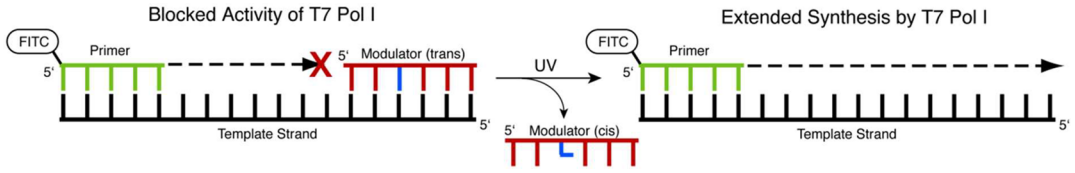

Figure 9. Application of the first generation azobenzene surrogate in the photocontrolled polymerization by T7 Pol I.[95] In the *trans* form the azobenzene-modified strand labeled modulator (red) blocked polymerization of FITC labeled DNA primer (green) to longer strand lengths. Irradiation with UV light favored the *cis* state and destabilized the association of the modulator with the template strand so the polymerase could continue.

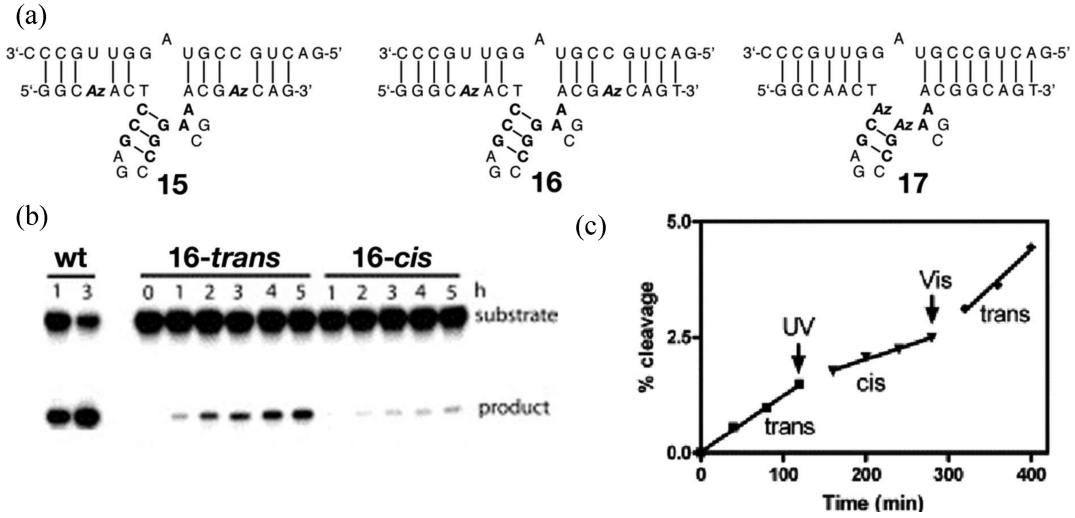

Figure 10. Photocontrol of 8−17 DNAzyme. (a) DNAzyme constructs synthesized. Catalytic core is in bold. Incorporation of **14** into 8−17 DNAzyme was done at positions marked *Az*. Two switches were introduced into (i) the 7-nt substrate binding arm (**15**); (ii) the 8-nt substrate binding arm (**16**); and (iii) the "required" G-C position in the catalytic core (**17**). (b) Gel showing time dependent cleavage of 5′-^{32}P labeled RNA by excess 8−17 DNAzyme. Control experiments with unmodified DNAzyme are labeled wt. *trans*-**16** is **16** irradiated with 422−438 nm light. *cis*-**16** is **16** irradiated with 322−338 nm light. (c) Cleavage rate modification by wavelength-specific light. DNAzyme started in the *trans* form and was then irradiated with UV light ("UV" arrow) to favor the *cis* form. Subsequent irradiation with visible light ("Vis" arrow) returned the DNAzyme to the *trans* state and the original cleavage rate. Irradiation times were approximately 40 min. Adapted with permission from ref 96. Copyright 2004 Elsevier B.V.

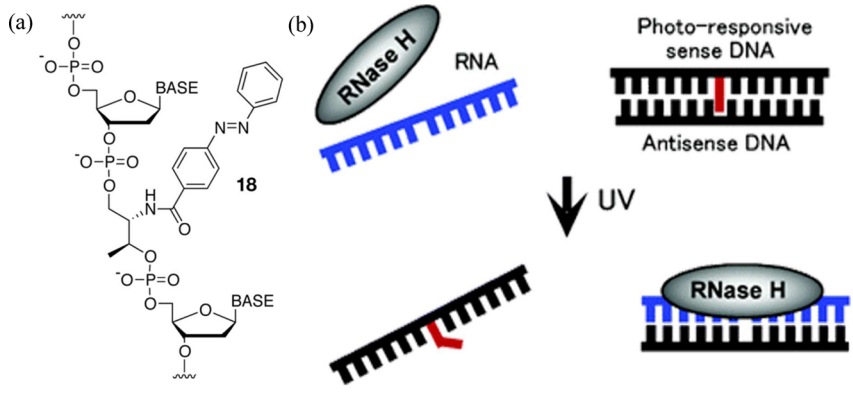

Figure 11. Incorporation of an enantiopure nucleoside surrogate for photocontrol of RNA digestion.[101] (a) Asanuma and co-workers' second generation azobenzene nucleoside surrogate (**18**).[97,98] (b) Cartoon showing the mechanism for photoresponsive oligomer sequestering of a DNA antisense strand. Following UV light irradiation, the photoresponsive strand liberates the antisense DNA, allowing it to recognize complementary RNA. RNase H recognizes hybridized RNA and performs degradation upon antisense duplex formation with RNA.

the poly-T strand (ΔT_m = 19.2 °C), indicating a different steric consequence for this light mediated structural change.

As a testament to the modularity of the approach, this method saw rapid applications in the photocontrol of T7 DNA polymerase activity *in vitro*.[95] The azobenzene nucleoside surrogate was substituted into an oligomer strand that acted as a blocking unit, dubbed modulator, by forming a duplex with the polymerase-template strand (Figure 9). In the dark, the FITC modified primer strand was extended from an 18mer to a 34mer. Following irradiation with light, isomerization of the switch occurred, reducing the stability of the blocking oligomer with the template strand. The same primer strand could then be extended to a 54-mer. The authors were careful to note that the T_m value of the *cis* form was still higher than the reaction

dx.doi.org/10.1021/cr300179f | *Chem. Rev.* 2013, 113, 6114−6178

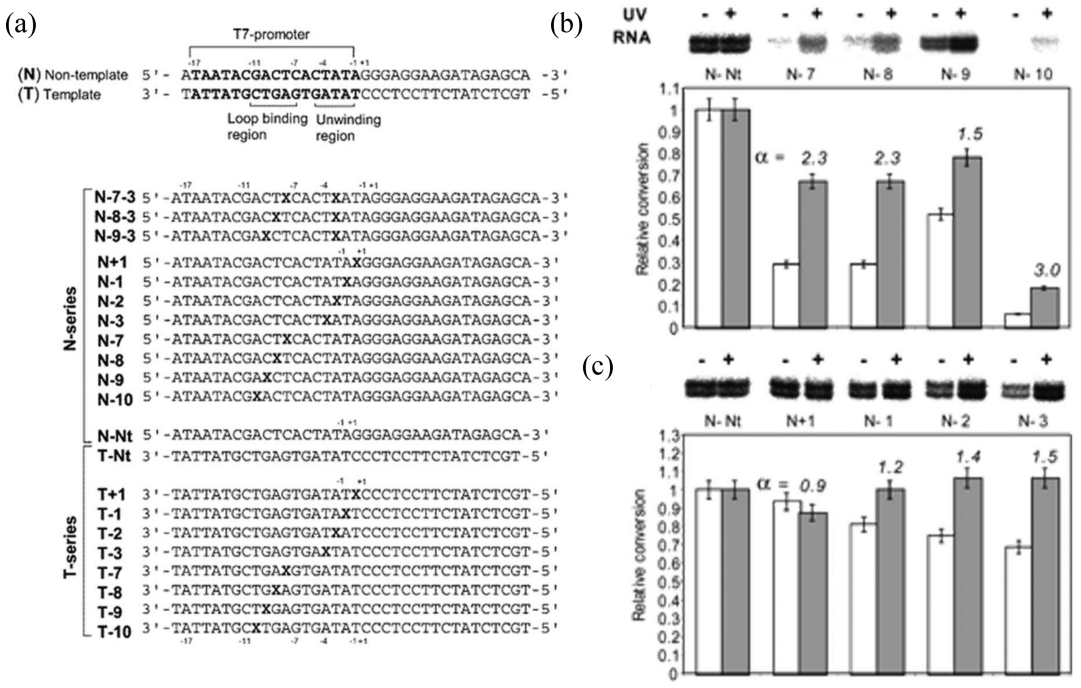

Figure 12. Photocontrol of transcription. (a) Incorporation of second generation nucleoside switch surrogate (**18**) into template (T) and nontemplate (N) dsDNA at positions X. The T7 RNAP promoter region is labeled and divided into the loop-binding and unwinding regions. (b and c) Nontemplate (N) switch insertion positions in the (b) loop binding region and the (c) unwinding region and the effect of UV light on transcription rate. N-Nt is unmodified dsDNA. Two gel bands account for full length and full length plus one. They were summed as total product. White bars were before UV irradiation (−). Gray bars were after UV irradiation (+). Adapted with permission from ref 102. Copyright 2006 American Chemical Society.

temperature (34 °C). That is, the strand should still have been in association with the template strand, though the stability should have been diminished. Exact T_m values were difficult to calculate based on fast thermal isomerization of the azobenzene switch at reaction temperature.

The first generation azobenzene nucleoside surrogate was also employed for spatial and temporal control of RNA-cleaving 8−17 DNAzyme (Figure 10).[96] This approach predated that previously discussed by Keiper and Vyle,[79] though the intended effect is largely the same (*vide supra*). The switch and the DNAzyme employed here were different, and this approach focused on single-turnover kinetics. Liu and Sen substituted two azobenzene nucleoside surrogates (Figure 10, **15**−**17**) in either the substrate binding arm or the catalytic core of the DNAzyme. The results of this investigation indicated that the introduction of **14** in two positions on the substrate binding arm allowed for photocontrol of DNAzyme activity. In the *trans* form (under visible light irradiation) the DNAzyme was active, and in the *cis* form (under UV irradiation) the DNAzyme showed 6-fold lower catalytic rates (Figure 10b). This process was shown to be reversible on the basis of wavelength of irradiation (Figure 10c). Interestingly, the inverse effect was seen when two positions on the catalytic construct were substituted with **14** (Figure 10, **17**). UV irradiation to the *cis* form led to a 5-fold *increase* in activity.

For a single incorporation site, racemic synthesis followed by purification of the diastereomeric oligomer is a useful approach. However, for the incorporation of *n* switches, the number of diastereomers increases 2^n for each incorporation. For this reason the enantiopure synthesis of a second generation of the azobenzene nucleoside surrogate (Figure 11, **18**) from Asanuma, Komiyama, and co-workers remains more useful.[97,98] The second generation was based on the chiral starting material D-threoninol. This starting material was chosen due its similarity to the structure used in the first generation approach and access to the chiral starting material. Comparison with the L-threoninol derived enantiomer showed the D-threoninol derived compound formed more stable duplexes in the *trans* form, could be incorporated at multiple sites without massively destabilizing duplex formation, and gave more dramatic shifts in T_m upon irradiation. Incorporation of this switch in a 20-mer could be performed easily using automated solid phase methods with substitutions of the enantiopure surrogate **18** in up to 10 positions without large problems with stability. "Clear-cut" photoregulation and reversibility were well characterized.[99] Structural modifications to the azobenzene switch were also performed to investigate the effects of increased sterics.[100] Surprisingly, in these cases, the introduction of methyl groups to the 2′ and 6′ positions on the azobenzene resulted in an increase in stability of the duplex for both the *cis* and the *trans* positions.

Photoregulation of RNA digestion by RNase H could be performed by substitution of the second generation nucleoside surrogate switch **18** (Figure 11a) into a DNA sense strand, allowing photocontrol of hybridization with a DNA antisense strand (Figure 11b).[101] A series of DNA strands were synthesized with an increasing number of azobenzene switches. These strands were the complementary sequence of the DNA antisense strand. Thus, in the *trans* form of the switch, hybridization takes place and the antisense DNA strand was sequestered. UV irradiation liberated the antisense strand, allowing it to hybridize target RNA. Once the duplex of the antisense DNA and RNA was formed, RNase H could bind the hybridized RNA and digest it. Asanuma and co-workers showed

dx.doi.org/10.1021/cr300179f | *Chem. Rev.* 2013, 113, 6114−6178

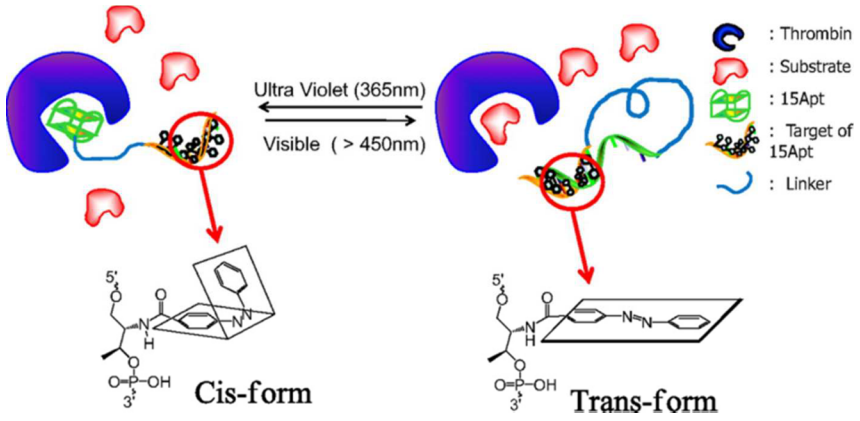

Figure 13. Photomodulation of thrombin activity *via* light controlled aptamer formation. The complement for the aptamer was modified with azobenzene switches and ligated to the aptamer sequence *via* a PEG chain. Under UV irradiation, duplex formation was discouraged, allowing the aptamer to fold for thrombin binding, inhibiting clotting. Visible light irradiation shifted the equilibrium to duplex formation, restoring thrombin activity by forming a duplex with the aptamer sequence. Reproduced with permission from ref 103. Copyright 2009 National Academy of Sciences, USA.

that when three or more azobenzene switches were incorporated into the sense strand, highly efficient on−off control of RNA digestion took place using UV light. Degradation of RNA was monitored by PAGE, and confirmation of the proposed mechanism was performed by fluorescent tagging of the RNA strand with FITC and the antisense strand with dabcyl. Upon UV irradiation, the DNA sense strand released the dabcyl tagged antisense strand, allowing it to hybridize the FITC tagged RNA strand. When in close proximity, dabcyl acts as a fluorescent quencher of FITC.

The second generation azobenzene nucleoside surrogate design has also been used to photoregulate transcription by incorporation into the T7 RNA polymerase (T7 RNAP) promoter region of DNA (Figure 12).[102] Asanuma and co-workers introduced the switch nucleoside in a series of 10 different positions on the template promoter region of T7 RNAP as well as on the nontemplate strand (see Figure 12a, for labels). The authors were careful to note that this approach differed from their other studies, as the focus was not control of hybridization, as the T_m is far above the temperature at which they are working. Instead, they were looking to change the local structure of the DNA duplex using light. The incorporation of the azobenzene switch into the 35-mer duplex sequence resulted in an isomerization to form between 20 and 40% of the cis isomer under UV irradiation. These values were uncharacteristically low for azobenzene substitution into DNA. We speculate this may be due to the length of sequence used, as the majority of the studies thus far have focused on sub-20-mer lengths. Incorporation of the switch was focused on the unwinding region and the loop-binding region of the T7 RNAP with the largest photoinduced change in activity, pointing to the cis form of the switch as the more active. Incorporation of the switch on the template strand resulted in diminished rates of conversion relative to the native strands even in the *cis* state while the rates of conversion, when the azobenzene was on the nontemplate strand, remained comparable to those of the native strand under UV irradiation (Figure 12b). A similar effect was seen when the switch was introduced to the unwinding region of the duplex (Figure 12c). Interestingly, the changes in relative transcription rates before and after irradiation remained similar whether the switch was on the template or nontemplate strand in the loop binding region or in the unwinding region (on average 1.5−2.0-fold increase under UV irradiation). A kinetic study revealed that azobenzene substitution in the loop-binding region primarily affected K_m, while those substitutions in the unwinding region affected k_{cat}. In other words, incorporation of the azobenzene in the loop-binding region affected enzyme binding, while incorporation in the unwinding region affected the rate of NTP incorporation. This effect, though it may be intuitive, is none-the-less elegant in application and proof. Incorporation of two switches, one in the loop binding and one in the unwinding region, resulted in an even larger discrepancy of on−off transcription behavior, with a 7.6-fold increase in rate of transcription when the *cis* form was present.[102]

Azobenzene nucleoside surrogate **18** was also used to modulate the binding of thrombin to a G-quadruplex aptamer.[103] This approach differed from the above-discussed Ogasawara and Maeda's inhibition of thrombin,[83] as the azobenzene switches were introduced to a complement strand for the aptamer rather than the aptamer itself (see Figure 13 for design). Photocontrol of the complement of the aptamer allowed for photoregulating of the aptamer concentration in solution without needlessly affecting the quadruplex structure and accidentally reducing thrombin−aptamer association (Figure 13). The aptamer sequence and a series of complement strands with varying incorporation of azobenzene switch positions and number were ligated together by a PEG strand. The effects of azobenzene position and state were tested for melting temperature, binding affinity to thrombin, and a clotting assay (a test for thrombin activity). To efficiently control hybridization of the aptamer and the complement, a minimum of one azobenzene per two nucleotides had to be used.[103] As thrombin is known to promote clotting, it was hypothesized that irradiation with UV light would liberate the aptamer, which would then bind thrombin, and clotting would decrease. Thus, following melting temperature experiments, blood clotting experiments were performed and the optimal azobenzene modified complement was chosen as the strand that gave the largest discrepancy in clotting time under UV irradiation and in the dark. The optimal azobenzene modified complement−aptamer conjugate was then employed in a microfluidic channel to show how this system could be used for spatial control of clotting. The *cis* form of the azobenzene-

dx.doi.org/10.1021/cr300179f | *Chem. Rev.* 2013, 113, 6114−6178

modified complement was formed using UV light, and the aptamer–thrombin complex was then annealed in a microfluidic chamber. Using radiation with visible light, clotting could be initiated in specific regions of the microfluidic chamber with submillimeter resolution in a matter of seconds.

An interesting investigation into the use of L-threoninol derivative **19** as a nucleoside surrogate was performed to assess the effect of stereochemical features of these hybrids (Figure 14).[104] Using this system, the *inverse* photocontrol process was

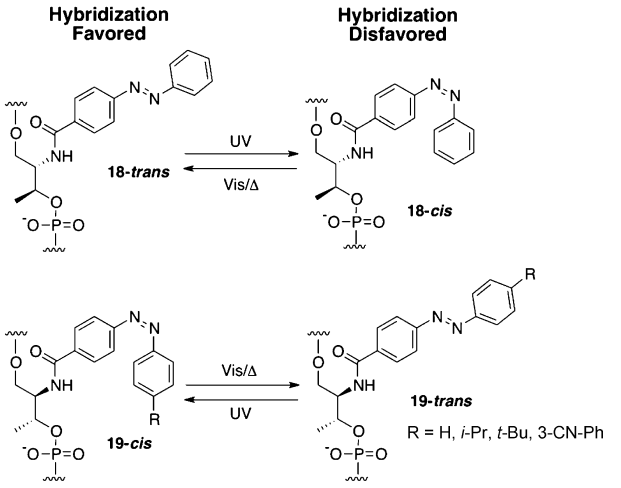

Figure 14. Development of a switch with inverse behavior.[104] Substituted L-threoninol derivative **19** served to give the inverse hybridization effects of the D-threoninol second generation derivative **18**. Under UV irradiation, duplex was favored with **19** while visible light and/or heat disfavored hybridization. R is a range of sterically different alkyl groups.

achieved. Irradiation with UV light to achieve the *cis* form of the switch resulted in duplex formation and *trans*-azobenzene destabilized duplex structure. The inclusion of **19** in nucleic acid oligomers characteristically lowered the T_m values between 1 and 3 °C when in the more stable *cis* form, depending on the steric effect of the R-substituent (Figure 14). After irradiation with visible light to achieve *trans*-**19**, the T_m values could be lowered between 7.3 and 0.9 °C from the *cis* form duplex, again depending on the size of the R-group. Characteristically, more sterically demanding substitutions to the azobenzene gave larger T_m shifts, with *t*Bu substitutions showing the largest effect. The reversibility of the system could be achieved with up to five "on–off" cycles confirmed by fluorophore and quencher tagging of the modified strand and its complement. However, in this case, the system had to be properly tuned with temperature to achieve this behavior. Furthermore, thermal isomerization was hypothesized to be a complication at higher temperatures, as complete hybridization was never achieved (~30% of the modified strand remained single stranded). Molecular modeling of the *cis* and *trans* states of the switch in the duplex showed that *cis*-**19** situated the switch outside of the duplex into the minor groove, while *trans*-**19** forced the sterically modified switch unit into the complement strand, causing duplex distortion. This remains the only system published to date in which the opposite hybridization behavior could be achieved for an established switchable system. This additional dimension of photocontrol could, in principle, cause two separate hybridization consequences with a single wavelength of light. In other words, UV irradiation would cause some strands to form duplexes while others would hybridize at a given temperature in a single flask. Such spatial and temporal control might be applied to some of the biological systems discussed above as well as have broader impacts in DNA-based logic systems or nanotechnology, and recent reports seem to indicate these applications are expanding.[105−108]

The extension of the nucleoside surrogate methodology has recently been applied to peptide nucleic acids (PNAs).[109] The move to this nucleic acid derivative allows expansion of scope as PNAs have been shown to be able to perform strand invasion on nucleic acid duplexes, elicit enhanced stability compared to native nucleic acids under physiological conditions, and cross cell membranes, while retaining the modularity of solid phase peptide synthesis. Stafforst and Hilvert showed[109] that the synthetic incorporation of azobenzene at the ends of PNA oligomers (neighboring the nucleobase) could be performed efficiently by synthesizing two strands: AcGlyLys-[Az_1]-(cattcatac)[Az_2]-LysGlyCONH$_2$, for duplex formation, and

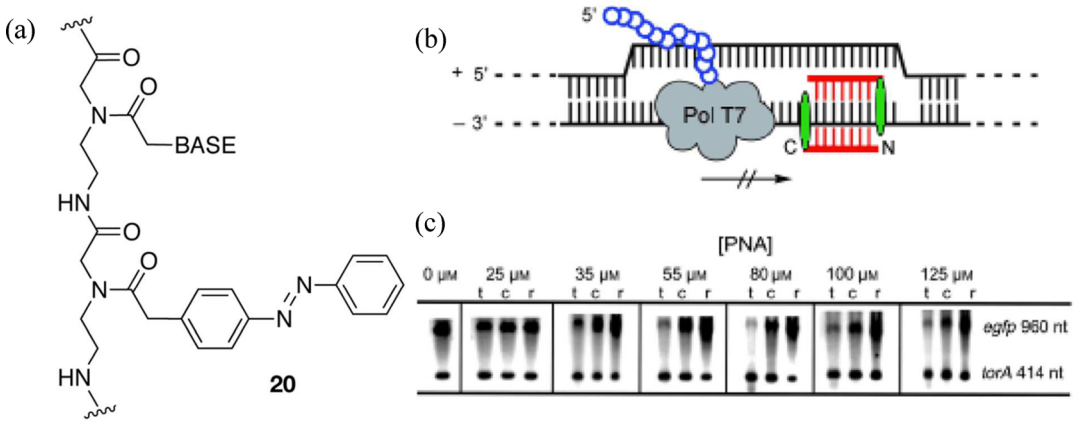

Figure 15. Triplex formation with azobenzene-modified PNA blocks gene transcription. (a) Peptide nucleic acid (PNA) derivative **20** was substituted as a surrogate base at the ends of a PNA oligomer, allowing for photomodulated triplex formation and consequently control of transcription. (b) Modulation of transcription by triplex formation. PNA is red. Azobenzene is green. Transcribed RNA is blue. Template DNA is black. (c) Formation of *egfp* transcripts (960 nt) and *torA* (414 nt, control) genes monitored by gel electrophoresis. The concentrations refer to amount of PNA added. *t* = ct_5c PNA containing azobenzene at the *C*-terminus. c = the same strand of PNA under irradiation with 360 nm light. r = reference PNA (minus the switch). Reproduced with permission from ref 109. Copyright 2010 Wiley-VCH Verlag GmbH & Co. KGaA.

dx.doi.org/10.1021/cr300179f | *Chem. Rev.* 2013, 113, 6114–6178

AcGlyLys-[Az_1](t_7)[Az_2]-LysGlyCONH$_2$, for triplex formation (see Figure 15a, **20** for the structure). [Az_n] signifies potential sites of azobenzene modification. Similar to the other discussed azobenzene derivatives, the switch existed up to 90% in the *trans* state and was isomerized up to 87% in the *cis* state with UV light. Thermal inversion back to the *trans* state was a facile process, especially at temperatures above 80 °C. Furthermore, irradiation with 425 nm light formed an 80:20 mixture of *trans*. The *cis* isomer was stable for hours up to 60 °C, allowing the monitoring of thermal denaturation curves below this temperature. Both substitution at the *C*-terminus and *N*-terminus further stabilized the duplex and triplex formation in the *trans* state to a substantial amount: ∼ +7 °C for the duplex with little variation between the *N* and *C* terminal substitution and +15 and +9 °C for the triplex at the *C*-terminus and the *N*-terminus, respectively. Following UV irradiation, all hybridization states were weakened, though the PNA strand with the switch in the *cis* state was still more stable than an unmodified PNA strand.

As photomodulation of triplex formation gave the most dramatic differences before and after irradiation, Stafforst and Hilvert investigated the spatial and temporal regulation of gene transcription using azobenzene-substituted PNA strands.[109] As stated earlier, PNAs can perform strand invasion. This principle has been applied to arrest transcription *in vivo* using triplex forming PNA strands. An analogous study was performed *in vitro* using the system described.[109] Comparison of the expression of the gene *egfp* with the control *torA* in the presence of an azobenzene modified triplex forming oligomer served as the test case (Figure 15b and c). Investigating a series of modified PNAs at seven concentrations between 0 and 125 μM showed that the *trans* isomer efficiently performed strand invasion on the *egfp* gene inhibiting transcription, while the *cis* isomer (formed *via* continuous irradiation with 360 nm light) showed a reduced ability to inhibit translation. Both azobenzene-modified oligomers were more efficient inhibitors than unmodified PNA. In an exquisite series of control experiments, the authors compared mixed sequences of the PNA strands and the gene, showing clear examples of specific triplex mediated inhibition of polT7 mediated transcription controlled by light.

2.5. Supramolecular Approaches to Photoresponsive Nucleic Acids

Supramolecular approaches to reversibly control nucleic acid hybridization consist of using a photochromic molecule that associates or dissociates from nucleic acids upon wavelength-specific irradiation of light. These approaches are attractive, as they circumvent the difficulty of introducing a switchable unit into the complex structure of nucleic acids. Furthermore, the potential for facile introduction to living systems exists, as the approach depends on small molecules rather than nucleic acid derivatives, potentially avoiding the need of transfection reagents to introduce the switchable small molecules into cells.

Andréasson and co-workers have recently reported evidence that cation-modified spiropyran **21** intercalates into nucleic acids in its open form, i.e. after exposure to UV light.[110] UV/vis spectra of **21o** in the presence of calf thymus DNA showed a significant blue shift in absorbance maximum from 512 to 420 nm in addition to a 45% hypochromic shift (i.e., decrease in absorbance), while the closed form of the cationic spiropyran (**21c**) showed no change in UV/vis spectrum in the presence of calf thymus DNA (Figure 16c). Both the blue shift and the hypochromicity were indicative of intercalation, as the

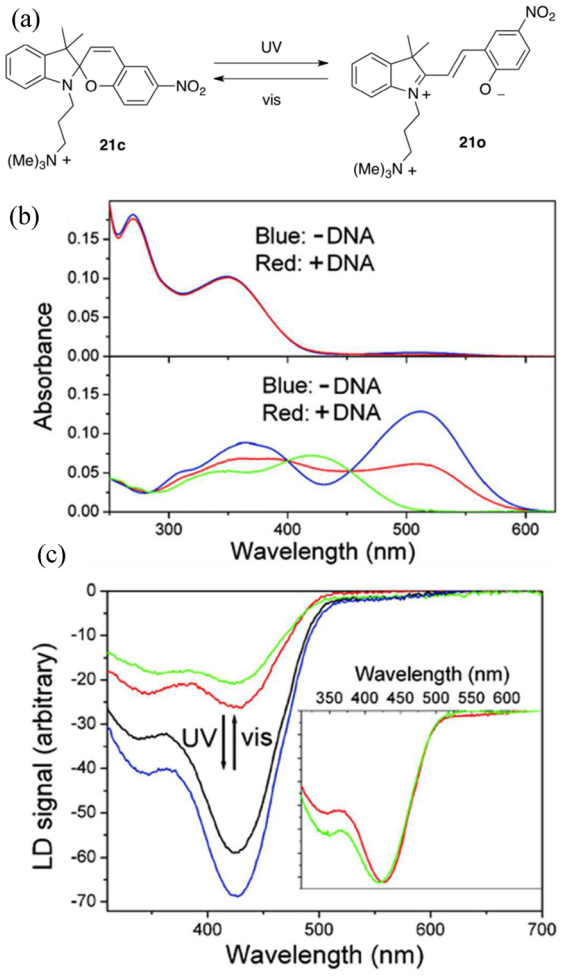

Figure 16. Photoswitchable nucleic acid intercalation. (a) Closed (**21c**) and open (**21o**) isomers of spiropyran derivative **21**. (b) UV/vis spectra of closed form (top) and open form (bottom) alone (blue line) and in the presence of calf thymus DNA (red line). The green line is a corrected spectrum for 100% spiropyran binding to DNA. (c) Flow oriented linear dichroism study of spiropyran **21** and calf thymus DNA. The green line is the start. The blue spectrum is after 5 min of UV irradiation. The red spectrum is after 5 min of visible light irradiation. The black spectrum is an additional 5 min of UV irradiation. The inset is the negative of the absorption spectrum for comparison. Reprinted with permission from ref 110. Copyright 2008 American Chemical Society.

hydrophobic environment between the nucleobases should favor a charge neutral resonance structure of **21o** while the zwitterion of **21o** should be favored in an aqueous environment. Comparison with the spectrum of **21o** in chloroform and water supported this argument. Further experiments using flow oriented linear dichroism also suggested intercalation, giving a value of 80 ± 5° for the angle between the transition moment of **21o** at 420 nm and the helix axis. These experiments also showed that intercalation could be triggered by light and was reversible as well as provided evidence that the light triggered events were due to the binding of the switch to calf thymus DNA and not due to switch decomposition (Figure 16).

The authors indicated cationic spiropyran **21** could be employed as a nucleic acid probe due to its distinctive blue shift, which occurred only with the open form despite a moderate binding value of 2×10^4 M^{-1}.[110] The effects of light-triggered spiropyran binding on hybridization or enzyme

dx.doi.org/10.1021/cr300179f | *Chem. Rev.* 2013, 113, 6114–6178

recognition remain to be seen, which currently limits application in biological settings, though the possibilities for this small molecule remain attractive. Further investigations would also require a comparison between repeated UV irradiation and potential competing nucleic acid cross-linking.

Nakatani and co-workers have developed a system they refer to as a "molecular glue for DNA": comprising a naphthyridine carbamate dimer connected by an azobenzene unit (**22**, Figure 17).[111−113] The naphthyridine carbamate dimer had previously been shown to stabilize duplex DNA containing G-G mismatches, effectively sequestering one of the mismatched nucleobases *via* groove binding while concomitantly displacing a neighboring nucleobase (Figure 17a).[114] By introducing an azobenzene to the dimer unit (**22**), the process could be spatially and temporally controlled with light. Incubation of *trans*-**22** with the mismatched hybrid sequence 5′-(CTAA ***CGG*** AATG)/5′(CATT ***CGG*** TTAG) gave a T_m value of 32.7 °C, an increase from 25.6 °C in the absence of *trans*-**22**. Following irradiation with UV light (5 min, λ = 360 nm) to form *cis*-**22**, the T_m increased again, this time by 15.2 °C to T_m = 48.0 °C. Interestingly, there was an increase in the photostationary state of *cis*-**22** to 75% in the presence of hybridized DNA. Cold-spray ionization time-of-flight mass spectrometry showed a distinct peak for DNA hybrid + *cis*-**22** while a mass for the duplex + *trans*-**22** could not be detected, offering support that the *cis*-**22** form binds DNA duplexes in the expected 2 to 1 ratio while the *trans*-**22** form does not.

Surface plasmon resonance (SPR) was used to monitor **22**-initiated DNA hybridization with a template strand attached to a gold surface (Figure 17b−d), and it was subsequently shown that the interaction was G−G mismatch specific and reversible following irradiation with 430 nm light.[111] By incorporating two G−G mismatches into a DNA sequence, the T_m change in the presence of **22** could be made very large. Using a special SPR-photoreactor cell, a solution including **22** and complementary DNA could be continuously irradiated while hybridization was monitored by SPR (Figure 17b). When additional tests with strands that substituted C, T, A, and G at position "X" in Figure 17b (DNA-3X) were performed, hybridization occurred immediately for the proper Watson−Crick partner C and after irradiation with 360 nm of light for the G mismatch indicating light induced transformation of *trans*-**22** to *cis*-**22** stabilized the duplex. Changing the irradiation conditions to 430 nm showed that the stabilization could be photochemically reversed (Figure 17d).

Nakatani and co-workers have continued to investigate the effects of linker length on the binding activity of **22**[115] as well as performed additional molecular modeling experiments to aid the structure elucidation and the design of further "switchable molecular glues for DNA". While this approach could benefit from the development of small molecules that target mismatches other than G−G, the approach has very clearly elucidated an "on−off" hybridization response to light, while other approaches described weigh the delicate balance between energy of hybridization and temperature. Furthermore, by avoiding synthetic modification to nucleic acids, the supramolecular approach benefits by retaining the modularity inherent in modern nucleic acid techniques. A limitation in this approach may be an inability to target specific sequences *in vitro*. Further experiments with larger libraries of sequences could illustrate how much of a potential complication this could be.

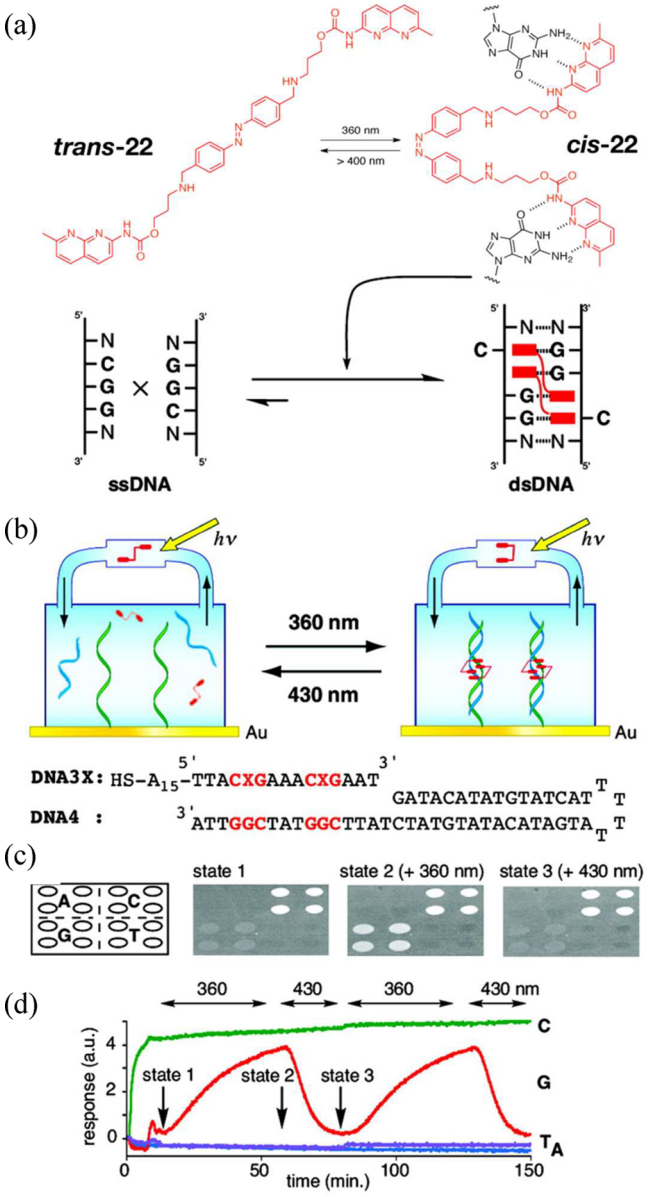

Figure 17. (a) Illustration of NCDA (**22**, red) assisted DNA hybridization. (b−d) SPR difference imaging experiments showing photoswitching. (b) Experimental setup and nucleic acid sequences studied. Thiol terminated sequence DNA-3X acts as a probe, while hairpin loop DNA4 acts a pseudocomplement. (c) SPR difference images of the DNA3X array. Strands are arranged according to the panel above, where "X" is a respective nucleobase. "State 1": image after addition of DNA4 and NCDA (**22**). "State 2": image after 40 min of irradiation at 360 nm. "State 3": image after 430 nm of irradiation of state 2 for 20 min. (d) Time course of intensities of the spots from part c. Horizontal arrows (top) indicate irradiation. DNA 4 and NCDA (**22**) were injected at 0 and 6 min, respectively. Reprinted with permission from ref 111. Copyright 2008 American Chemical Society.

2.6. Concluding Remarks

A number of methods have been developed for the photocontrol of nucleic acid structure and hybridization. A surprising result of the studies described above is the number of applications in which the nucleic acid oligomers are synthetically modified in different ways without massive losses to hybridization energy, and yet irradiation with light immediately has an effect on stability. This is no small feat, as synthetic

dx.doi.org/10.1021/cr300179f | *Chem. Rev.* 2013, 113, 6114−6178

modifications to nucleic acids are known to have complicated effects. The retention of solid phase synthetic methods for nucleic acid oligomers allows for a number of strands to be tested with varying numbers of switches incorporated in different positions, or with different sequences. Such modularity is key, not only to describing functional attributes of the light-sensitive systems but also toward fast and efficient applications in enzymatic systems.

The outlook for spatial and temporal control of nucleic acids remains bright, as new modifications continue to be published. Ample examples exist that show the potential for these approaches *in vivo*, including antisense and antigene technologies. Complications arising from excessive irradiation with UV light in a biological setting remain to be tested. Furthermore, using temperature to alter hybridization effects will also be limited in living systems. The development of switchable units with absorption maxima outside the UV range, in particular switching systems in the near-IR, would be extremely beneficial. We eagerly await the use of the above applications in an *in vivo* setting.

3. PHOTOCONTROL OF PEPTIDE CONFORMATION AND ACTIVITY

3.1. Introduction

The incorporation of molecular photoswitches into proteins could in principle allow for reversible control of protein structure and function *via* photoinduced isomerization. The small conformational changes within large and complex proteins are, however, difficult to predict and interpret, which limits their possible scope and applications.

It would be therefore advantageous to investigate the effects of photoinduced isomerization on structure and function in smaller systems, such as short model peptides. Furthermore, various bioactive peptides are present in living systems, offering the potential for the photocontrol of their biological activity, thus reaching beyond influencing solely protein conformation. Examples of such peptides include the hormones somatostatin, insulin, and leptin or naturally occurring bioactive peptides such as cyclosporin and apicidin. Additionally, photocontrol of peptide structure could influence the properties of peptide-based materials, such as polymers, gels, and fibers. Three different methods used to incorporate photoresponsive switches in peptides are depicted in Figure 18. This section, inspired in its structure by a report from Renner and Moroder,[23] describes the most significant photoresponsive effects observed on peptide conformation and properties using these approaches. Novel molecular photoswitches and potential future applications are also discussed. For another recent review on photoresponsive peptides, the reader is referred to the work of Ciardelli, Pieroni, and co-workers.[116]

3.2. Peptides with Photoresponsive Amino Acid Residues

Peptides are known to be good synthetic analogs of protein motifs and can exist in disordered or regularly folded structures, such as random-coil, β-sheet, and α-helix structures, depending on reaction medium, pH, and temperature.[17] Incorporating photoresponsive amino acid residues into peptide structures allows for photochemical control of molecular recognition and organization.

Photoresponsive peptides were investigated for the first time by Goodman,[117−121] who employed optical rotatory dispersion (ORD) to demonstrate the effects of photoisomerization and the accompanying structural changes of peptide derivatives.

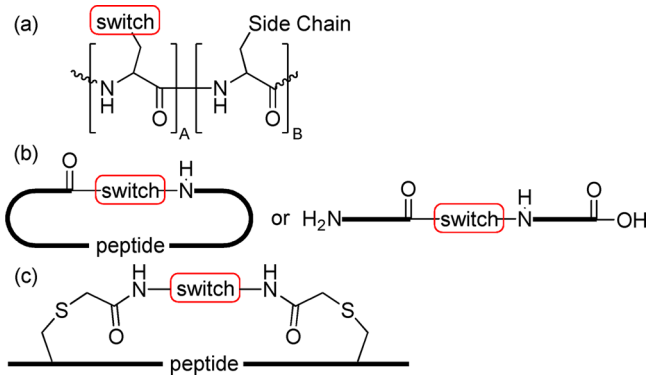

Figure 18. Three approaches used to incorporate molecular switches in peptides. (a) Copolymers of an amino acid and molecular switch-functionalized amino acid derivative have been used to photomodulate the conformational states of poly-α-amino acids. (b) Molecular switches have been introduced into the backbone of both cyclic and linear peptides. (c) Peptides have been cross-linked with a molecular switch between side chains. Adapted with permission from ref 23. Copyright 2006 Wiley-VCH Verlag GmbH & Co. KGaA.

Copolymers of phenylazophenylalanine and γ-benzyl-glutamic acid (Figure 18A) were used to photomodulate the ratio of conformational states of these poly-α-amino acids. Changes in Cotton effect were observed upon irradiation, indicating a light-induced change in the structure of the polypeptide backbone.

Photoregulation of azobenzene-modified poly(L-glutamic acid) **1** was studied by Pieroni et al.[122] Irradiation of the *trans*-azobenzene-modified polypeptide at 350 nm induced isomerization to the *cis* form. This process could be reversed to give the *trans* isomer by irradiation at 450 nm or *via* thermal isomerization (Figure 19). CD measurements of the peptides,

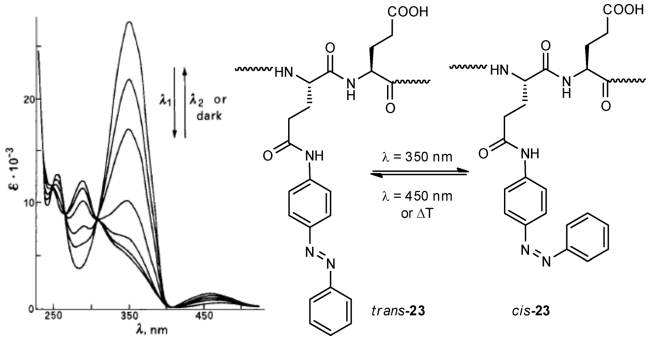

Figure 19. Reversible light-induced variations (λ_1 = 350 nm and λ_2 = 450 nm) of the absorption spectra in *azo*-modified poly(L-glutamic acid) **23**. Reproduced with permission from ref 123. Copyright 1992 Elsevier B.V.

containing 13−56 mol % of azobenzene-derived amino acid residues, dissolved in trifluoroethanol and trimethyl phosphate (TMP), indicated the presence of an α-helix structure for both the *trans*- and *cis*-isomers.

In aqueous solution, the photoresponsive peptide behavior differed and was shown to be dependent on pH or the presence of surfactants.[124] UV irradiation of the peptide in water, at pH 5−7, caused a decrease in ordered structure, which was then restored *via* dark adaptation. However, at pH 7.6 the peptide, containing 20 mol % of azobenzene units, showed the CD pattern of a random coil structure and was no longer influenced by photochemical isomerization. Addition of the surfactant,

dx.doi.org/10.1021/cr300179f | *Chem. Rev.* 2013, 113, 6114−6178

dodecylammonium chloride (DAC), at its critical micelle concentration, resulted in a coil-to-helix transition upon irradiation at 350 nm (*trans* to *cis*). The mechanism for this reversible, photomodulated process was explained by favorable interactions of the apolar *trans* form and the hydrophobic core of the micelles, which resulted in the coiled conformation of the peptide. It was hypothesized that photoisomerization to the more polar *cis*-azobenzene disrupted the hydrophobic interactions and caused the peptide to separate from the micelles, allowing the polypeptide chains to adopt an α-helix structure (Figure 20).

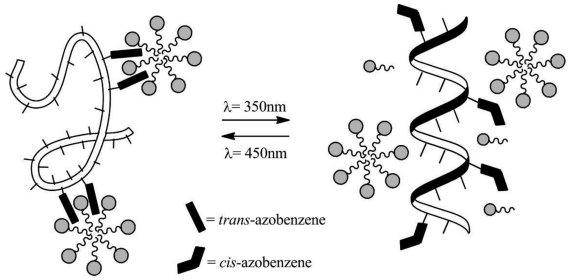

Figure 20. Schematic illustration of the proposed photoresponsive effect of *azo*-modified poly(glutamic acid) in the presence of DAC micelles. Reproduced with permission from ref 124. Copyright 1988 Wiley-VCH Verlag GmbH & Co. KGaA.

Pieroni and co-workers achieved similar photoregulation of polypeptide structures using spiropyran-containing poly(L-glutamate)[125,126] and poly(L-lysine) modified with spiropyran[127] or azobenzene units.[128] The large differences in polarity between the two forms of the switch units were suggested to strongly affect the conformation of the macromolecules.

Poly(L-glutamic acid), containing nitrospiropyran units, dissolved in hexafluoro-2-propanol (HFP) adapted a random coil conformation, as revealed by CD spectroscopy. A "negative photochromism" behavior was observed; that is, the opened, merocyanine form of spiropyran was observed in a non-irradiated sample. The authors hypothesized that HFP stabilized the photoswitch in the merocyanine form *via* protonation. Exposure to visible light for a few seconds induced isomerization of the photoswitch to the spiropyran form with full conversion, which was accompanied by a random coil to α-helix transition of the peptide. Dark adaptation to the merocyanine form restored the original random coil conformation.[125] Similar photocontrol was observed for spiropyran-modified poly(L-lysine), when appropriate amounts of triethylamine (3−15%) were added to the HFP−polymer solutions.[127] The driving force for the photoinduced ordering of the spiropyran-modified peptide was attributed to the hydrophobic properties of the closed photoswitch that did not disturb the formation of intramolecular H-bonds in the polymer, which are responsible for its α-helical structure. Isomerization to the merocyanine form, and subsequent protonation, likely results in electrostatic repulsion between the positively charged photochromic units, and as a consequence, the α-helix structure is disrupted.

An interesting effect was observed upon the addition of a small amount of trifluoroacetic acid (TFA) to spiropyran-modified poly(L-glutamate) dissolved in HFP. A random coil structure for both the spiropyran- and merocyanine-modified peptides was observed.[126] It was proposed that the repulsive electrostatic interactions in the now protonated peptide-switch force the macromolecule to adopt an extended random coil structure. Random coil to α-helix transitions were again observed when methanol (5−40%) was added as a cosolvent. It was hypothesized that the addition of methanol shifts the equilibrium between the protonated and deprotonated spiropyran units, favoring the neutral form.

Similar behavior was observed for spiropyran-[129] and azobenzene-[128] modified poly(L-lysine). Poly(azobenzenesulfonyl-L-lysine) **24**, dissolved in HFP, showed a typical CD spectrum of a random coil for both the *trans* and *cis* configurations of the azobenzene switch. When methanol was added at concentrations below 15%, irradiation of the sample at 340 nm resulted in a coil to α-helix transition, indicated by the increased CD ellipticity at 222 nm. At methanol concentrations of 15% or higher, both *trans*- and *cis*-azobenzene-modified peptides adopt an α-helical structure (Figure 21).

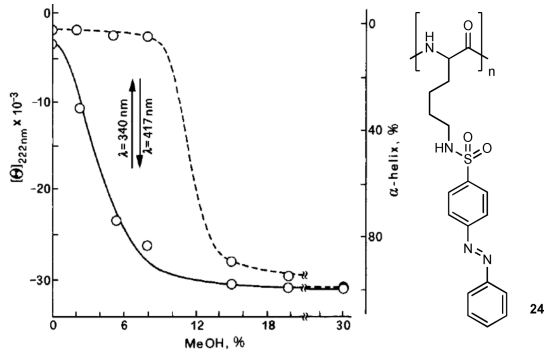

Figure 21. CD elipticity at 222 nm and the content of the α-helix of poly(azobenzenesulfonyl-L-lysine) **24** in hexafluoro-2-propanol/methanol (HFP/MeOH) solvent mixtures as a function of MeOH concentration for samples irradiated at 417 (−) and 340 nm (- - -). Reproduced with permission from ref 128. Copyright 1996 American Chemical Society.

Ueno et al.[130,131] investigated the photoisomerization of azobenzene-modified poly(L-aspartate) in a solvent mixture of 1,2-dichloroethane (DCE) and TMP. CD spectroscopy revealed an exclusive left-handed helix conformation for the polypeptide with *all-trans*-azobenzene units using DCE as solvent. This peptide structure could be changed to a predominantly right-handed helix (74−81%) upon irradiation to the *cis* form of the azobenzene at increased TMP concentrations (25−30%). The peptide helix inversion was accomplished with 9.7% *azo* groups incorporated in the polymer.

These studies show that photoisomerization of photochromic residues in polypeptide side chains can induce major conformational changes in the peptide structure. The choices of solvent, pH, and temperature were shown to be crucial for tuning of the photoresponsive behavior of the polypeptides. Further research could improve thermal stability and fatigue resistance of the chromophores described, and determine the scope of these polymer systems for future applications, which include photocontrol of solution viscosity and the properties of polypeptide-based materials. However, the need for multiple chromophores to be incorporated in the peptide structure in order to obtain these conformational changes is a limiting factor in tuning the photoresponsive behavior. More recently developed methods for incorporating molecular photoswitches in peptides, discussed in the following sections, show enhanced

dx.doi.org/10.1021/cr300179f | *Chem. Rev.* 2013, 113, 6114−6178

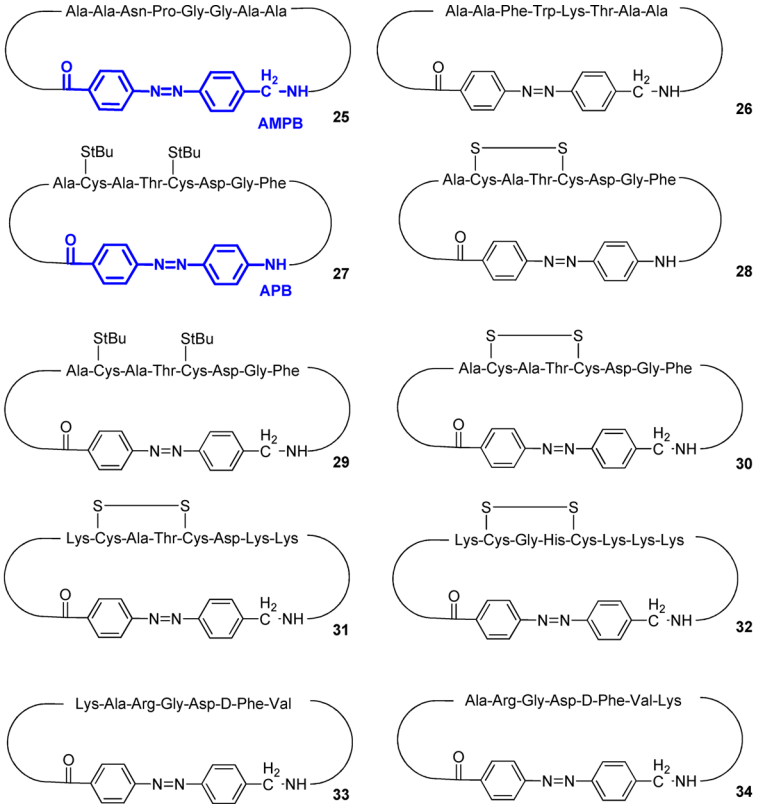

Figure 22. Structures of the monocyclic and bicyclic peptides with azobenzene-based APB and AMPB linkers.[134,135,137,138,140−146]

photoresponsive behavior with a better control of the structural changes elicited by the peptides.

3.3. Photoresponsive Molecular Switches Incorporation into the Backbone of Peptides

3.3.1. Photoresponsive Switches in Cyclic Peptides. The β-turn is a common motif in bioactive proteins and peptides, shown to be important in various peptide−protein and protein−protein interactions.[132,133] Photoregulation of β-turn conformations could be a useful step toward controlling biologically active peptides (Figure 22).

Chmielewski and co-workers incorporated a photoresponsive amino acid into β-turn mimicking cyclic peptides and investigated the effects of photoisomerization on their conformation.[134] A Gly-Gly-Pro-Asn sequence was flanked on both sides by two alanine residues that were then joined by 4-[(4-aminomethyl)phenylazo]benzoic acid (AMPB) to give peptide **25**. *trans*-**25** showed a β-strand conformation interrupted by a bend at the Pro residue. Irradiation of *trans*-**25** resulted in the isomerization to the *cis*-form, and consequently, the cyclic peptide adopted a typical β-turn conformation.

More recently, Chmielewski et al. reported photoresponsive cyclic peptide **26**, in which the pharmacophoric tetrapeptide turn sequence of the decapeptide somatostatin was incorporated.[135] Somatostatin is a peptide hormone that regulates a range of biological functions, including cell growth, and, hence, is of interest in the treatment of certain cancers.[136] Isomerization of the *trans* isomer of somatostatin derived photoresponsive cyclic peptide **26** to the *cis* form induced the formation of a β-turn within the pharmacophore Phe-Trp-Lys-Thr somatostatin sequence. An enhanced affinity to a somatostatin receptor was observed (Table 2).

Table 2. Binding Affinities to a Somatostatin Receptor of *trans*-26 and *cis*-26, Bearing the Pharmacophore Turn Sequence of Somatostatin[135]

	trans (μM)	*cis* (μM)
IC_{50}	3.6 ± 0.3	1.7 ± 0.1
K_i	2.6 ± 0.2	1.0 ± 0.1

Moroder and co-workers studied related photoswitchable cyclic peptides containing various sequences of seven to eight amino acids. In the first approach, 4-(4-aminophenylazo)-benzoic acid (APB, Figure 22) was incorporated in a cyclic peptide comprised of the pharmacophore for thioredoxin reductase (TRR) recognition (peptide **27**, Figure 22).[137,138] TRR enzymes are able to reduce oxidized thioredoxin (Trx) proteins. Proteins reduced by Trx play an important role in various biological processes (i.e., cell growth, apoptosis inhibition, etc.).[139] Photoisomerization of a photoresponsive monocyclic APB-peptide was reversible, with both *cis* and *trans* isomers adopting well-defined conformations. Additional conformational constraints were introduced *via* an intramolecular disulfide bridge to form a bicyclic APB-peptide (peptide **28**, Figure 22).[140] However, this generated a so-called "frustrated" system for both isomers. The use of an AMPB chromophore introduced enhanced flexibility and was found to be of more use (peptides **29** and **30**, Figure 22).[141] The AMPB-peptide **30** (Figure 22) was made water-soluble by replacing all the residues outside the Cys-Ala-Thr-Cys-Asp motif with Lys residues to investigate the photomodulation of the redox potential under aqueous conditions (**31**, Figure 22).[142,143]

The redox potential was determined by performing thiol/disulfide exchange experiments with GSH/GSSG (glutathione) as a reference redox pair. The potential measured for the

dx.doi.org/10.1021/cr300179f | *Chem. Rev.* 2013, 113, 6114−6178

bicyclic *trans*-**31** was very similar to that for the native linear active site fragment of thioredoxin reductase (Table 3, entries 2 and 1, respectively). Irradiation at λ = 360 nm resulted in photoisomerization of the switch-linked peptide backbone and a concominant shift in oxidation potential for the *cis*-**31** isomer to a higher value (Table 3, entry 3). This redox potential closely resembles that of a native enzyme, protein disulfide isomerase (PDI). PDI catalyzes disulfide formation in protein folding by connecting the proper cysteines linkages in proteins.[144] Formation of the disulfide bridge using *cis*-**31** proved to be highly unfavorable, with a K_{ox} value ($K_{ox} = k_{ox}/k_{red}$) that was nearly 3 orders of magnitude lower than that of the *trans*-**31** (Table 3, entries 2 and 3).

Table 3. Apparent Redox Potentials and K_{ox} Values ($K_{ox} = k_{ox}/k_{red}$) of Linear and Bicyclic Peptides Containing the Thioredoxin-Derived Cys-Ala-Thr-Cys Sequence at pH 7.0[143]

entry	compd	K_{ox} (M)	E'_0 (mV)
1	H-Ala-Cys-Ala-Thr-Cys-Asp-Gly-Phe-OH	0.123	−210
2	*trans*-**31**	0.050	−200
3	*cis*-**31**	8×10^{-4}	−146

The ability of the AMPB-modified bicyclic peptide **31** to mimic thiol/disulfide oxidoreductases was investigated by catalyzing the oxidative refolding of reduced ribonuclease A (RNase A). In both *trans* and *cis* configurations, the peptide catalyzed the folding; however, higher initial rates were observed for the *cis* isomer.[143,145] Finally, a cyclic AMPB-peptide **32** (Figure 22) was constructed with the Cys-Gly-His-Cys-Lys active-site motif of PDI incorporated. *Trans* to *cis* isomerization induced a conformational change in the cyclic peptide, going from an extended to a β-turn conformation, as observed by NMR (Figure 23).[146]

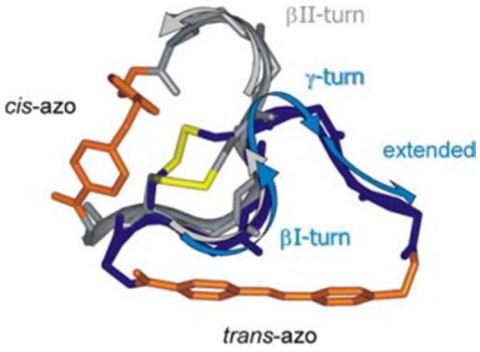

Figure 23. Overlay of the structure of the *cis*-**32** (gray backbone) and *trans*-**32** (blue backbone). The arrows highlight the structural elements. Reproduced with permission from ref 146. Copyright 2006 Elsevier B.V.

For further studies on the conformational and redox properties of cyclic peptides, presented in Figure 22, the reader is referred to a review by Moroder and co-workers.[147]

The kinetics of the photochemically controlled peptide folding processes were studied with femtosecond time-resolved UV/vis-spectroscopy for the following cyclic and bicyclic peptides: APB-peptides,[148] AMPB-peptides,[149] a water-soluble AMPB-peptide with the TRR sequence,[150] and AMPB-peptides with the PDI sequence[146] (Figure 22). These studies were recently reviewed in depth by Renner and Moroder.[23]

Ultrafast IR spectroscopy allowed for monitoring of structural changes upon photochromic isomerization in cyclic and bicyclic AMPB-peptides with TRR sequences. The study was based on the change in two characteristic IR bands: the amide I band (between 1625 cm^{-1} and 1725 cm^{-1}) reflected the carbonyl-stretching vibrations in the peptide backbone, and the amide II band (below 1630 cm^{-1}) reflected the structural changes of both the peptide and the chromophore (Figure 24).[151] The results obtained for **28** showed that the main

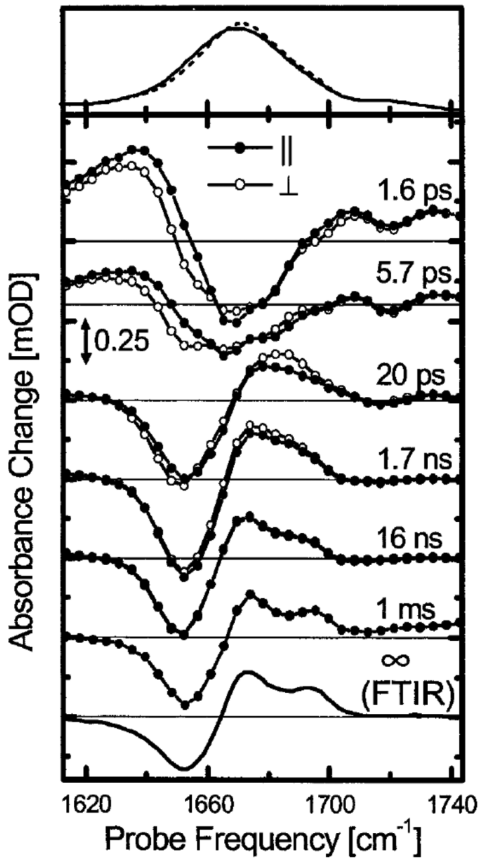

Figure 24. Absorption spectra of the *cis*-**28** (*Top*, solid line) and *trans*-**28** (*Top*, dashed line), transient difference spectra at selected delay times (*Middle*) and stationary *cis*−*trans* difference spectrum measured by the FTIR (*Bottom*). DMSO was used as a solvent. Reproduced with permission from ref 152. Copyright 2003 National Academy of Sciences, USA.

conformational changes of the backbone were completed after only 20 ps. However, equilibration of the entire peptide was not completed even 16 ns after irradiation (Figure 24).[149,151,152] These studies also showed that light-induced conformational rearrangements of the peptides could still be observed at temperatures below the freezing point of the solvent.[153]

The changes in IR spectra observed for the *cis* to *trans* isomerization of **27** closely resembled those of **28**.[154] Conformational relaxation of the peptidic portion was not completed even after 3 ns, and modeling studies predicted that it would require ~23 ns for the peptide to completely relax.[154] This contradicted the conclusions derived from the UV/vis spectroscopy study[148] and demonstrated IR spectroscopy to be more sensitive for detecting the structural relaxation events. Additional insight into the folding processes of the peptide backbone could be obtained with the use of isotope labeled

dx.doi.org/10.1021/cr300179f | *Chem. Rev.* 2013, 113, 6114−6178

azobenzene **35** (Figure 25a).[155] The labeling shifted the aromatic valence vibrations of the azobenzene out of the region in which the peptide vibrations are observed to 1576 cm^{-1} (Figure 25b).

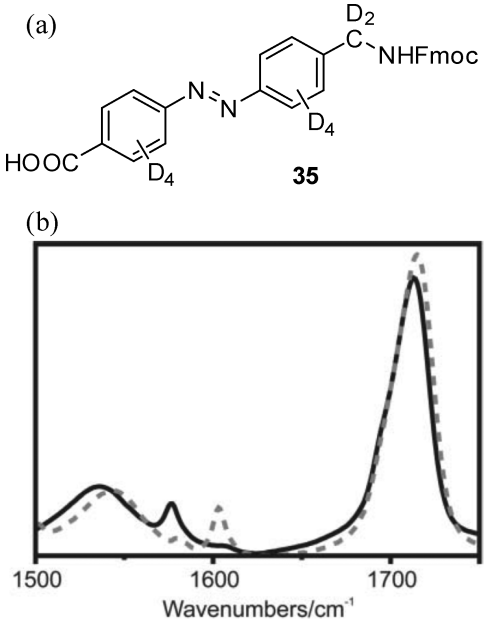

Figure 25. (a) Structure of D-labeled AMPB molecular photoswitch **35**. (b) FTIR spectrum of the $\nu_{C=C}$ stretching and amide I and II regions of **35** in DMSO (black line, spectral resolution 2 cm^{-1}) in comparison with the unlabeled sample (dotted line). Reproduced with permission from ref 155. Copyright 2008 The Royal Society of Chemistry.

Photocontrol of cell adhesion was illustrated with photoresponsive cyclic heptapeptide **33** (Figure 22).[156] The Arg-Gly-Asp (RGD) sequence is recognized by integrin cell-surface receptors of a large number of adhesive extracellular matrices, blood cells, and cell-surface proteins. Photocontrol of this ubiquitous recognition system for cell adhesion could be used to investigate or modify events of intermolecular adhesion.[157] The binding affinity of the cyclic azobenzene peptide **33** to immobilized $\alpha v\beta 3$ integrin was investigated with surface-plasmon enhanced fluorescence spectroscopy (SPFS) by attaching a fluorophore to the Lys side chain of peptide **33**. The conformationally more constrained *trans*-azobenzene-modified cyclic peptide showed a higher binding affinity for $\alpha v\beta 3$ integrin than the *cis* form (Figure 26). Shifting the position of the Lys residue (peptide **34**) was shown to reduce integrin affinity significantly. However, the difference in affinity between the *cis*- and *trans*-peptides increased by more than a factor of 2 and photomodulation of integrin affinity was more efficient for peptide **34** (Figure 26).[158]

Rück-Braun and co-workers synthesized a cyclic, AMPB-modified peptide derived from the binding site of the PDZ domain of neuronal nitric oxide synthase (nNOS) (Figure 27).[159] PDZ domains, approximately 90 residues long, are

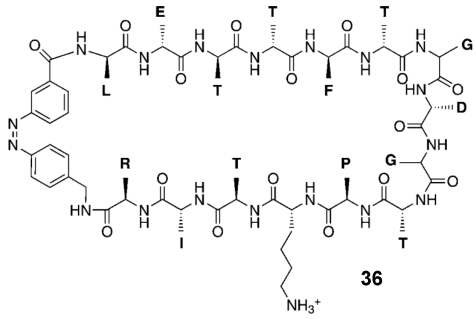

Figure 27. Cyclic peptide **36** is related to the β-finger peptide of nNOS with the added modification of an AMPB photoswitch.[159] Side chains are abbreviated by their one-letter codes for clarity, with the exception of the lysine side chain used for immobilization on a sensor chip. Reproduced with permission from ref 159. Copyright 2009 Wiley-VCH Verlag GmbH & Co. KGaA.

frequently encountered domains found in a diverse collection of signaling proteins that mediate protein−protein interactions.[160] The PDZ domain of nNOS heterodimerizes with the PDZ domain of α-1-syntrophin. The internal recognition motif, L-E-T-T-F, in the extended PDZ domain of nNOS is crucial for binding. α-1-Syntrophin is present in skeletal muscle, and its association with nNOS induces the production of second messenger nitric oxide (NO) for muscle contraction.[161] The cyclic AMPB-peptide **36** (Figure 27) adopted a β-hairpin structure analogous to the structure of the native protein enabling **36** to act as a light-controlled ligand. The peptide was immobilized *via* the Lys side chain on a chip to study the interactions of the switchable peptide with α-1-syntrophin. Surface plasmon resonance spectroscopy (SPR) revealed almost no binding for the purely *trans*-**36**, while photoisomerization to *cis*-**36** resulted in binding (K_D = 10.6 μM). The binding affinity of the *cis*-**36** was comparable to that of the unmodified model peptide (K_D = 5.4 μM).[159]

Recently it was shown that peptide **36** could also be used *in vivo* to photoregulate the contraction of muscle fibers when

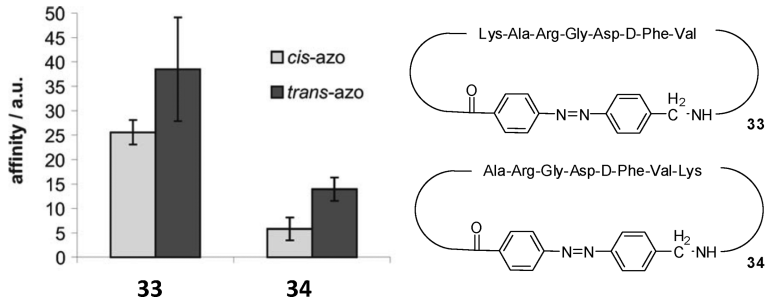

Figure 26. Affinity of two fluorescently labeled peptides **33** and **34** to surface-immoblized $\alpha v\beta 3$ integrin.[158] "*cis*" relates to the photostationary state with ~80% *cis*-azo isomer, and "*trans*" relates to the thermally relaxed molecule with 100% *trans*-azo isomer. Reproduced with permission from ref 23. Copyright 2006 Wiley-VCH Verlag GmbH & Co. KGaA.

dx.doi.org/10.1021/cr300179f | *Chem. Rev.* 2013, 113, 6114−6178

transfected to living cells.[32] A fluorophore (nitrobenzoxadiazole) was attached to the lysine residue to enable the visualization of peptide uptake into skeletal muscle fiber (Figure 28a), demonstrating that the modified peptide was

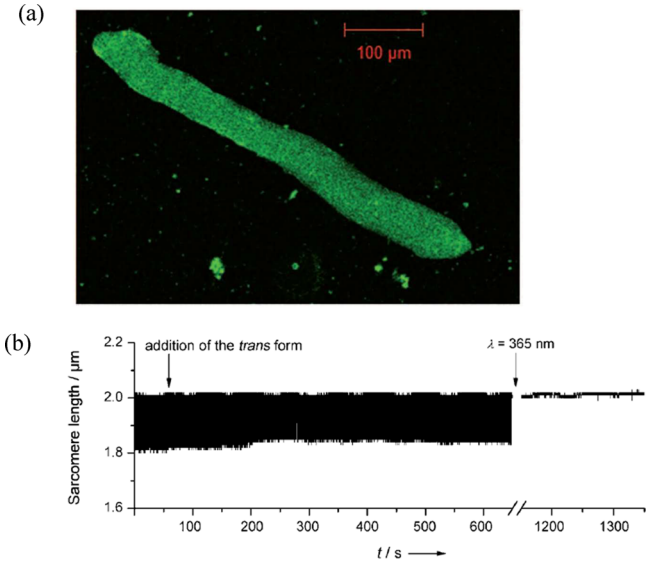

Figure 28. (a) Fluorescence-based visualization of the uptake of nitrobenzoxadiazole-labeled, photoswitchable peptide **36** into a single skeletal muscle fiber from *Flexor digitorum brevis* from three-month-old mice. (b) Recordings of sarcomere shortening in the presence of the *trans* form and after illumination at λ = 365 nm for 15 min. Reproduced with permission from ref 32. Copyright 2011 Wiley-VCH Verlag GmbH & Co. KGaA.

capable of crossing the membrane. C2C12 myotubes incubated with *trans*-**36** were shown to produce higher levels of NO than cells exposed to the peptide in the *cis* configuration.

The shortening of the sarcomere length of skeletal muscle fibers from the *Flexor digitorum brevis* (FDB) of three-month-old mice could be observed in the presence of **36** (Figure 27). FDB fibers were stimulated to contract at 1 Hz. Addition of the *trans*-isomer of the peptide resulted in no significant change in amplitude (Figure 28b). Illumination of the fibers at 365 nm reduced the amplitude. This effect was shown to be irreversible following attempted reisomerization of the photochromic unit in the peptide to the *trans* form. The authors hypothesize that the lack of reversibility could be explained by the loss of nNOS from the sarcolemma caused by the perturbation of syntrophin−nNOS interactions. This research constitutes a unique example of the use of a photoswitch-modified peptide for the control of physiological function, albeit not in a reversible way.

3.3.2. Photoresponsive Switches as Mimics of the β-Hairpin Motif. The stability of β-hairpins depends on the interaction between linked antiparallel peptide strands (i.e., hydrogen bonding and side chain−side chain interactions).[161−163] Ghadiri et al. have shown that the incorporation of an azobenzene photoswitch in a linear peptide could allow reversible switching between inter- and intramolecular hydrogen bonding (in *trans*- and *cis*-azobenzene-modified peptides, respectively) in which the chromophore functions as a β-turn element.[164]

Hilvert et al.[165,166] designed and synthesized a photoswitchable β-hairpin **37** (Figure 29) by replacing the turn residues D-Pro-Gly with an azobenzene switch in a 12-residue

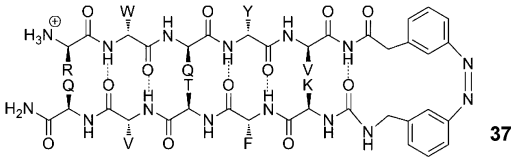

Figure 29. Model hairpin sequence **37** containing a *cis*-azobenzene (3-(3-aminomethylphenylazo)phenylacetic acid, AMPP) turn element with the hydrogen bonding pattern of the β-hairpin.[165−167]

peptide sequence derived from protein GB1[167] (Figure 29). MD simulations showed that [3-(3-aminomethyl)phenylazo]-phenylacetic acid (AMPP) linker would be the most promising conformational switch.[165] NMR spectroscopy revealed that *cis*-**37** adopted a well-defined β-hairpin structure resembling the model peptide. However, the azobenzene unit introduced more flexibility, affecting the intramolecular interactions between the two strands. Higher order aggregates were formed if the peptide was in a *trans* configuration. This peptide could be switched reversibly until the aggregates precipitated from solution.[166]

Subsequently, Hilvert and co-workers[168] inserted the same AMPP-azobenzene moiety in a 36 amino acid sequence, derived from avian pancreatic polypeptide (aPP), again by replacing the β-turn segment (Figure 30). The modified aPP

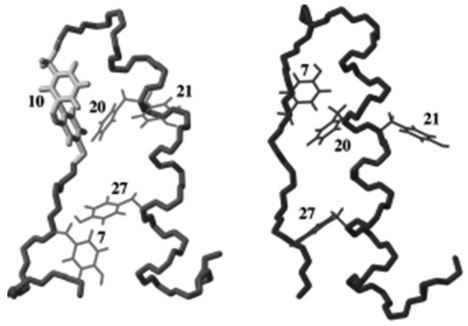

Figure 30. Backbone representation of the monomeric subunits of *cis*-AMPP-aPP (pancreactic polypeptide) (left) and aPP (right) including the side chains of aromatic residues. *cis*-AMPP is presented in light-gray. Reprinted with permission from ref 168. Copyright 2006 Wiley-VCH Verlag GmbH & Co. KGaA.

showed the same degree of helicity as the natural aPP, and reversible isomerization using light was observed. *cis*-AMPP-aPP was tetrameric in solution and adopted a back-folded structure (Figure 30), while *trans*-AMPP-aPP formed larger aggregates. The observed photoswitching between two different tertiary structures could be a promising approach for controlling larger and more complex peptide systems in the future.

Another route to obtain well-folded, highly stable β-hairpins proceeds *via* the inclusion of tryptophan (Trp) zippers in 12- or 16-residue peptides, as even two Trp-Trp pairs have been shown to stabilize β-hairpin formation.[169] Moroder and co-workers synthesized a photoresponsive β-hairpin peptide **38** based on the Trp zipper motif (Figure 31) and could control the degree of folding by irradiation of the incorporated AMPP chromophore.[170] Additional investigation with ultrafast UV pump, IR probe spectroscopy combined with MD simulations revealed the dynamics of the β-hairpin folding and unfolding process. *Trans* to *cis* isomerization of **38** was completed within picoseconds and resulted in the formation of a stable β-turn

dx.doi.org/10.1021/cr300179f | *Chem. Rev.* 2013, 113, 6114−6178

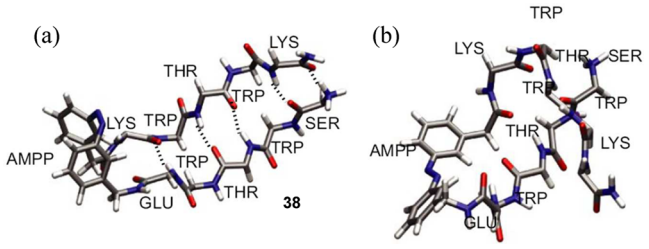

Figure 31. NMR-derived structures of (a) *cis*-**38** and (b) *trans*-**38**. Reprinted with permission from ref 171. Copyright 2007 National Academy of Sciences, USA.

structure in the peptide. However, the transition into a well-ordered hairpin required an additional 30 μs and was shown to be the rate-limiting step.[171]

Gogoll et al. incorporated a stilbene chromophore in peptides. Despite the intrinsic drawbacks of this photoswitch (see section 1.3.2), stilbene is an interesting alternative for the more common azobenzene, as stilbene is not as sensitive to reduction and *E*−*Z* photoisomerization is not thermoreversible.[172,173] The linear peptide sequence Leu-Leu-Val-Ile-D-Phe-Gly-Thr-Thr-Ala-Leu is known to fold into β-sheets and is present in the TATA-box-binding protein (TBP). TBP is a protein that binds to specific DNA sequences to initiate transcription and is active in cells and tissues throughout the human body.[174] The D-Phe-Gly β-turn inducer in the peptide sequence was replaced with a stilbene chromophore.[173] The observation of unfolded protein conformations for both the *E* and *Z* forms of the photoswitch indicated that switching did not induce β-hairpin formation.[173] An alternative peptide **39** (Figure 32), based on the Trp zipper motif, was used to

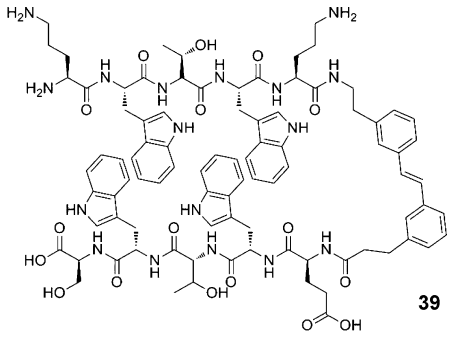

Figure 32. Model hairpin **39** based on a Trp(W) zipper motif containing a photoswitchable stilbene unit. Reprinted with permission from ref 175. Copyright 2009 Wiley-VCH Verlag GmbH & Co. KGaA.

overcome the lack of sufficient stabilizing forces between the peptide strands in the first system. NMR spectroscopy, translational self-diffusion studies, and CD spectroscopy on this second peptide sequence with the *Z*-isomer of stilbene allowed the observation of β-hairpin formation to a considerable extent, similar to the previous Trp zipper motif reported by Moroder.[170] Switching to the *E*-isomer in this case disrupted the β-hairpin motif.[175]

3.3.3. Additional Motifs with Switches in the Peptide Backbone. Gogoll et al.[176] expanded their study to a larger system, incorporating a stilbene chromophore into the turn region of an artificial hydrolase (HN1). The hydrolytic activity of HN1 depends on the spatial proximity of two helical segments, in particular the histidine amino acids in those segments (Figure 33). The catalytic activity of the photoresponsive peptide was determined using the hydrolysis of

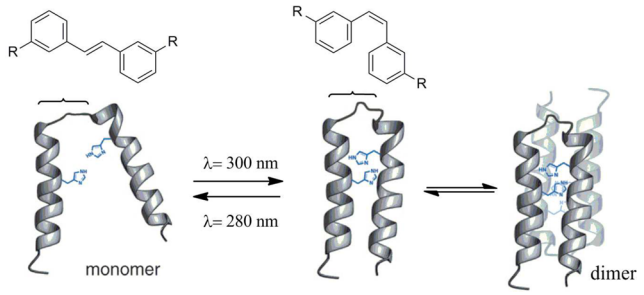

Figure 33. Schematic representation of the helical peptide HN1 and the photoisomerization of the incorporated stilbene chromophore. Reprinted with permission from ref 176. Copyright 2009 Wiley-VCH Verlag GmbH & Co. KGaA.

para-nitrophenyl acetate. The observed rate constants showed a 25% increase in activity for the Z isomer and a 12% decrease in activity for the *E* isomer compared to unmodified HN1. Isomerization of the stilbene unit to the Z-isomer was shown to induce dimerization of the peptides, changing the arrangement of the helical segments and, consequently, the catalytic activity.

A similar approach was used by Mascarenas and co-workers[177] to photoregulate the site-specific DNA binding affinity of a model peptide. Selected peptide segments were linked by an azobenzene moiety. These segments consisted of amino acids 226−248 from the basic regions (BR) of the yeast transcription factor GCN4, a well-studied bZIP (basic leucine zipper domain) protein known to recognize and bind DNA. For this study an additional Gly-Gly-Cys linker was placed at the C termini of the helices. *trans* to *cis* isomerization of the azobenzene unit in the peptide resulted in 60−70 times more efficient DNA binding by the GCN4 derivative. The peptide segments changed from a random coil to an α-helix structure upon DNA binding (Figure 34), which could be followed using

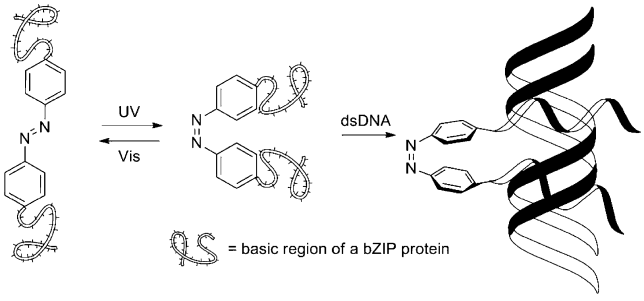

Figure 34. Schematic illustration of the *cis* to *trans* isomerization of the *azo*-peptide and the sequence-specific DNA binding of the *cis* form accompanied by a random coil to α-helix transition. Adapted with permission from ref 177. Copyright 2000 Wiley-VCH Verlag GmbH & Co. KGaA.

CD spectroscopy. Sequence-specific DNA binding could be controlled by irradiation with UV light. However, this process was shown to be irreversible due to the stability of the DNA−*cis*-azopeptide complex. Woolley et al.[178] subsequently achieved reversible binding/dissociation of azobenzene-modified GCN4-bZIP proteins, which will be discussed in the following section.

Another important biological recognition event is the interaction between an antigen and an antibody. Nakanishi et

dx.doi.org/10.1021/cr300179f | *Chem. Rev.* 2013, 113, 6114−6178

al.[179] used a hapten peptide (Glu-*azo*Ala-Gly_2) that carried an azobenzene switch at the amino acid side chain (similar to the approach described in section 3.2). The monoclonal antibody (Z1H01) was shown to reversibly bind and release the hapten peptide upon irradiation. Freitag et al.[180] demonstrated similar changes in antigen−antibody interactions between a FLAG-tag peptide and its analogs, with an azobenzene switch replacing three internal amino acid residues and monoclonal anti-FLAG-tag antibody M1.[180] Two specific azobenzene-bearing FLAG-tag peptide analogs showed significant differences in binding affinities, with the *cis* form approaching the value of the natural FLAG-tag peptide.

The introduction of molecular photoswitches has also been used to regulate zinc finger binding to DNA.[181] Zinc fingers are motifs that appear in transcription factors that can sequence-specifically bind double-stranded DNA. The folding of zinc fingers into the active $\beta\beta\alpha$ secondary structure is coupled with Zn^{2+} binding.[182]

A 59-amino acid photoresponsive double zinc finger, Sp1 (Figure 35), was prepared by conjugating an azobenzene

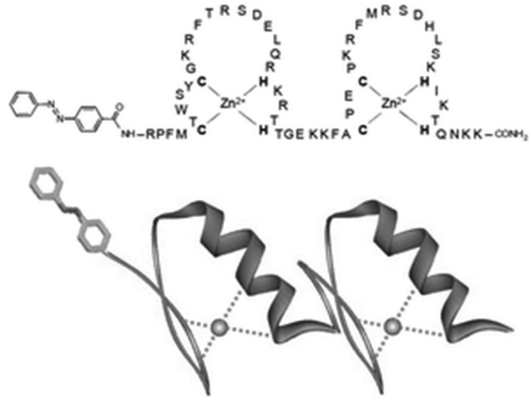

Figure 35. Sequence and proposed structure of a photoresponsive zinc finger motif. Reproduced with permission from ref 181. Copyright 2009 The Royal Society of Chemistry.

moiety to the *N*-terminus, which is known to recognize the GGGGCG DNA sequence. The ligation site was chosen due to the ease of modification as well as the proximity to the DNA-binding region.

Photoinduced *trans* to *cis* isomerization at λ = 365 nm took place efficiently, and it did not influence the α-helix folding structure according to CD measurements. Reisomerization back to the *trans* form, upon irradiation at >420 nm, proceeded with low conversion and could be brought to completion only after denaturation of the protein. The retarded reversible isomerization was explained by strong interaction of the *cis* form of the photochromic unit with the folded protein. The dissociation constants calculated by gel mobility shift assay were 0.73 ± 0.18 and 0.32 ± 0.08 μM for the *trans* and unmodified forms, respectively. The K_D value for the *cis* form could not be determined. To estimate the difference in the binding between the two photoisomers, the cleavage of a model DNA strand by the *AciI* restriction enzyme was studied. *AciI* is known to bind to the CCGC sequence of DNA. The activity of *AciI* can be inhibited by the native zinc finger Sp1. In the presence of the *trans* form of the photoresponsive zinc finger, no cleavage of DNA by *AciI* was observed. After irradiation, the affinity of the photoisomerized zinc finger to DNA was diminished and over 50% DNA cleavage was observed in 30 min. Considering the rise in interest in zinc finger proteins,[183] this approach provides a promising and simple methodology to control peptide binding to DNA.

Nakatani and co-workers[184,185] also investigated photocontrolled binding of a small photoresponsive peptide, KR-Az-R, where Az is AMPB (**40**, Figure 36), to RNA aptamers,

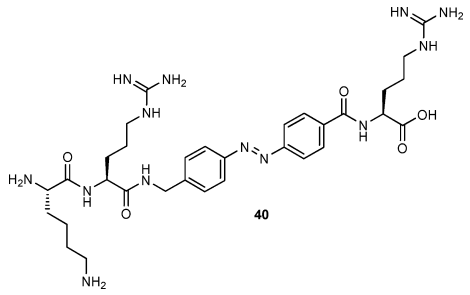

Figure 36. Photoresponsive peptide *trans*-KR-Az-R (**40**) used in the study of photocontrolled binding to RNA aptamers.[184,185]

aiming to control the activity of riboswitches by light. In KR-Az-R the AMPB moiety was flanked on both sides with arginine residues, which can interact with RNA by electrostatic interactions and hydrogen bonding. The *N*-terminal lysine residue was used to immobilize the photoresponsive peptide to an agarose gel. The RNA aptamer sequence was optimized by eluting random sequences through an agarose column containing immobilized KR-A-zR over eight cycles of selection. Three of the obtained RNA sequences were further characterized with respect to photocontrolled binding to KR-Az-R. The binding of RNA aptamer-19 to the peptide immobilized *via* the *N*-terminal lysine residue on the gold surface decreased by more than 90% upon *trans* to *cis* photoisomerization, as measured by SPR, and the effects were completely reversible. In a follow-up study,[185] another two cycles of RNA sequence selection were applied, followed by *in silico* analysis of the structure-binding relationship. The study revealed the secondary structure of the selected aptamers and showed that conserved residues were important for peptide binding.

Various photoresponsive peptide systems have shown the possibility of mimicking a β-turn upon irradiation and inducing the formation of folded conformations (i.e., β-hairpins). However, folded conformations are present in both isomers and larger conformational differences between the two isomers are desired to gain more control over the relative activities. The use of a more rigid switch or perhaps alternate switches could promote more dramatic conformational effects in future studies.[172,186,187]

3.4. Molecular Photoswitches as Amino Acid Side-Chain Cross-Linkers

The α-helix is an additional key structural element in peptides and proteins, including DNA binding motifs such as helix−turn−helix structures and leucine zippers. Such motifs are essential for many processes, including DNA replication, recombination, scission, and transcription.[188,189] Photocontrol of α-helical content in peptides and proteins could in essence offer photocontrol of gene modification and expression.

Woolley and co-workers achieved photocontrol over α-helix folding by introducing two cysteine (Cys) residues into peptides and cross-linking these with photoresponsive bridging unit **41** (Figure 37), an iodoacetamide-modified azobenzene.[190]

dx.doi.org/10.1021/cr300179f | *Chem. Rev.* 2013, 113, 6114−6178

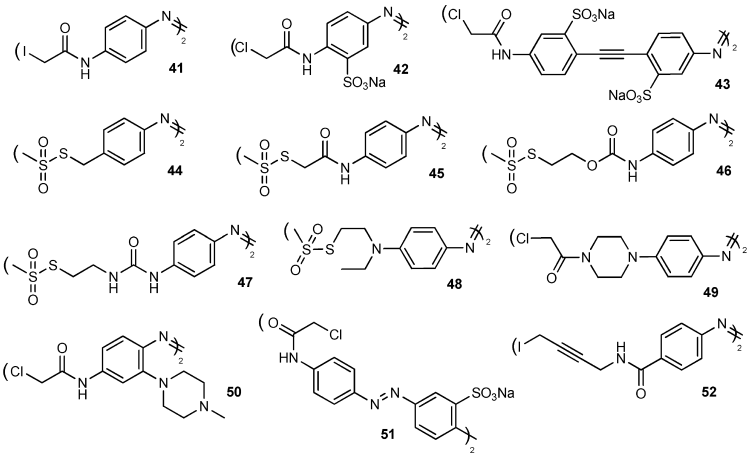

Figure 37. Selected molecular photoswitches used for the cross-linking of peptide side chains.[190,200−208]

The Cys residues were introduced at *i*, *i* + 7 spacing in the JRK-7 peptide to match the linker length of the switch in the *cis* conformation (Figure 38a and b). As indicated by CD

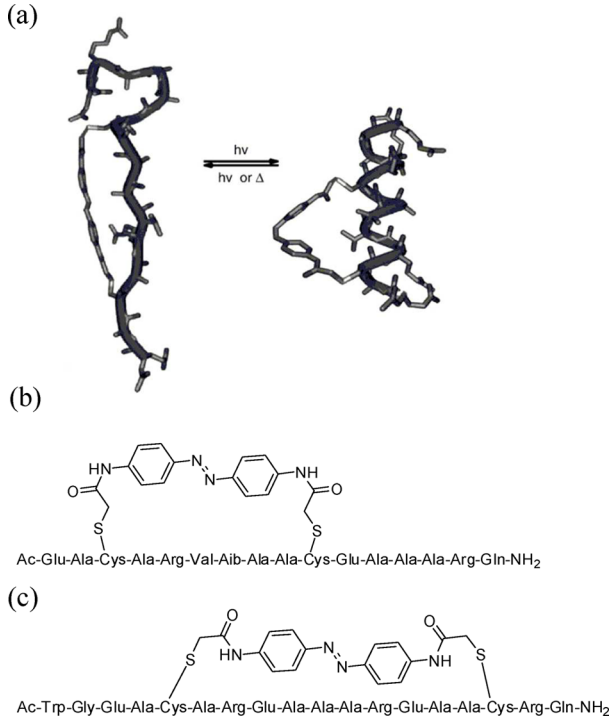

Figure 38. (a) Model showing the increased helicity induced in the JRK-7 peptide upon *trans* to *cis* isomerization of the attached azobenzene cross-linker **41**. Primary sequences of the cross-linked peptides: (b) JRK-7 (azobenzene reacted *via* Cys residues spaced *i*, *i* + 7); (c) FK-11 (azobenzene *via* Cys residues spaced *i*, *i* + 11). Reproduced with permission from ref 192. Copyright 2005 Elsevier B. V.

measurements, the isomerization of the azobenzene switch from the *trans* to *cis* configuration increased helical content from 12% to 48%. At first it was expected that steric interactions between residues *i* + 3, *i* + 4 and the cross-linking switch would influence the photosensitive behavior.[190] However, altering these two residues showed that steric interactions did not seem to have a large effect on the conformational transition.[191]

Alternative Cys spacing was also investigated in this study. Peptides with *i*, *i* + 4 spacing behaved similarly to the JRK-7 peptides described, and peptides with *i*, *i* + 11 spacing (FK-11, Figure 38c) showed the reverse behavior, with significant helical content for the *trans* isomer (66%).[193] The possibility to alter the spacing of the cross-linking positions allowed additional control over the peptides. It was shown to be advantageous to have the dark-adapted, >99% *trans* state as the inactive state of the system. The isomerization to the *cis* form then resulted in the largest change in activity. To further increase the versatility of the approach, a procedure was developed to calculate the approximate distance between Cys sulfur atoms in noncross-linked peptides to determine which linkers would fit in the S−S distance and stabilize/destabilize α-helix formation.[194]

Kinetic measurements on JRK-7 and FK-11 azobenzene **41** cross-linked peptides (Figure 38), using time-resolved ORD and IR techniques, showed fast isomerization of the azobenzene photoswitch moieties (picoseconds), while peptide folding/unfolding occurred at the 100 ns to 1 μs time scale.[195,196] The folding and unfolding kinetics were shown to be strongly dependent on temperature, and lower temperatures resulted in higher helical content but slower (un)folding rates.[196,197] Single $^{13}C{=}^{18}O$ isotope labeling provided further insights into the rates of hydrogen bond formation for the α-helix structure.[198] Two-dimensional IR spectroscopy on single site $^{13}C{=}^{18}O$ isotope-labeled peptides proved to be a useful method to measure the extent of hydrogen bonding at any given position along the helical peptide and allowed examination of the local folding behavior in photoresponsive peptides.[199]

The practicality of compound **41** as a cross-linker was limited by its poor water-solubility and the short half-life of the *cis* form (~12 min at 25 °C). Addition of sulfonate groups to the aromatic rings of the azobenzene chromophore at the *meta* position (compound **42**, Figure 37) increased the water solubility. The FK-11 peptide was cross-linked with the new, sulfonated switch and showed similar conformational behavior to that of the original photoresponsive peptide, with a longer half-life of 35 min.[200] Thus, an extended and more rigid, water-soluble azobenzene cross-linker **43** (Figure 37) was prepared in an attempt to generate larger conformational changes in the peptide upon isomerization. However, irradiation of the switch at 400 nm at room temperature yielded only small amounts of the *cis* isomer and induced only small conformational changes in the model peptides.[201]

dx.doi.org/10.1021/cr300179f | *Chem. Rev.* 2013, 113, 6114−6178

An additional series of methanethiosulfonate (MTS)-bearing azobenzene cross-linkers **44**−**47** (Figure 37) provided a large range of thermal stabilities of the *cis* isomer.[202] FK-11 peptides were cross-linked with MTS-alkyl-, -amide-, -carbamate-, and -urea-azobenzenes, and half-lives for the *cis* to *trans* isomerization process ranged from 43 h to 26 s, respectively (Table 4).[202] The MTS-dialkylaminoazobenzene **48** showed both a considerable red-shift of the absorption and extremely short half-lives for *cis* cross-linked JRK-7 and FK-11 peptides (Table 5, entry 1).[203] The introduction of a piperazine substituent at the azobenzene unit (compound **49**, Figure 37) resulted in a shift to shorter wavelengths relative to the related azobenzenes bearing acyclic substituents along with longer half-lives of thermal isomerization (Table 5, entry 2).[204] Finally, a series of *ortho*-amino-substituted azobenzenes was synthesized allowing for photoswitching at longer wavelengths ranging from 435 up to 530 nm (morpholine to pyrrolidine) and thermal relaxation on time scales of seconds to minutes (Table 5, entry 3). Moreover, these photoswitches showed enhanced resistance to reduction because of the electron-rich nature of the azobenzenes.[205]

Table 4. Absorption Wavelength of the *trans* Isomer and Thermal Relaxation Half-Lives of *cis*-Azobenzene Cross-Linked FK-11 Peptides in 5 mM Phosphate Buffer at 25°C.[202]

entry	photoswitch	λ_{max} (nm)	$\tau_{1/2}$
1	**44**	342	43 h
2	**45**	366	8 min
3	**46**	372	96 s
4	**47**	382	26 s

Table 5. Absorption Wavelength of the *trans* Isomer and Thermal Relaxation Half-Lives of *cis*-Azobenzene Cross-Linked Peptides

entry	photoswitch	λ_{max} (nm)	$\tau_{1/2}$
1	**43**	400	53.9 min (i, i + 14),[a] 37.2 min (i, i + 21)[a]
2	**48**	480	0.0065 s,[a] 12.1 s[b] (JRK-7); 0.076 s,[a] 8.2 s[b] (FK-11)
3	**49**	400−450	190 s (JRK-7),[b] not (FK-11), 15 s (i, i + 14),[b] 11 s (i, i + 15)[b]
4	**50**	437	∼300 s (JRK-7)[a]
5	**51**	365	12.6 min (i, i + 11), 10.6 min (i, i + 14), 29.1 min (i, i + 19), 16.0 min (i, i + 21)

[a]Aqueous phosphate buffer, pH 7.0, 25 °C. [b]50% MeOH in aqueous phosphate buffer, pH 7.0, 25 °C.[200,201,203−206]

Moroder and co-workers demonstrated photoresponsive folding and unfolding of triple-helix structures in collagen model peptides. The sequence Ac-(Gly-Pro-Hyp)$_n$-Gly-X-Hyp-Gly-Pro-Hyp-Gly-Pro-X-(Gly-Pro-Hyp)$_m$-Gly-Gly-NH$_2$ (Hyp = hydroxyproline) was chosen for the model peptide, as the tripeptide unit Gly-Pro-Hyp is known to stabilize the triple helix structure.[207,208] In the initial approach,[208] mercaptoproline residues (X) were incorporated in the sequence (n, m = 2) and cross-linked with an azobenzene chromophore **52** (Figure 37). *Trans* to *cis* isomerization at ambient temperatures unfolded or distorted the triple-helix structure, and thermal relaxation induced refolding. Subsequently, an approach analogous to that followed by Woolley and co-workers (X = Cys),[190] was used to cross-link the peptide sequence (n = 3, m = 5) with the azobenzene chromophore (Figure 39). Unfolding in response to photoinduced isomerization of the triple helix was limited and only observed in the region spanned by the azobenzene switch.[207] Additional folding studies and further investigation into the optimal peptide sequence and structure of the switch may be required to improve the photoresponsive effect.

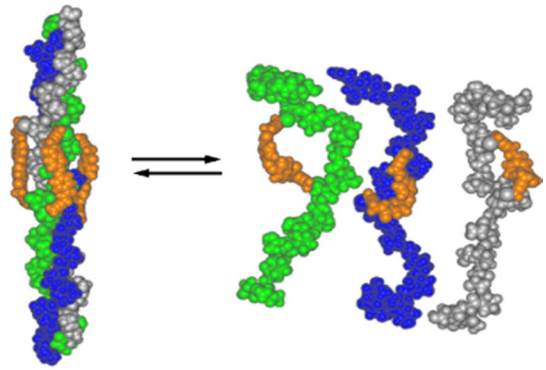

Figure 39. Schematic illustration of the unfolding/distortion of triple-helix structure upon *trans* to *cis* isomerization. Reproduced with permission from ref 208. Copyright 2006 Wiley-VCH Verlag GmbH & Co. KGaA.

Photocontrol over helix formation *via* side-chain cross-linking with a biofunctional photochromic residue has been taken a step further to control a biological process, exemplified here by the study on an 18-residue peptide sequence HDH-3 containing DNA binding residues. Cross-linking i, i + 11 Cys residues in the HDH-3 peptide with an azobenzene switch **42** (Figure 37) resulted in DNA binding by the α-helix with high affinity and specificity (to the known QRE sequence) when the switch was in the *trans* configuration. Photoisomerization to the *cis* isomer prevented the formation of an α-helix structure between the Cys residues and significantly reduced the binding affinity of the helix to DNA (Table 6).[209]

Table 6. DNA Binding Parameters for HDH-3, Dark Adapted -HDH-3, and Irradiated -HDH-3 (ref 209)[a]

	K_D (nM)		
	QRE	ERE	MCK-S
dark-adapted HDH-3	7.5 ± 1.3	140 ± 11	>6000
irradiated HDH-3	140 ± 25	160 ± 15	>6000
native HDH-3	200 ± 11	175 ± 16	n.d.

[a]Sequences: QRE = 5′-CGCAGTGTAATCCCCTCGAC-3′; ERE = 5′-CGCAGTGTAATTACCTCGAC-3′; MCK-S = 5′-CAGGCAG-CAGGTGTTGG-3′.

Another photoactive DNA-binding peptide, from the group of Woolley, was based upon the introduction of an azobenzene-derived cross-linker **42** (Figure 37) into the DNA-recognition helix of the muscle-specific transcriptional activator MyoD.[21]

MyoD is produced in various cell types and relies on the dimerization of a basic helix−loop−helix (HLH) domain for DNA binding (Figure 40a). Cysteine residues were introduced into positions 116 and 123 of MyoD and cross-linked, in i, i + 7 spacing, with 3,3′-bis(sulfonato)-4,4′-bis(chloroacetamido)-azobenzene (BSBCA), to give photochemically active MyoD

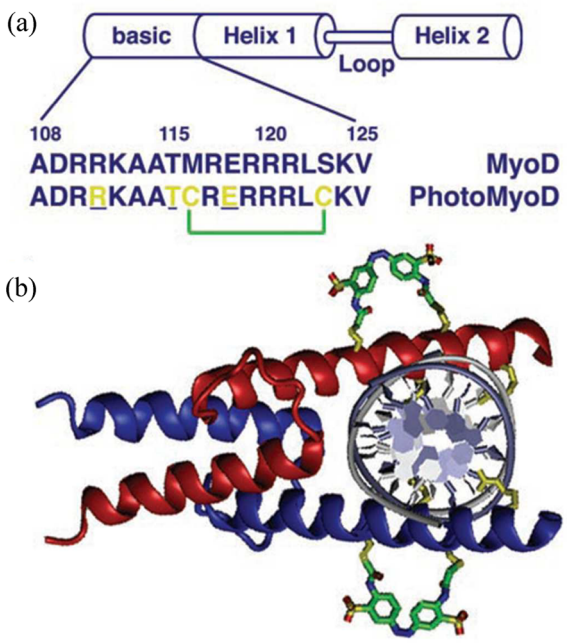

Figure 40. Reinforcing the native structure of DNA-recognition elements. (a) Structures of MyoD and PhotoMyoD. (b) Model of the complex between DNA and *cis*-photo-MyoD. Reprinted with permission from ref 210. Copyright 2005 Wiley-VCH Verlag GmbH & Co. KGaA.

(photo-MyoD). Both the non-cross-linked and the *trans*-photo-MyoD existed predominantly in a random coil conformation, which is typical for the parent domain that adopts a helical conformation only upon DNA binding. Irradiation at 360 nm gave a PSS with 61% of *cis* isomer (determined by HPLC), resulting in increased helicity in the region spanned by the cross-linker, as determined by CD spectroscopy.[210] The affinity of different forms of MyoD was measured with MCK-S oligonucleotide, which includes the MyoD recognition sequence, "E-box" (CAGGTG). The K_D values for *trans*-photo-MyoD and non-cross-linked-MyoD were similar (1.5 ± 0.38 and $0.88 \pm 0.22 \times 10^{-14}$ M^2, respectively). The stability of the complex increased by 3 orders of magnitude following the photoisomerization of the *trans* form to the *cis* form ($K_D = 4.4 \pm 0.16 \times 10^{-18}$ M^2). This constitutes an interesting approach based on reinforcing the native structure of DNA-recognition elements.

After establishing the precedence for photocontrol of coiled coil interactions in a leucine zipper peptide GCN4-p1,[211] Woolley et al. studied the reversible binding-dissocation of azobenzene-modified GCN4-bZIP proteins to the AP1 transcription factor binding site in DNA (5′-TGACTCA-3′, Figure 41).[178] The azobenzene photochromic unit **42** (Figure 37) was introduced by cross-linking Cys residues at positions 262 and 269 within a bZIP domain. The *trans* form of the azobenzene destabilized the helical structure of the coiled-coil region of GCN4-bZIP, resulting in lower DNA binding affinities. *trans* to *cis* photoisomerization resulted in a substantial increase of helical content and a 20-fold increase in DNA-binding affinity as measured by kinetic capillary electrophoresis. This process was fully reversible upon thermal isomerization of the azobenzene unit. Further adaptation to this system could be considered (i.e., location, spacing or number of cross-linked azobenzenes) to obtain an even larger change in DNA binding affinities.

A similar system that allows for the photocontrol of AP1 transcription factor activity was recently reported (Figure 42a).[212] AP1 is formed by dimerization of CJun and CFos proteins. Photoswitchable cross-linker **42** was introduced into AP-1 dominant, negative peptide AFosW, allowing photocontrol over helicity. Helical AFosW inhibits the heterodimer cFos/cJun binding to DNA, but it is inactive in the unfolded state (Figure 42a). As a result, the photoswitching between the two states could allow for control over the activity of AP1 in a living cell.

Azobenzene-modified AFosW (XAFosW) was transfected into HEK293T cells, in which the luciferase reporter was under the control of an AP-1 promoter. Activity ratios of luciferase and β-galactosidase, the latter being under the control of a constitutive promoter, were used as an indication of specific inhibition of AP-1 activity (Figure 42b). Unmodified AFosW was used as a control. The activity of AP1 was shown to decrease by 40% upon irradiation. This effect was observed only for azobenzene-modified AFosW. Flow cytometry-based determination of living/dead cells ratio's excluded possible effects of UV phototoxicity. Ease in uptake of XAFosW, combined with the diversity of the colied coil targets, renders this approach a general strategy for the effective control of a broad range of activities in living systems.

Another interesting example showed photocontrolled peptide binding to Bcl-x_L (B-cell leukemia) proteins, which are overexpressed in many cancer cells and inhibit apoptosis. The photoresponsive peptides were based on the Bcl-x_L-binding Bak and Bid proteins. The azobenzene switch **42** (Figure 37) was

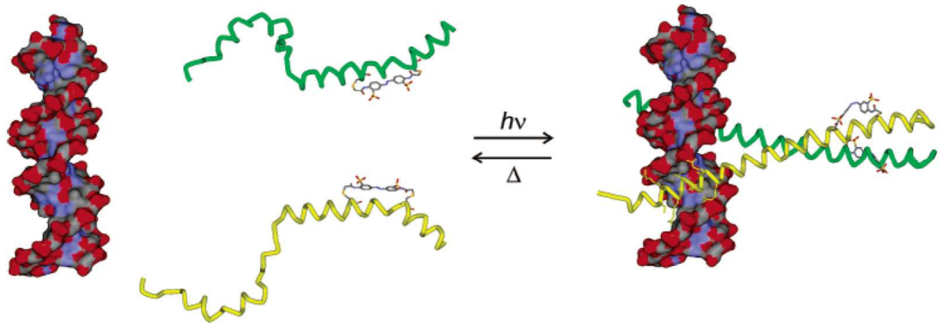

Figure 41. Models showing the photocontrol of DNA binding by *azo*(*i*, *i* + 7) GCN4-bZIP. In the *trans* conformation, the cross-linker induces a bend in the helix, which destabilized folding and consequently DNA binding (left). In contrast, the *cis* conformation of the cross-linker is compatible with zipper formation and thus DNA binding (right). Reprinted with permission from ref 178. Copyright 2006 American Chemical Society.

dx.doi.org/10.1021/cr300179f | *Chem. Rev.* 2013, 113, 6114–6178

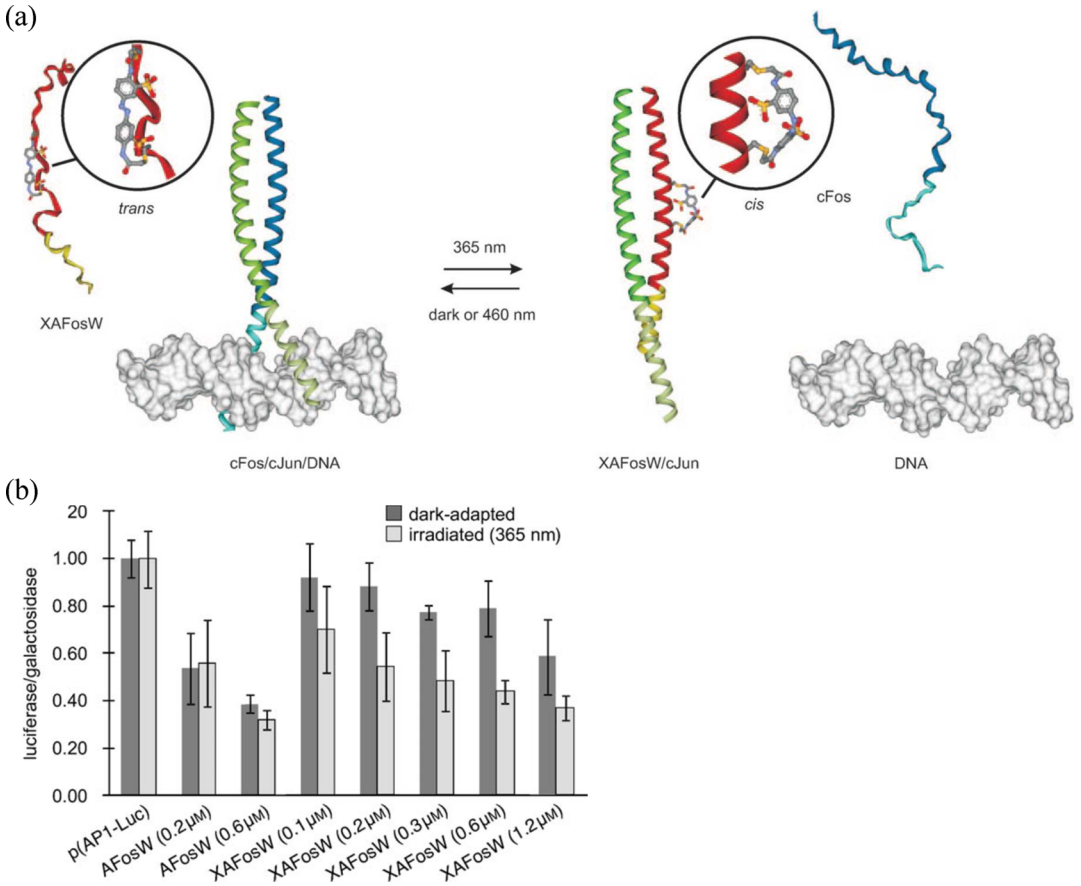

Figure 42. (a) Photocontrolled enhancement of helicity in an azobenzene-cross-linked, AP-1 dominant negative peptide XAFosW results in coiled-coil formation with cJun protein, thereby inhibiting DNA binding. (b) Effect of photoirradiation on cellular AP-1 activity in XAFosW-transfected cells. Reprinted with permission from ref 212. Copyright 2010 Wiley-VCH Verlag GmbH & Co. KGaA.

used as a cross-linker in three different examples at *i*, *i* + 4, *i*, *i* + 7, and *i*, *i* + 11, respectively. The *trans* configuration of the azobenzene units in Bid^{i+4} and Bak^{i+7} destabilized the helix structure, preventing binding to Bcl-x_L. Photoisomerization of the switch to this *cis* form resulted in a 20-fold increase of the binding affinity of Bid^{i+4} and Bak^{i+7}. However, the photoisomerization of the azobenzene in Bak^{1+11} had little effect on binding affinity (Table 7).[213]

Table 7. Dissociation Constants to Bcl-x_L for Three Different Unmodified and *azo*-Modified Peptides[213,207]

	K_D (nM)		
peptide form	$Bak^{i+7}{}_{72-78}$	$Bak^{i+11}{}_{72-87}$	$Bid^{i+4}{}_{91-111}$
parent	134 ± 16	328 ± 19	117 ± 48
dark-adapted	825 ± 157	21 ± 1	1275 ± 139
irradiated	42 ± 9	48 ± 10	55 ± 4

An alternative approach for the introduction of azobenzene-based photochromic cross-linker into peptides has been reported recently by Beyermann and co-workers.[214] This methodology relies on the introduction of vinyl-azobenzene-substituted amino acids, dubbed photoswitchable click amino acids (PSCaa), into the sequence of the peptide, during solid phase peptide synthesis. Additionally, cysteine residues were introduced in the *i* + 4 position, enabling cross-coupling with the vinyl group of the PSCaa *via* a light-induced thiol−ene reaction (Figure 43). This approach results in the selective

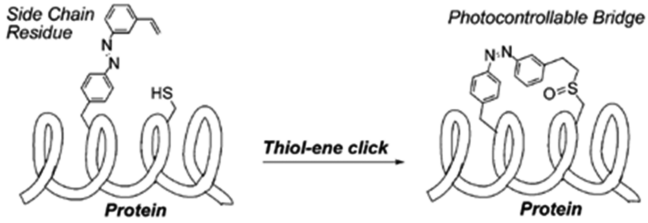

Figure 43. Cross-linking of amino acid residues using the thiol-click reaction. Reprinted with permission from ref 214. Copyright 2012 Wiley-VCH Verlag GmbH & Co. KGaA.

formation of a photoresponsive bridge within a peptide and can therefore be used *in vivo*. This is an advantage as compared to the methods relying on cross-linking with activated compounds **41**−**52** (Figure 37), which may react nonspecifically with other reactive thiols present in the cells.

This methodology was used for the control of the α-helix formation in an artificial helical linker that connected the two binding sites of urocortin-1 (Ucn). Ucn is an endogeneous peptide that targets the CRF-R1 receptor responsible for the response to stress and is involved in numerous diseases.[215] The cross-linked peptide elicited a disorded conformation that switched to the α-helix upon photoisomerization of the azobenzene unit to the *cis* state following the irradiation at λ = 360 nm. The hybrid system, composed of the *C*- and *N*-terminal Ucn binding sites connected with the photoresponsive azobenzene unit, has been shown to be roughly ten times more

dx.doi.org/10.1021/cr300179f | *Chem. Rev.* 2013, 113, 6114−6178

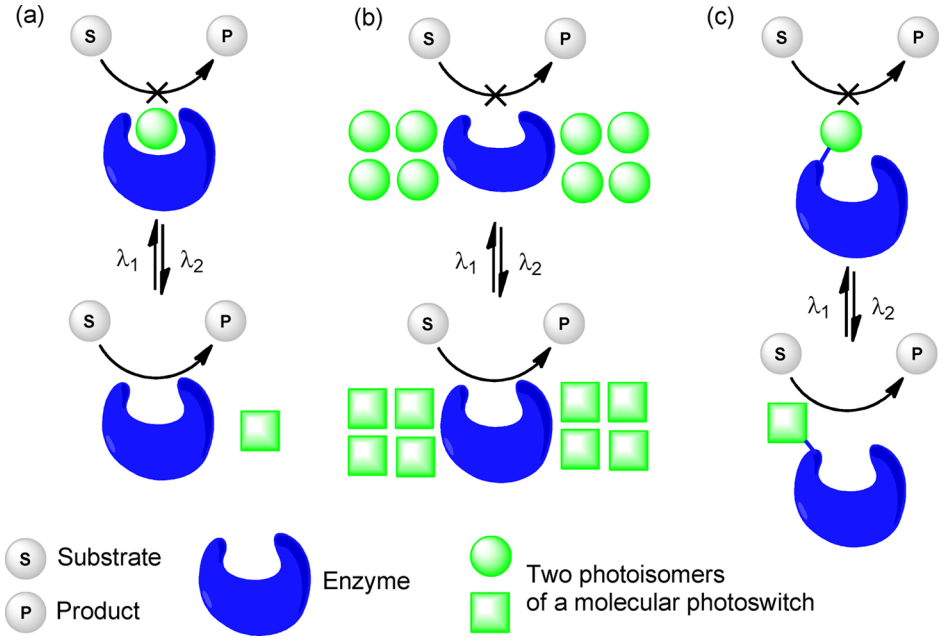

Figure 44. Three general strategies for the preparation of enzymes with photocontrolled activity: (a) The use of photoswitchable inhibitors; (b) application of photoresponsive environments; (c) direct incorporation of molecular photoswitches into the protein.

efficient in inducing the receptor activation in the *cis* form as compared with the nonirradiated sample, although the activity was 4 orders of magnitude lower than that of unmodified Ucn.

The helical structures discussed here illustrate the progress in the understanding of photocontrol of peptides. It is also evident that the introduction of a photoswitchable unit by cross-linking holds great promise, as this approach retains the modularity inherent in peptidic systems. That is, the photoswitchable unit can be inserted in a number of sequences and at a number of positions without disturbing folding until the proper wavelength of light is used. We eagerly await attempts at applying these photoactive and biologically relevant hybrid systems in living organisms.

3.5. Concluding Remarks

The application of the first of the methods described here, i.e. the preparation of peptide polymers with photoresponsive amino acid residues, demonstrates the feasibility of photocontrolling peptide structures by switching photochromic molecules. The effect of the photoisomerization on the peptide backbone is, however, usually small and depends heavily on the experimental conditions (solvent, pH, temperature) and number of chromophores present. Furthermore, the use of photoactive peptides in a biological context is limited so far, as these approaches seem to be focused more toward the applications in material sciences.

Incorporating a photochromic switch in the backbone of a peptide or by cross-linking the side chains of a peptide resulted in more dramatic photoresponsive effects on peptide conformation. The most relevant structures in proteins (α-helix, β-turn, β-hairpin) could be induced or distorted upon irradiation of a photoswitch incorporated in the peptide. Moreover, the approaches allowed for time-resolved ORD-, IR-, and UV-studies showing, in most cases, an initial fast photoisomerization of the chromophore followed by a considerably slower reorganization of the peptide backbone. These approaches also retain the modularity inherent in amino acid-based systems, allowing for the chromophore to be introduced at a number of positions with a range of structural effects.

A long-term goal of producing efficient light-sensitive peptides is complete photocontrol of conformation, allowing for "on−off" switching of biologically relevant molecular recognition events. This could enable scientists to investigate the role of certain proteins in living systems or to create photoresponsive biomaterials, such as light induced cell adhesion on surfaces. However, switching between completely ordered and disordered peptides has been shown to be challenging, though many of the above systems are very well-behaved. The effects of limited conformational control on peptide interactions in living systems remain to be seen. The use of additional switchable units could induce larger conformational changes, though it can be complicated to introduce these units without disrupting the proper peptide conformation too much.

Alternative photoswitches are also needed in order for the photoresponsive peptides to be more useful for *in vivo* applications. Irradiating cellular systems with UV light, for instance, can lead to unwanted side reactions such as DNA cross-linking. The use of longer switching wavelengths, such as near-infrared, will be necessary for deeper penetration of tissues. The reducing intracellular environment and the possibility of proteolysis must also be taken into consideration, as these kinetic events may be difficult to foresee.

Therefore, more efficient molecular switches could be designed and investigated, and hemithioindigo switches,[187] overcrowded alkenes,[216] or the improved azobenzenes discussed in this review seem to be the most promising follow-up candidates.

4. PHOTOREGULATION OF ENZYMATIC ACTIVITY

Biocatalysts with light-regulated properties have many potential applications, which stem mainly from the possibility of controlling enzymatic activity with high spatial and temporal resolution. These applications include the following: signal

dx.doi.org/10.1021/cr300179f | *Chem. Rev.* 2013, 113, 6114−6178

amplification, diagnostics, biosensoring, optobioelectronics, affinity separations, and photodynamic therapy.

In the following section, an overview of the methods for the preparation of light-addressable biocatalysts and the photocontrol of enzyme function will be presented, focusing on three general methods:[1] the use of photoswitchable enzyme inhibitors (section 4.1, Figure 44a), the embedding of proteins in photoresponsive environments (sections 4.2 and 4.3, Figure 44b), and the incorporation of molecular photoswitches into the structure of biocatalysts (sections 4.4 and 4.5, Figure 44c).

4.1. Photoregulation of Enzyme Function by Photoswitchable Inhibitors and Activators

The activity of enzyme effectors depends strongly on their structure and conformation, which influence the strength of their interactions with the proteins. By incorporating molecular photoswitches into enzyme effectors (i.e., inhibitors and activators), it is possible to alter enzyme properties with light, thus altering activity. This part of the review focuses on the more recent implementations of this approach (since the year 2000), with selected earlier examples. For attempts at regulating enzyme activity with photoswitchable effectors prior to 2000, the reader is referred to an earlier, extensive review by Willner and Rubin.[1]

Two main strategies were used in the design of photoswitchable enzyme effectors (Figure 45). One of them relies on

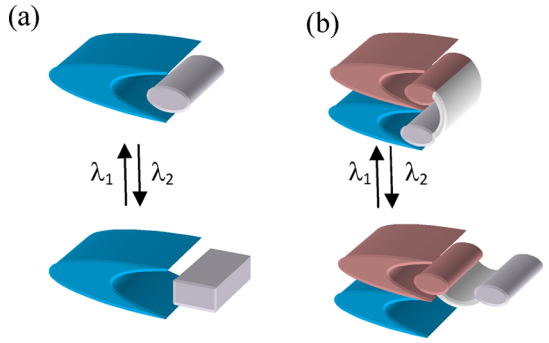

Figure 45. Schematic representation of the two main strategies used in the design of photoswitchable effectors (gray) of enzymes (blue).

the incorporation of a photochromic moiety into the structure of a known effector (Figure 45a). The photoisomerization would then change the properties of the compound, thereby changing its interactions with the target protein. The second approach (Figure 45b) is applicable in the situations where two ligands within the effector interact with two binding sites in the target. Introduction of a photoisomerizable linker between the ligands enables photocontrolled changes in the distance and alignment between the active groups and, thus, results in changes in the effector activity.

The prospect of using photoswitchable inhibitors of the first type (Figure 45a) was recognized as early as in 1969, with a series of reports from the group of Erlanger on the photoregulation of various enzymes. The initial research[221] focused on the use of compound **53** (Figure 46), a photoswitchable inhibitor of acetylcholinesterase (AChE, E.C. 3.1.1.7). The design of **53** was based upon a known reversible AChE inhibitor **54**[222] (Figure 46), that contains trimethylammonium ion in its structure. Both photoisomers of **53** were shown to be active as AChE inhibitors. The differences in activity, albeit reproducible and reversibly addressable, did not

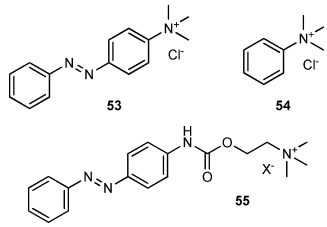

Figure 46. Photoswitchable and model inhibitors of AChE.

exceed 20%, with the *trans* isomer being a slightly more potent inhibitor.[221] These results were followed up with a study on using sunlight and darkness for photocontrolling AChE activity with compound **55** (X = I) and a discussion on possible biological implications of this phenomenon.[223]

In a follow-up report,[224] the group of Erlanger used AChE inhibitors **53** and **55** (X = Cl) for the photoregulation of the electric potential difference across the excitable membrane of cells from the electric organ of electric eels. This membrane undergoes depolarization in response to carbamylcholine. This interaction is inhibited by compounds **53** and **55**. For both compounds **53** and **55**, the *trans* isomer was more efficient as an inhibitor, since at a given concentration the loss in depolarization is considerably higher than in the case of the *cis* form. The control experiments ruled out the influence of irradiation on the membrane in the presence of carbamylcholine. This research was one of the first examples of directly affecting a biologically relevant system with the use of photochromic molecular switches.

An attractive approach to photoregulating enzymatic activity with a photoswitchable cofactor molecule was reported by Sisido and co-workers.[225] In this method, a photochromic NAD^+ (nicotinamide adenine dinucleotide) analog **56** (Figure 47a) and its reduced form bound reversibly and with photocontrollable affinity to an NAD^+-specific monoclonal antibody. Using light, these compounds could therefore be efficiently and reversibly removed from the reaction system. This system was used for the control of a bienzymatic redox reaction, in which an alcohol dehydrogenase (ADH) oxidizes ethanol using **56** as a cofactor. The reduced cofactor was regenerated by the diaphorase-catalyzed reduction of blue 2,6-dichlorophenol-indophenol sodium salt, which yields a colorless product, allowing for the spectroscopic monitoring (Figure 47b).

When compound **56** was in its *trans* state, binding to the antibody was very strong and no conversion was observed in the enzymatic reaction. Photoisomerization to the *cis*-**56** state recovered 72% of the activity as compared to a reaction without the antibody added, and this phenomenon was shown to be reversible.[225] This system, while demanding in terms of antibody preparation, is promising due to the very high influence of photoirradiation on the observed biological activity.

Proteases are enzymes that have been targeted the most with photoswitchable inhibitors. These approaches began in the early nineties with reports from Smith and co-workers.[226] Bifunctional compounds **57** and **58** (Figure 48), which consist of a photochromic portion and a recognition moiety (aldehyde or boronic acid) known to bind reversibly to the enzyme active site, were prepared and used as photoswitchable inhibitors of papain (E.C. 3.4.22.2), α-chymotrypsin (E.C. 3.4.21.2), and subtilisin (E.C. 3.4.21.62). The results are summarized in Table 8.

dx.doi.org/10.1021/cr300179f | *Chem. Rev.* 2013, 113, 6114–6178

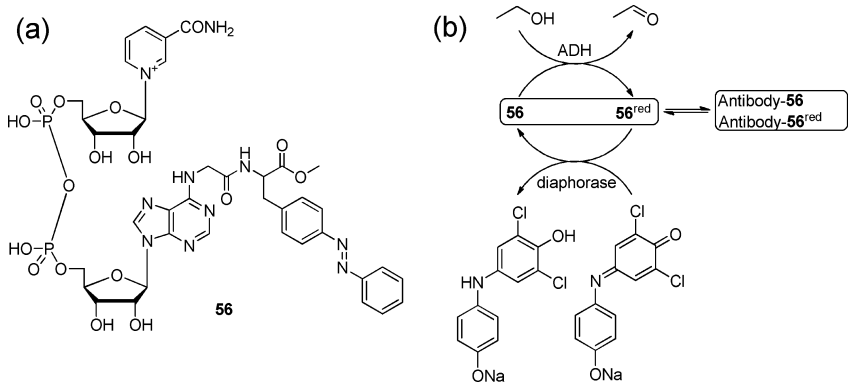

Figure 47. Photocontrol of enzymatic acitivity by changing affinity of a photoswitchable cofactor to an antibody:[225] (a) the structure of cofactor **56**; (b) bienzymatic catalytic system.

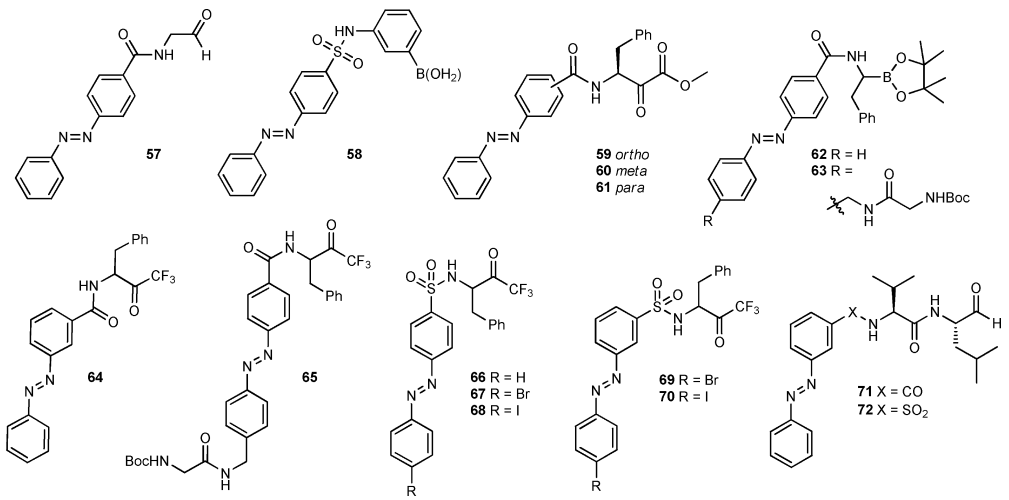

Figure 48. Photoswitchable inhibitors of proteases.[226−230]

Table 8. Photocontrolled Inhibition of Proteases

entry	enzyme	inhibitor	K_i *trans*	K_i*cis*	*trans* PSS	*cis* PSS	ref
1	papain	**57**	2.1 μM	8.8 μM	not given	83%	226
2	α-chymotrypsin	**58**	11 μM[a]	41 μM[a]	not given	80%	226
3	subtilisin	**58**	0.9 mM[a]	1.4 mM[a]	not given	80%	226
			0.5 mM[b]	0.3 mM[b]			
4	α-chymotrypsin	**59**	240 nM	130 nM	74%	73%	227
5	α-chymotrypsin	**60**	80 nM	40 nM	72%	54%	227
6	α-chymotrypsin	**61**	1200 nM	360 nM	68%	75%	227
7	α-chymotrypsin	**62**	3.0 μM	4.7 μM	>95%	>95%	228
8	α-chymotrypsin	**63**	10 μM	7 μM	>95%	60%	228
9[c]	α-chymotrypsin	**64**	>65 μM	16 μM	>95%	78%	229
10[c]	α-chymotrypsin	**65**	32 μM	13 μM	>95%	93%	229
11[c]	α-chymotrypsin	**66**	46 μM	10 μM	>95%	68%	229
12[c]	α-chymotrypsin	**67**	>108 μM	23 μM	93%	77%	229
13[c]	α-chymotrypsin	**68**	>86 μM	17 μM	89%	90%	229
14[c]	α-chymotrypsin	**69**	46 μM	8.5 μM	92%	89%	229
15[c]	α-chymotrypsin	**70**	>60 μM	27 μM	>95%	86%	229
16	m-calpain	**71**	45 nM	175 nM	83%	81%	230
17	m-calpain	**72**	40 nM	100 nM	77%	79%	230

[a]These results were obtained with KCl and bovine serum albumin as stabilizers. [b]These results were obtained with only bovine serum albumin as a stabilizer. [c]IC_{50} values are reported in these cases.

Compound **57** was used as a photoswitchable inhibitor of papain,[226] an enzyme from the group of cysteine proteases. A clear difference in efficiency in response to photoswitching was reported (Table 8, entry 1), and the activity of the enzyme could be reversibly altered over two irradiation cycles. In the case of chymotrypsin, the addition of stabilizers (KCl and

dx.doi.org/10.1021/cr300179f | Chem. Rev. 2013, 113, 6114−6178

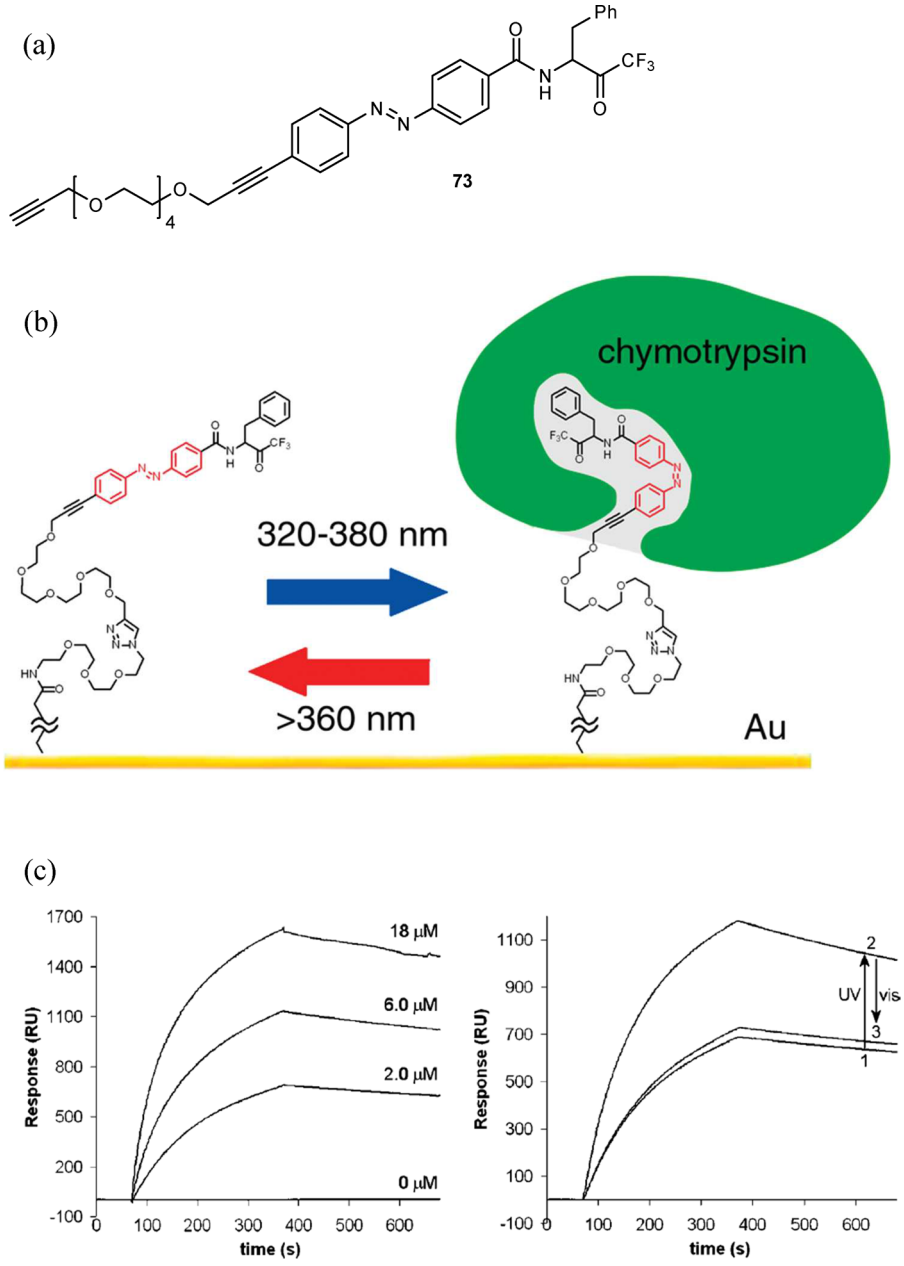

Figure 49. Photocontrolled binding of α-chymotrypsin to a gold surface. (a) The structure of the inhibitor **73**. (b) Reversible protein binding. (c) left graph: binding of the enzyme to a nonirradiated surface (see explanation in the text); right graph: reversible photocontrol of enzyme binding at 2.0 μM protein concentration; 1: nonirradiated surface; 2: UV-irradiated surface; 3: surface irradiated subsequently with UV and visible light. Reprinted with permission from ref 232. Copyright 2007 American Chemical Society.

bovine serum albumin) was necessary to ensure enzyme stability during the assay. For compound **58**, again the inhibitor in the *trans* state proved to be ~4 times more potent (Table 8, entry 2), and its reversible behavior was demonstrated.[226] Interestingly, when the photocontrolled inhibition of subtilisin with **58** was studied, opposing effects of irradiation on the activity were reported in the presence and in the absence of stabilizers (Table 8, entry 3). However, no explanation was provided for this phenomenon.

Further developments in photocontrolled inhibition of α-chymotrypsin were presented by the group of Abell in a series of reports (Table 8, entries 4–15).[227−229,231,232] All of the studied compounds incorporated azobenzene in their structure, linked to a phenylalanine that orients the compounds in the active site. Additionally, a reactive electrophilic group (such as ketoester, trifluoromethyl ketone, aldehyde, or boronic acid), to which the catalytic serine of the enzyme reversibly binds (a so-called "warhead"), is also attached. Initially,[227] α-ketoesters **59**–**61** (Figure 48) were used to serve the role of the "warhead" (Table 8, entries 4–6). While the reported photostationary states for both isomers were low, an over 3-fold change in enzymatic activity upon irradiation was reported. The preparation[228] of inhibitors with a boronate ester moiety as the warhead was subsequently presented. Two of these derivatives, unsubstituted inhibitor **62** and its analog **63** with an amino acid residue added to increase its peptidic character, were used in a photocontrolled inhibition study (Table 8, entries 7 and 8). While the photostationary states were generally high, a low and irreproducible level of activity change

dx.doi.org/10.1021/cr300179f | *Chem. Rev.* 2013, 113, 6114–6178

upon irradiation was reported, which was explained by the possible degradation of boronate ester upon irradiation.[228]

To overcome this hurdle, the trifluoromethyl ketone was used as a "warhead" in the follow-up design (compounds **64**–**70**, Figure 48).[229] In some of the molecules, a sulfonamide linker was used instead of the amide, to increase the proteolytic stability of the inhibitor. Additionally, in some compounds, halide substituents were included in the 4′ position of the azobenzene structure to increase its bulkiness. The photochromic molecules could be switched with UV light (λ = 320–380 nm) from *trans* isomers (PSS > 89%) to *cis* isomers (PSS = 68–93%) with high selectivity (Table 8, entries 9–15). Compound **67**, a sulfonamide derivative with a bromo-substituent, proved to be the most effective photoswitch with an >4.7-fold change in activity upon photoirradiation.

An interesting extension of the designed inhibitors was reported more recently by Abell and co-workers.[231,232] Immobilization of a photoswitchable inhibitor **73** (Figure 49a) on a gold surface allowed photocontrol over protein binding (Figure 49).[232] The structure of compound **73** was derived from a previously published inhibitor of α-chymotrypsin (**64**)[229] with a substituted tetraethylene glycol chain, bearing a terminal acetylene residue. This residue was used for the attachment of compound **73** to an azide-decorated gold surface *via* Cu^{I}-catalyzed azide–alkyne cycloaddition.

Compound **73** was first studied in solution and showed a reversible change in activity upon irradiation, giving the K_i values of >51 μM for the *trans* isomer (92% PSS) and 14 μM for the *cis* isomer (85% PSS).[232] After immobilization of compound **73** on a gold surface, the photocontrolled binding of α-chymotrypsin to the surface was studied by SPR (Figure 49c). In the initial experiments, the enzyme was bound to the nonirradiated surfaces at different concentrations (Figure 49c, left graph, enzyme injection at t = 70 s, binding time 300 s, washing time 300 s) and the concentration-dependent response was recorded. This showed that the surface with *trans*-**73** attached was able to bind the protein. In the following experiment, the surface was irradiated with UV light and the enzyme binding was repeated at 2.0 μM protein concentration (Figure 49c, right graph). A reversible influence of irradiation was recorded with the UV irradiated surface being more efficient in protein binding. Subsequent attempts to optimize the structure of the photoswitchable inhibitor failed to provide a more pronounced effect.[231]

An important structural insight into the change of activity of protease inhibitors upon irradiation came from a report[230] on the use of photoswitchable dipeptide aldehydes **71** and **72** (Figure 50). These compounds are inhibitors of m-calpain (E.C. 3.4.22.17), a Ca^{2+}-dependent cysteine protease implicated in the development of cataracts.[233] In both cases, the extended *trans* isomer proved to be more potent (Table 8, entries 16 and 17). This observation was explained by the results obtained from molecular modeling (Figure 50), showing that the peptide portion of the inhibitor binds in an extended β-strand conformation, while the *trans*-azobenzene moiety extends deep into the S3 binding pocket. The photochromic unit in its *cis* form, on the other hand, has an unfavorable interaction with the hydrophobic patch on the mobile loop that defines the calpain active site.[230] This model provides a structural explanation for the light-induced differences in activity of these photoswitchable enzyme inhibitors (Figure 50a).

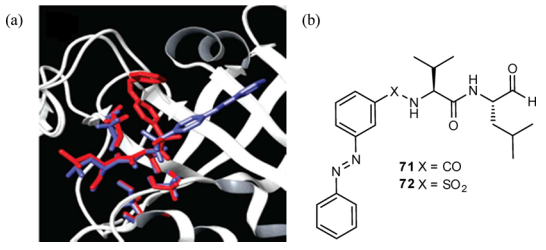

Figure 50. (a) Induced-fit overlay of the S3 subsite of calpain with docked *trans*-**72** (blue) and *cis*-**72** (red); (b) Structures of compounds **71** and **72**. Reprinted with permission from ref 230. Copyright 2007 American Chemical Society.

Bis-azobenzene-based compound **74** (Figure 51a), a photochromic inhibitor of bovine heart mitochondrial NADH ubiquinone oxidoreductase (complex I), was studied by Miyoshi and co-workers.[234] Its design was inspired by the influence on activity of the aromatic substitution pattern of known inhibitor **75** (Figure 51a).[235] Compound **75**, with both *n*-butyl groups in the *para* position, was a potent inhibitor of mitochondrial complex I with an IC_{50} value of 0.83 nM.[234] When these groups were both present in the *ortho* position, no inhibition activity was found. Upon the basis of these observations, compound **74** (Figure 51a) was prepared, in which the relative position of the *n*-butyl groups with respect to the tetrahydrofuran moieties could be changed upon photoirradiation. The influence of the photoswitching on the activity of the inhibitor is presented in Figure 51b.

The reversibly photocontrolled inhibition of mitochondrial complex I activity was shown at two different concentrations of the inhibitor; albeit, the changes were relatively small. The low photostationary state of *cis*,*cis*-**74** in bovine heart submitochondrial particles and its possible residual activity were suggested as the explanation for the unsatisfactory level of photocontrol.

König and co-workers used a diarylethene derivative **76** (Figure 52a) for the photocontrolled inhibition of human carbonic anhydrase I (hCAI).[236,237] This approach and the others described below are examples of the second type of inhibitor design (Figure 45b), in which two ligands in the effector are connected by a photoswitchable linker. Inspired by literature reports,[238] the diarylethene scaffold was functionalized with a sulfonamide group that acts as an inhibitor and with a copper(II) iminodiacetate moiety that reversibly coordinates to the imidazole side chains of the histidine residues in the active site of the enzyme.

Photoisomerization of **76** was achieved by irradiation with 312 nm light and yielded a very high photostationary state of >99%.[236] The closed form was found to be highly thermostable and could be converted back to the open form by irradiation with visible light. The inhibition study (Figure 52b) showed that the open form was a much more potent carbonic anhydrase inhibitor with an IC_{50} value of 8 nM. The closed form shows an IC_{50} value of 400 nM, and its activity is similar to the one of a known inhibitor, sulfanilamide. These differences in activity were attributed to geometrical constraints in the closed form.

Control experiments, performed with symmetrically substituted compounds **77**–**79** have shown that compounds **77** and **78**, which include the structural elements of **76**, also inhibit the enzyme, albeit with activities lower than that of sulfanilamide. Photoisomerization had no effect on activity. The lack of activity of compound **79** showed that the diarylethene moiety has no influence on the enzyme.[236] In

dx.doi.org/10.1021/cr300179f | *Chem. Rev.* 2013, 113, 6114–6178

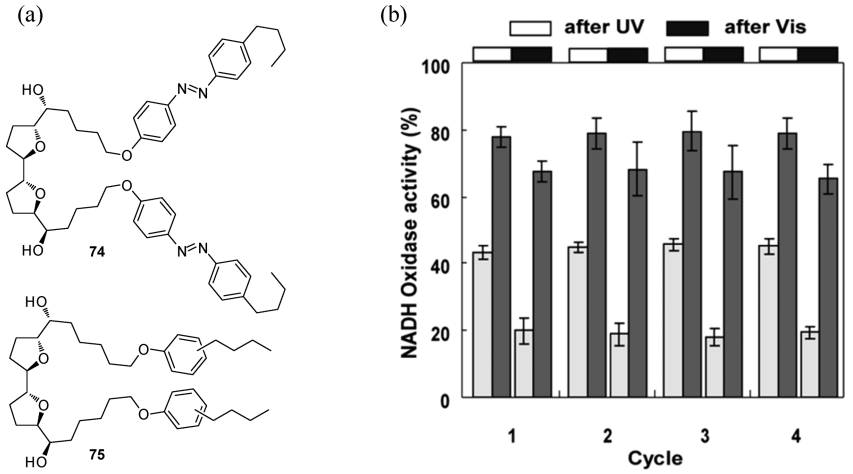

Figure 51. Photocontrolled inhibition of mitochondrial complex I. (a) The photoresponsive inhibitor **74** and its parent structure **75**; (b) the changes in the activity of NADH oxidase, incubated with **74**, upon alternating photoirradiation with UV and visible light. Two concentrations of **74** were studied: 9.6 nM (dark gray bars) and 96 nM (light gray bars). Reprinted with permission from ref 234. Copyright 2006 American Chemical Society.

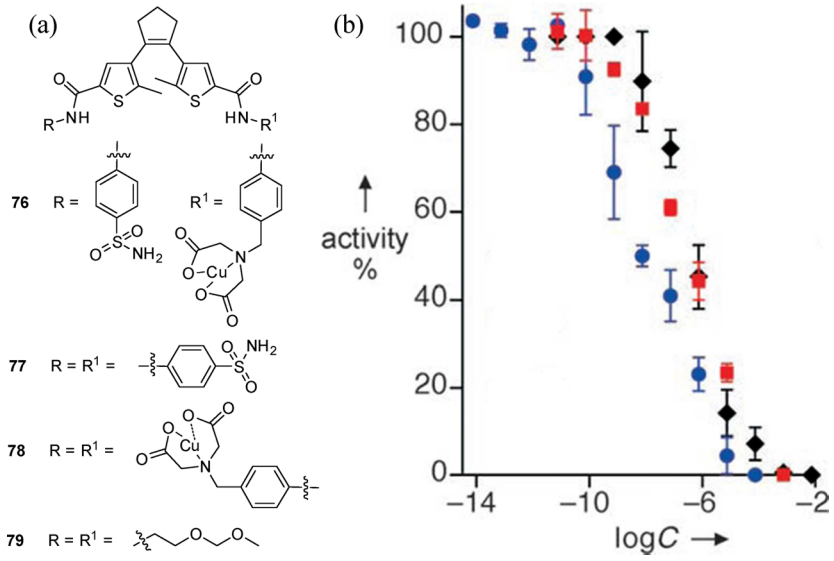

Figure 52. Photocontrolled inhibiton of human carbonic anhydrase I. (a) The structure of the inhibitors. (b) Activity profile; (blue circles) **76** in an opened form; (red squares) **76** in a closed form; (black diamonds) sulfanilamide, a known inhibitor of human carbonic anhydrase I. Reprinted with permission from ref 236. Copyright 2008 Wiley-VCH Verlag GmbH & Co. KGaA.

the follow-up report,[237] the activity of compounds **76**−**79** was assayed on a set of five physiologically relevant isoforms of carbonic anhydrase. It was shown that, for select isoforms, photocontrolled inhibition with symmetrically substituted compounds **77**−**79** was also possible.

The strategy of designing bifunctional effectors in which the distance and alignment of both moieties that interact with the target enzyme is controlled with a photoswitchable group (Figure 45b) was applied in a more systematic manner by the group of Liskamp.[239,240] The chosen target was the spleen tyrosine kinase (Syk) protein. This protein takes part in a number of signaling pathways in human cells, including the high affinity IgE receptor (FcεRI) signaling cascade. The γ part of this receptor contains the immunoreceptor tyrosine-based activation motif (ITAM peptide, **80**, Figure 53a). When the ITAM of FcεRI is phosphorylated, the Syk binds to it and becomes activated, triggering a series of events in the cell. An important feature of the ITAM−Syk interactions is its divalency; that is, two motifs (epitopes) in the ITAM peptide are recognized by the two SH2 domains in Syk (Figure 53b). This opens the possibility of controlling Syk activation by ITAM-analogs where the distance and alignment of the epitopes are controlled by a photoisomerizable linker.

Compounds **81**−**84** (Figure 53a) were prepared, in which the epitopes were separated with photoswitchable linkers of different lenghts. Their binding to Syk was examined using SPR, and the obtained K_D values are summarized in Table 9.

Photoirradiation of compound **81** resulted in an over 10-fold change in binding affinity to Syk (Table 9, entry 1). This was attributed to the change in the length of the linker, which forces the activator to shift from a divalent interaction to a monovalent one. The authors note, however, that the K_D value for the *cis* isomer still differs from the one observed for the pure monovalent interaction (K_D = 27 μM). They attribute this to the flexibility of the linker that exists between the two SH2 domains in Syk.[239] This flexibility allows Syk to adopt different conformations and adjust its geometry to the demands

dx.doi.org/10.1021/cr300179f | *Chem. Rev.* 2013, 113, 6114−6178

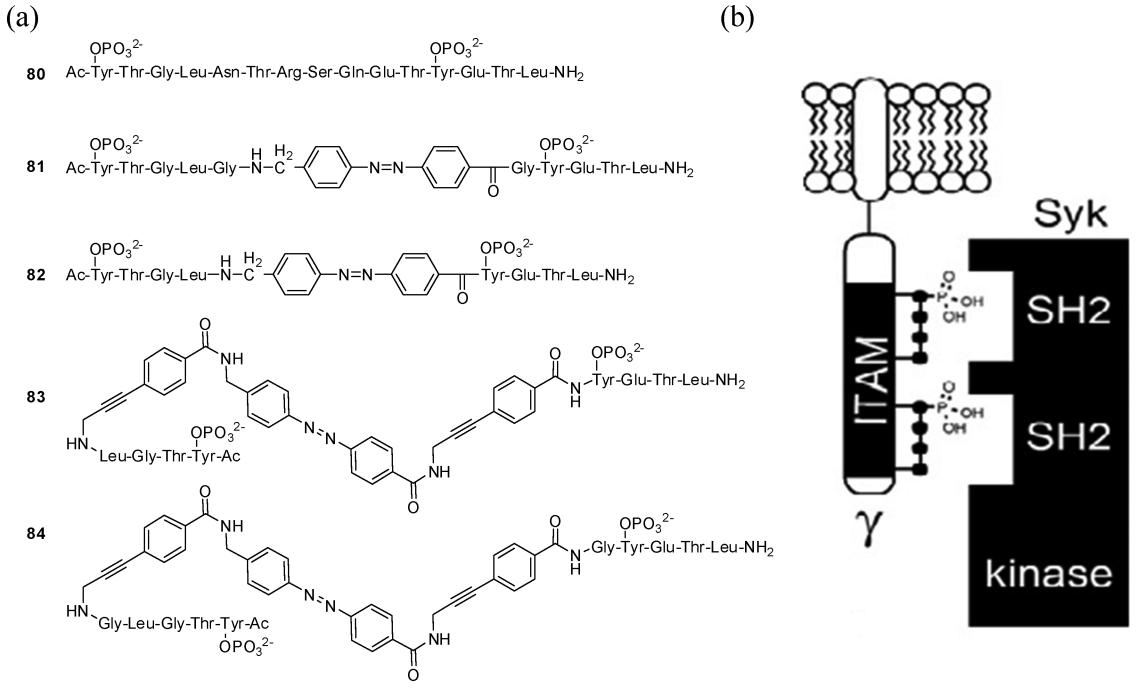

Figure 53. Photocontrolled activation of spleen tyrosine kinase.[239,240] (a) The structure of inhibitors **80**–**84**. (b) Schematic representation of ITAM–Syk interactions. Adapted with permission from ref 239. Copyright 2008 Elsevier B. V.

Table 9. Photocontrolled Binding of ITAM-Analogs to the SH2 Domains of Spleen Tyrosine Kinase[240]

		trans		*cis*	
entry	compd	epitope dist	K_D (nM)	epitope dist	K_D[a] (nM)
1	**81**	18.6 Å	65 ± 8	7.2 Å	860
2	**82**	12.0 Å	91 ± 10	6.2 Å	>10 000
3	**83**	23.4 Å	196 ± 35	11.0 Å	147
4	**84**	30.2 Å	77 ± 13	17.8 Å	49

[a]These values were calculated for pure *cis* isomers, assuming 66% PSS in the real samples.

of the ITAM-analog. The influence of the flexibility of the ITAM-analog itself also cannot be excluded.[239]

In the follow-up study,[240] compound **82** (Figure 53a), a truncated analog of **81**, was prepared and tested, showing a very large change in activity upon photoirradiation (Table 9, entry 2). Since compound **82** binds Syk more strongly in its *trans* configuration and it was impossible to reach high PSS levels of *cis* isomer upon photoirradiation, complete on–off photocontrol could not be achieved. Therefore, two more analogs, **83** and **84** (Figure 53b), were prepared. These analogs were designed to better fit to the SH2-SH2 domains distance (14.1–16.4 Å) in their *cis* states. While this aim was achieved (Table 9, entries 3 and 4), the differences in activity upon photoisomerization were considerably lower than in the case of compound **82**, indicating that not only distance constraints are important.[240]

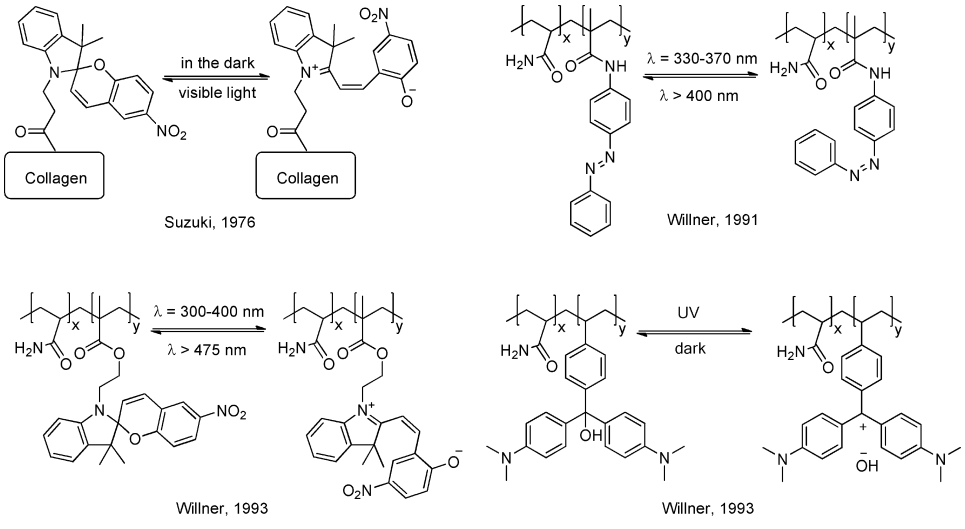

Figure 54. Photoswitchable supports used for the immobilization of enzymes.[241–244]

dx.doi.org/10.1021/cr300179f | *Chem. Rev.* 2013, 113, 6114–6178

In summary, the use of photoisomerizable ligands for the photocontrol of enzymatic activity is a valuable tool, which has yet to show its full potential in *in vivo* studies. The results published so far usually show small change in activity upon irradiation, especially for designs of the first type (Figure 45a).[221,224,226−229] The second approach (Figure 45b) seems to be more promising in terms of photocontrol[236,237,239,240] but is restricted to divalent systems. While the use of photoisomerizable effectors is facile from an experimental point of view, requiring less effort than the site-selective, covalent incorporation of photochromic residues into enzymes (see sections 4.4 and 4.5 of this review), it is considered a drawback that it has lower othogonality toward the other elements of the studied systems. The effector compounds may influence other proteins present in living systems. Furthermore, the introduction of a photoswitch unit into the structure of the effector can have a considerable effect on activity and often lowers the affinity to the enzyme.

4.2. Photoresponsive Immobilization Supports

One of the first attempts toward regulation of enzymatic activity by light was based upon the immobilization of a biocatalyst in a membrane that had been modified by the incorporation of molecular photoswitches. The group of Suzuki reported[241] the preparation of a collagen membrane modified by spiropyran residues that underwent reversible isomerization by irradiation with visible light (Figure 54). Urease (E.C. 3.5.1.5), an enzyme that hydrolyzes urea to ammonium ion and bicarbonate, was entrapped in the photoresponsive support and cross-linked with glutaraldehyde.

The study on the activity of the resulting immobilized enzyme revealed that, in the dark, the k_{cat} value was almost twice as high as under visible light irradiation, while the K_M value remained virtually unchanged. Diffusion of urea and ammonium ion through the membrane was reported to be the rate limiting step in this system.[242] However, more detailed studies on the spiropyran-modified membrane revealed only a slight difference of diffusion coefficients of these compounds in the dark and under irradiation. Therefore, the lack of change in the K_M values upon isomerization of the photoswitch led to the conclusion that the difference in enzymatic activity was not caused by the differences in diffusion. Instead, it was proposed that, in the dark, the spiropyran residue is charged, which results in the formation of hydrophilic microenvironment around the enzyme, increasing its activity. A shift in the optimum pH of the enzyme upon irradiation of the immobilized enzyme was also reported.[242]

The concept of using photoresponsive supports for the immobilization of enzymes has been further explored by the group of Willner.[243] The immobilization of α-chymotrypsin (E.C. 3.4.21.1) was carried out by radical copolymerization of acrylamide, *N*,*N*′-methylenebis(acrylamide) (as a cross-linker) and photoswitchable azobenzene derived monomer (up to 1%) in the presence of the enzyme (Figure 54). A strong influence of the concentration of the photochromic component on the activity of immobilized enzyme has been observed. At higher loadings (0.75−1.0%), no difference in the enzymatic activity could be observed upon irradiation by light. However, when 0.5% of the photoswitch was used in the polymerization mixture, the change in activity of the immobilized biocatalyst upon irradiation exceeded 90%. Further studies revealed that the polymer in its *trans* state is virtually impermeable with respect to the substrate as opposed to the *cis* state. This effect is considered to be at the origin of the difference in the rate of product formation.

Subsequently, a variety of different polymers were applied as immobilization supports (Figure 54).[244] In all cases, complete and reversible control over enzymatic activity was obtained after optimization; that is, the immobilized biocatalyst was active in one photostate of the switch and inactive in the other. Furthermore, it was estimated that ∼100−200 cycles of enzyme-switchable activities can be achieved prior to degradation of the polymers. Permeability studies using a flow-dialysis cell confirmed that in all of the studied cases the change of polymer permeability upon irradiation was responsible for the observed effects of light on enzymatic activity.

The preparation of photoresponsive immobilized biocatalysts is an interesting approach that gives remarkably good results with respect to the degree of changes in enzyme activity upon irradiation. It is, however, mainly dependent on the changes in permeability of the support toward the substrate, which might limit this methodology to selected cases.

4.3. Photoresponsive Surfactants

Photoisomerization of photoresponsive surfactants results in changes in their polarity. This can effect electrostatic interactions with proteins, allowing for the manipulation of their structure and activity.[245,246] A representative example for such an approach is presented below.

The group of Lee studied the changes in bovine serum albumin (BSA) structure in response to the increasing concentration of the *trans* and *cis* forms of azobenzene-based photoswitchable surfactant **85** (Figure 55a) that interact with the anionic residues on the surface of the protein.[247,248]

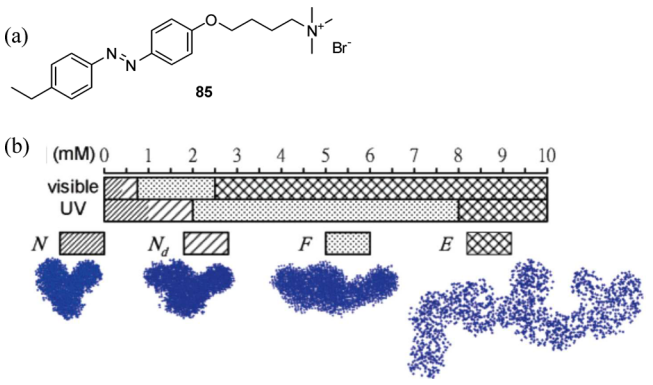

Figure 55. Use of photoresponsive surfactant for the control of BSA structure. (a) The structure of the photoresponsive surfactant. (b) The influence of the concentration of surfactant in both forms on the tertiary structure of bovine serum albumin. N: native heart-shaped structure; N_d: distorted heart-shaped structure; F: partially unfolded; E: elongated. Reprinted with permission from ref 248. Copyright 2006 American Chemical Society.

Four distinct protein structures have been observed using small-angle neutron scattering (SANS) (Figure 55b), and their distribution was strongly dependent on the concentration of the cationic surfactant **85**. Compound **85** was shown to have different effects on the structure of BSA in its *trans* and *cis* forms (Figure 55b). In general, the UV-irradiated samples showed weaker influence of increasing surfactant concentration on protein unfolding, as the *cis* from of the azobenzene is less hydrophobic. At a fixed concentration of **85**, the changes of

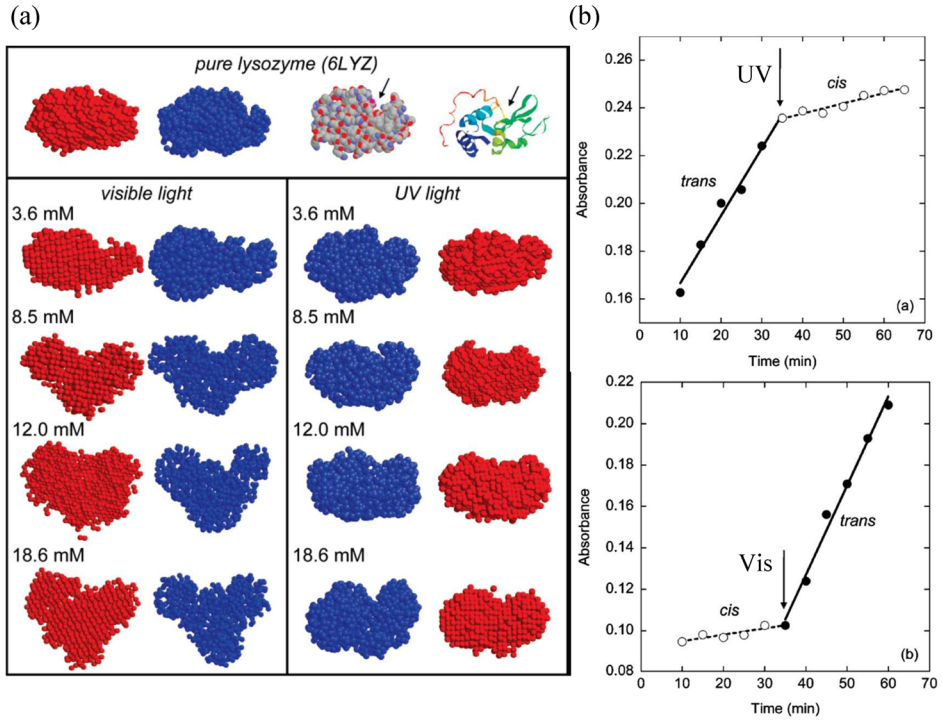

Figure 56. Use of photoresponsive surfactant for the control of lysozyme structure and activity. (a) *In vitro* conformations of lysozyme determined from shape-reconstruction analysis of the SANS data at different concentrations of photoresponsive surfactant **85** in *trans* and *cis* forms. Best-fit structures are shown in blue, and consensus envelopes are shown in red. The arrows in the upper part show the active-site cleft between α and β domains. (b) Photoregulation of lysozyme activity with the reaction initiated with *trans*-**85** (upper) and *cis*-**85** (lower). The arrows indicate the initiation of irradiation. Reprinted with permission from ref 246. Copyright 2007 American Chemical Society.

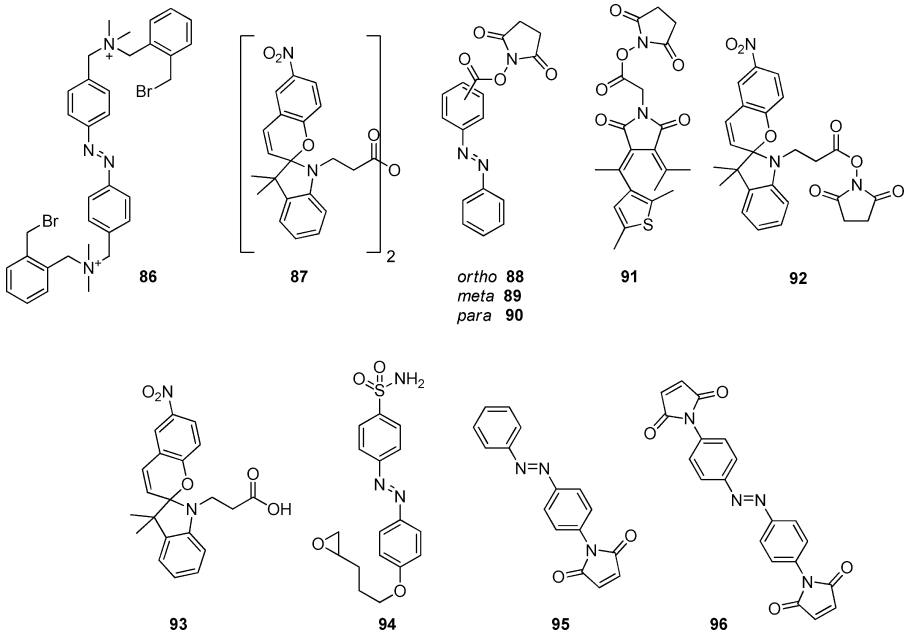

Figure 57. Compounds used for the random, semirandom, and directed incorporation of molecular switches into the structure of enzymes.[47,48,249−256,264,265,285−289,291]

protein structure in response to the photoisomerization were shown to be reversible.[247]

Having established the proof of principle for the photocontrol of BSA folding/unfolding behavior, the group of Lee also used photoswitchable surfactant **85** for the control of the enzymatic activity of lysozyme (E.C. 3.2.1.17),[246] an enzyme responsible for damaging bacterial cell walls (Figure 56a).

The kinetic analysis of lysozyme activity in the presence of 0.2 mM **85** has revealed reversible changes in enzymatic activity upon irradiation (Figure 56b). Interestingly, the activity was increased ∼5-fold when the surfactant was in its more hydrophobic, *trans* form and the protein was unfolded to a greater extent. The sample irradiated at 350 nm exhibited enzymatic activity comparable to that of the sample without

dx.doi.org/10.1021/cr300179f | *Chem. Rev.* 2013, 113, 6114−6178

surfactant. This effect has been explained by the introduction of additional flexibility in the partially unfolded enzyme, which promotes conformational changes along the reaction pathway.[246] However, additional experiments need to be performed to gain insight into this intriguing dynamic effect.

The use of photoresponsive surfactants for the photocontrol of enzymatic activity is a simple solution, which may even lead to the establishment of "superactivity",[246] i.e. the formation of enzymes with increased catalytic properties as compared to the native proteins. However, it is difficult to envisage the application of this protocol for the control of activity of a biocatalyst in living systems without affecting other enzymes/proteins present in the studied system. This, together with the potential disturbance of biological membranes by added surfactants, currently limits these studies to fundamental investigations of surfactants and proteins.

4.4. Random Incorporation of Molecular Switches into the Structure of Enzymes

The first reports on the random incorporation of molecular photoswitches directly into the structure of biocatalysts date back to the mid-1970s. Erlanger and co-workers studied the incorporation of azobenzene derivative **86** (Figure 57) into chymotrypsinogen A.[249] The modification had to be done at the proenzyme stage, since activated chymotrypsin lost about 75% of its activity upon attachment of the photoswitch. The level of incorporation of **86** into the proenzyme was estimated by UV/vis measurements to be one switch molecule per biocatalyst. The exposure of the modified chymotrypsinogen A to trypsin released the activated, photoresponsive π-chymotrypsin. Kinetic studies revealed that it had similar K_M values to those of the unmodified enzyme, while the k_{cat} was increased 4 times. Upon irradiation with 330 nm light, activity was reduced 2-fold. It was suggested that the increase of activity upon modification with the photoswitch is allosteric in nature.

The group of Suzuki[250] described the random modification of urease with spiropyran residues and subsequent immobilization of the photorosponsive biocatalyst. Nucleophilic groups on the enzyme surface were modified using spiropyran anhydride **87** (Figure 57). The biocatalyst was subsequently purified and immobilized on a collagen support. It was shown that the enzyme retained 62% of its activity after UV irradiation and that this effect was derived from changes in k_{cat} values, as the K_M remained the same. This observation was explained by the interactions of the charged merocyanine with one of the intermediates of the enzymatic reaction. A shift of the optimum pH upon irradiation was also observed, but only in the case of immobilized enzymes and not for soluble catalyst. Interestingly, the immobilized enzyme modified with photoresponsive residues showed higher thermostability than the unmodified one. This observation was attributed to hydrophobic intermolecular interactions between spiropyran moieties attached to an enzyme molecule.

A similar approach was used[47,48] for the preparation of photoresponsive α-amylase (E.C. 3.2.1.1). Compound **87** was employed for the random incorporation of spiropyran residues *via* the amino groups of lysine side chains present in/on the biocatalyst. The modified protein was purified from unreacted protein with a DEAE-Sephadex column. It was shown that, on average, two amino groups in the enzyme were conjugated with the photoswitch. The incorporation was further confirmed by UV/vis spectra and isoelectric point measurements. The photoresponsive α-amylase showed a 36% decrease in activity upon UV irradiation, and the activity was fully recovered upon incubation in the dark. The pH optimum shifted by approximately 0.5 units upon photoswitching. Kinetic analysis showed that the UV irradiation results in a change in the K_M value of the enzyme, and it was hence concluded that the reduced affinities of enzymes toward the substrates were responsible for the observed changes of enzymatic activity upon irradiation. This methodology was also applied to other hydrolytic enzymes: α-chymotrypsin, β-glucosidase (E.C. 3.2.1.21), and β-amylase (E.C. 3.2.1.2).[251] The results of the studies are summarized in Table 10. The enzymes modified with spiropyran derivative **87** showed up to 87% change in activity (in case of β-amylase), and the effect in all cases originated from the difference in the change of affinity of the enzymes to the substrates upon photoirradiation.

Table 10. Kinetic Parameters of the Enzymes Modified with Spiropyran Derivative 87[251]

		relative activity		K_M (mM)	
enzyme	substrate	opened	closed	opened	closed
α-chymotrypsin	*N*-benzoyl-L-tyrosine ethyl ester	100	150	15	4.3
β-glucosidase	phenyl-β-D-glucoside	100	115	4.0	3.3
α-amylase	amylose	100	64	12	15
β-amylase	amylose	100	13	3.4	60

Willner et al. have expanded the methodology of random introduction of photoswitches into the structure of the protein by optimizing the structure of the switch.[252] Various carboxyazobenzene isomers **88**−**90** (Figure 57), in the form of activated esters, were introduced into lysine residues of papain (E.C. 3.4.4.10) and were tested for their influence on enzymatic activity. The enzyme modified with *para*-substituted compound **90** was examined in more detail, as it showed the least loss in activity upon modification. The average efficiency for the attachment of switch units was estimated by UV/vis measurements to be about 54%; that is, on average 5 out of 10 lysine residues present in the protein structure were modified. The enzyme, immobilized in alginate beads, showed a moderate, yet reversible, change in activity upon irradiation. Kinetic measurements revealed that the K_M value changed upon switching of the system, while k_{cat} remained virtually the same. This phenomenon, characteristic for competitive inhibition, was attributed to structural changes in the protein that influenced substrate binding but did not disturb the active site itself. It was also suggested that only the lysine groups exposed to the solvent could be modified with compounds **88**−**90**, which may have resulted in a rather low level of photocontrol.

The photoregulation of the activity of α-chymotrypsin, randomly modified with thiophenefulgide derivative **91**, has been compared in aqueous and organic medium.[253] While in water no difference in activity upon irradiation was observed, in cyclohexane the enzyme exhibited a 5-fold increase in activity upon photoswitching. The difference in photoresponse between the two solvents has been explained by increased perturbation of enzyme-bound water molecules in nonaqueous media. Interestingly, the change in activity upon irradiation was less pronounced when enzyme imprinting was been used, i.e. when the biocatalyst was crystallized in the presence of its substrate, prior to being used as a catalyst in organic medium. This was explained by an increase in enzyme rigidity, which

dx.doi.org/10.1021/cr300179f | *Chem. Rev.* 2013, 113, 6114−6178

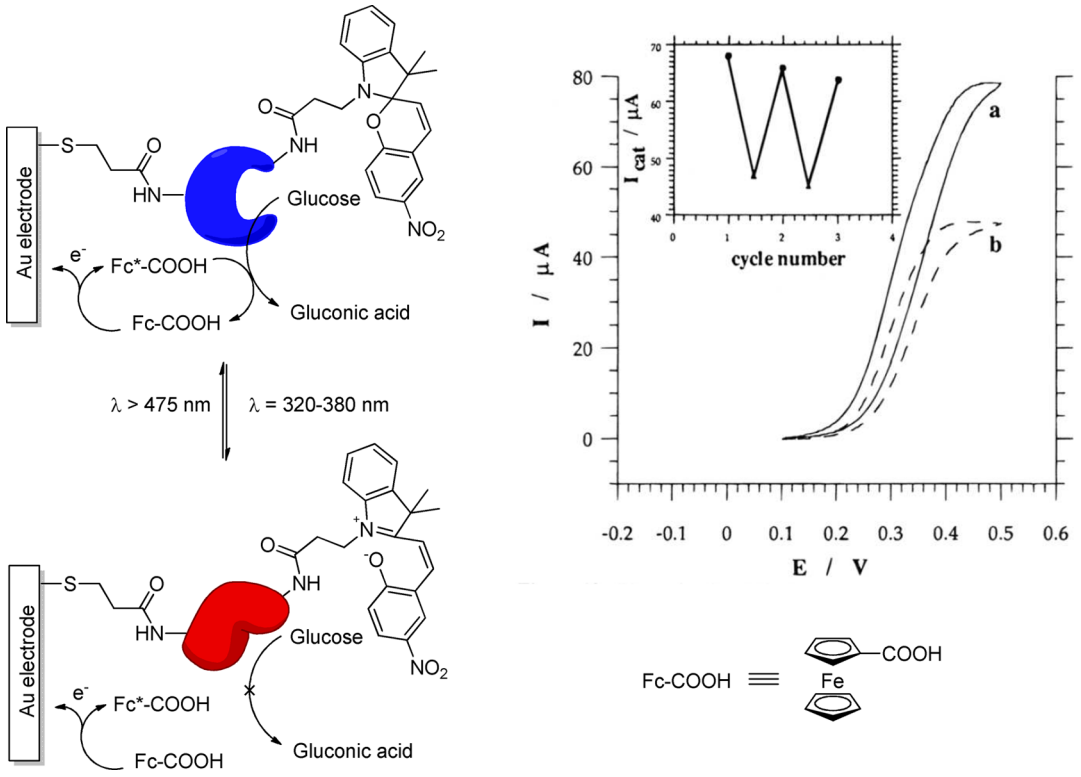

Figure 58. Effect of photoirradiation on glucose oxidase immobilized on a gold electrode. Reprinted with permission from ref 254. Copyright 2007 American Chemical Society.

made the enzyme less susceptible to undergoing light-effected perturbation.

The amplification of light signals using photoresponsive enzymes, obtained by the method of random incorporation of photoswitches, was reported by Willner and co-workers in the mid-1990s.[254] Spiropyran derivative **92** (Figure 57) was introduced into the structure of glucose oxidase (E.C. 1.1.3.4), resulting in the modification of, on average, 21 out of 54 lysine residues. The modified enzyme showed roughly a 50% change in activity upon irradiation. The biocatalyst was immobilized on a rough gold electrode (Figure 58).

The addition of an electron mediator, ferrocene carboxylic acid, facilitated electron transfer between the enzyme and the electrode. When the enzyme was in its active state, the bioelectrocatalyzed oxidation of glucose proceeded at a higher rate and an anodic current was recorded (Figure 58, curve a). UV irradiation transformed the enzyme into a less active state (Figure 58, curve b). The changes were reversible (Figure 58, inset), although a drop of activity was observed. This slow inactivation was attributed to the denaturation of the enzyme caused by UV irradiation, seen to an even higher extent for the photoswitch-modified but nonimmobilized enzyme. Although it does not show a complete on−off control of activity, this system represents one of the few reported direct applications of photoswitchable enzymes.

Additional insights into the phenomena responsible for changes in enzymatic activity upon irradiation were provided by Cullen and co-workers, when studying the EDC-mediated modification of horseradish peroxidase (E.C. 1.11.1.7) with spiropyran derivative **93** (Figure 57).[255] The efficiency of the incorporation of **93** depended on the reaction time for conjugation, and a maximum of nine switching units per enzyme could be introduced. The level of photomodulation was strongly influenced by the amount of the introduced photoswitches. The difference in activity before and after irradiation with UV light was as high as 92% and was observed when, on average, 8.5 dye molecules per enzyme were attached. Interestingly, spectroscopy studies on the biocatalyst after irradiation revealed that only two to three photoswitches were in the merocyanine state. From these observations, it was concluded that the influence of the dye on the enzyme activity occurred *via* local interaction with the active site.

A semirandom approach toward the preparation of light-responsive biocatalysts has been recently reported by Trauner and co-workers.[256] They introduced the photoswitchable affinity label (PAL) concept, which relies on the use of a bifunctionalized compound (e.g., molecule **94**, Figure 57) for enzyme modification. The enzyme chosen for this study was bovine carbonic anhydrase II (E.C. 4.2.1.1), which, as has been previously mentioned, is inhibited by sulfanilide. The PAL is comprised of three parts: the ligand that binds noncovalently into the enzyme active site, the photoswitch, and the reactive group (arylsulfonamide, azobenzene, and epoxide moieties in **94**, respectively). The binding of the ligand to the active site allows the reactive group to conjugate to the most geometrically available nucleophile on the enzyme surface (Figure 59).

The yield of carbonic anhydrase modification with PAL **94** was estimated by LC-MS to be in the range 65−85%, and the level of reversible photocontrol was measured to be 50%. MS/MS studies revealed that **94** was introduced to positions H2 and H3. The relatively low value of photocontrol was explained by the fact that these histidine residues are placed at the flexible *N*-terminus of the enzyme, which does not always reside in the vicinity of the active site. The obtained data pointed also to an important observation: the photostationary state of the

dx.doi.org/10.1021/cr300179f | *Chem. Rev.* 2013, 113, 6114−6178

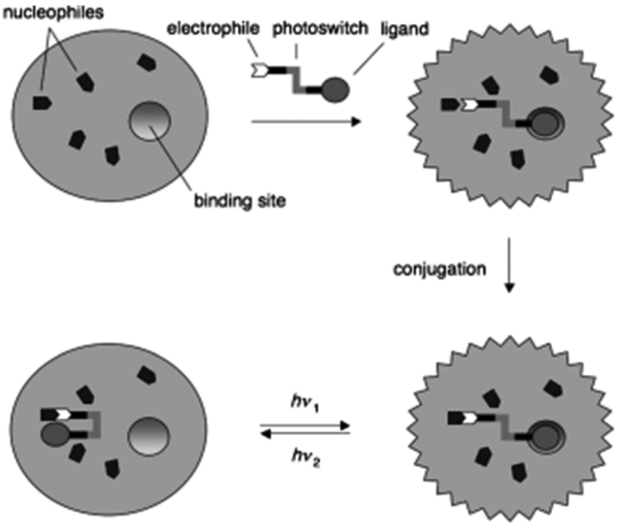

Figure 59. Use of PAL for the photocontrol of enzymatic activity. Reproduced with permission from ref 256. Copyright 2008 Wiley-VCH Verlag GmbH & Co. KGaA.

azobenzene switch changes significantly upon bioconjugation.[256]

In summary, the random introduction of photoswitchable compounds into the structure of enzymes is a simple method for the preparation of photoresponsive biocatalysts, which in selected cases allows up to >90% change in activity upon irradiation.[255] Whole systems can easily be optimized with regard to the structure of the photoswitch, although the control over the position and number of introduced molecules is statistical at best,[255] leading to the formation of heterogeneous mixtures of differently modified enzymes. The recently introduced PAL approach[256] might help to solve this issue. The studies on photoresponsive biocatalysts revealed that the change of activity upon irradiation is mainly caused by the alteration of enzyme's affinity to the substrate (K_M),[47,48,251,252] which is caused by the switching of compounds in the vicinity of the active site[252,255] or allosteric sites.[249] The changes of k_{cat} value upon irradiation were also reported in a few cases.[249,250]

4.5. Site-Selective Incorporation of Molecular Switches into Enzymes

Site-selective incorporation of molecular switches into enzymes offers the possibility of structure-based design and optimization of photoresponsive bioconjugates. Three major approached have been followed (Figure 60): (a) preparation of a modified fragment of an enzyme and its subsequent attachment to the remaining part of the protein (section 4.5.1); (b) introduction of a reactive amino acid side chain at a chosen position and subsequent modification thereof with a a photochromic unit (section 4.5.2); and (c) introduction of photoswitchable amino acids during *in vivo* or *in vitro* synthesis of the enzyme (section 4.5.3).

4.5.1. *De Novo* Synthesis of a Part of the Enzyme. The simplest approach uses standard peptide synthesis methods (Figure 60a) for the *de novo* preparation of a terminal fragment of a catalytically active protein. This step allows for convenient introduction of the photoswitchable amino acid(s) at a chosen position(s). The prepared fragment is subsequently conjugated to the main body of the protein. This approach was first reported in the preparation of photosensitive phospholipase A_2 (E.C. 3.1.1.4), an enzyme responsible for the hydrolysis of phosphoglycerides.[257] It is known that the α-helix conformation of the *N*-terminal fragment of this enzyme plays a key role in the action of the interface-recognition site, which is responsible for anchoring the enzyme at the lipid–water interface.[258] Therefore, the *N*-terminal region of the enzyme was a promising candidate for the incorporation of photoswitchable compounds in order to achieve photoregulation of the catalytic activity.

Azobenzene-derived amino acid **97** (Figure 61) was introduced into the 3-position of the *N*-terminal tripeptide of phospholipase A_2.[257] The modified tripeptide was further transformed into a *N*-hydroxysuccinimidyl ester. In parallel, the

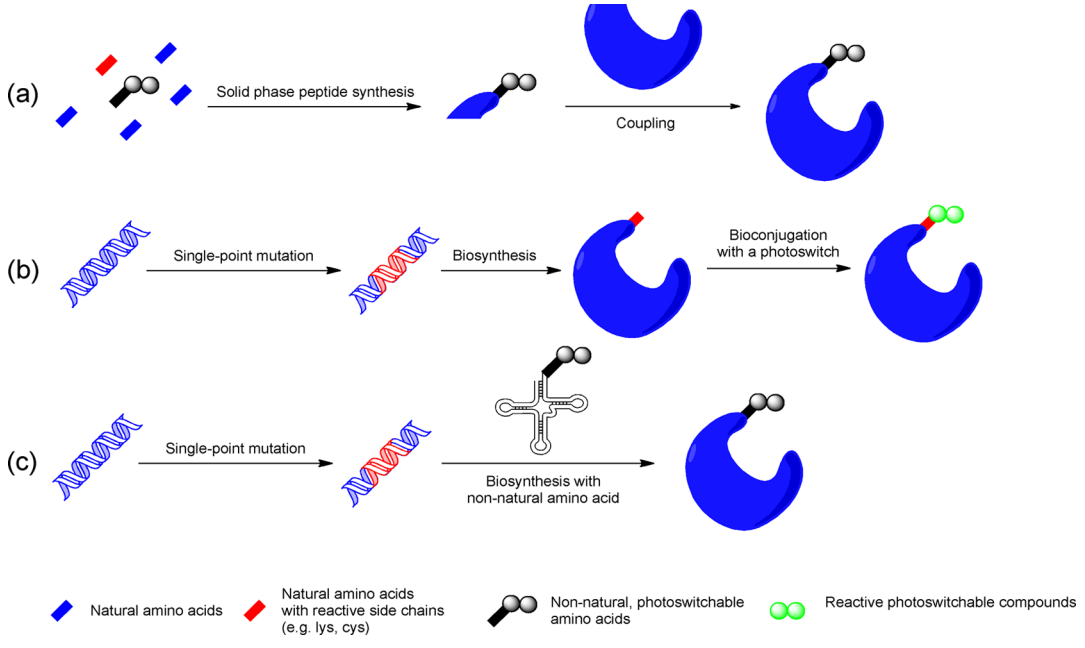

Figure 60. Methodologies used for the site-selective incorporation of molecular switches into the structure of enzymes (see text for description).

dx.doi.org/10.1021/cr300179f | *Chem. Rev.* 2013, 113, 6114–6178

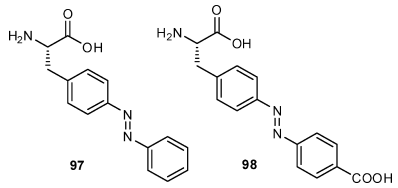

Figure 61. Photoswitchable amino acids used for the preparation of photoresponsive proteins.[257,269,272,290]

fully amidated enzyme was subjected to three cycles of Edman degradation, yielding a protein missing the first three *N*-terminal residues. The coupling of the activated tripeptide with the truncated protein followed by the removal of protecting groups yielded a catalytically active enzyme. CD studies confirmed that the α-helix content of the protein was higher when the azobenzene was in its *cis* form, as compared to the *trans* form. This change in structure was reflected in a difference in activity, which was higher for the *cis* form of the bioconjugate. The effect was attributed to better anchoring of the *cis* form at the lipid−water interface.

Another enzyme targeted with the semisynthetic method was ribonuclease S. This RNA hydrolyzing biocatalyst is a variant of ribonuclease A (E.C. 3.1.27.5, Figure 62) in which the amide

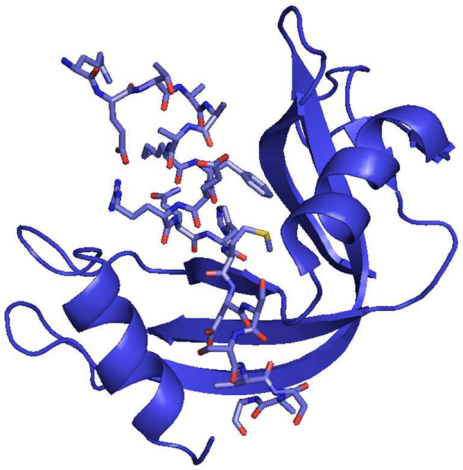

Figure 62. Structure of ribonuclease A. The *N*-terminal fragment, which corresponds to the S-peptide in ribonuclease S, is shown in detail. Adapted from coordinate data (1FS3)[260] of bovine pancreatic ribonuclease A from the protein databank, using PyMOL software.

bond between residues 20 and 21 has been hydrolyzed, giving rise to two parts: a smaller 20 amino acid S-peptide and a larger S-protein. Separately, these two parts are catalytically inactive, while it was shown that by noncovalent self-assembly they can form an active catalyst.[259] The S-peptide was conveniently prepared using standard, Fmoc-based solid phase peptide synthesis, opening the possibility of facile introduction of unnatural, photoswitchable amino acids into its structure.

This approach was independently investigated by the groups of Woolley[261] and Hamachi.[262] The first of these reports describes the modification of positions 4, 8, and 11 of peptide S, while the latter focuses on residues 1, 8, 13, and 16. In the first case,[261] a strong influence of the positioning of photoswitch **97** was observed, as the S-peptide modified in the 8-position failed to produce an active enzyme upon self-assembly with the S-protein, and the variant modified in the 11-position showed no activity change upon irradiation. The enzyme modified in the 4-position of the S-peptide, however, showed 4 times more activity in the *cis* state, as compared to the *trans* state. A strong influence of the incorporation site was confirmed by the study of Hamachi and co-workers.[262] Small changes in activity upon irradiation were observed for the enzyme modified in the 1- and 16-position of the S-peptide. Introduction of compound **97** into position 8 or 13 resulted in a decrease of activity; albeit, for position 13 almost complete (on−off) and reversible photocontrol was reported. The observations were explained by the proximity of the ribonuclease active site histidine H12.

In a follow-up study,[263] Woolley and co-workers determined the kinetic parameters of ribonuclease S with amino acid **97** introduced in positions 4, 7, 8, 10, 11, and 13. The results indicated that the response to the photoswitching was a combined effect of peptide binding, substrate binding, and the rate constant of the reaction. Furthermore, the observation of Hamachi and co-workers[262] of the complete photocontrol of the enzyme activity in the case of the variant modified in postion 13 could not be confirmed experimentally. It has also been disproved on the grounds of incomplete photoswitching of the azobenzene derivative under the given conditions.

In summary, the *de novo* approach for the preparation of light responsive biocatalysts offers tantalizing possibilities, as it allows optimization of the position of the photoswitchable amino acid and, potentially, the photochromic unit structure. It is particularly useful in situations where either an easy assembly of the synthesized peptide and the remaining part of the enzyme is possible[261−263] or the *N*-terminus of the protein requires modification.[257]

4.5.2. Introduction of a Reactive Amino Acid Side Chain into the Structure of the Enzyme. Another approach to site-selective introduction of photoswitches into the structure of enzymes takes advantage of reactive groups present in naturally occurring amino acid side chains (e.g., the amine group of lysine or thiol group of cysteine). Codons for these amino acids can be introduced into the gene of the target enzyme by site-directed mutagenesis methods (Figure 60b). Upon expression of such genes, a mutant protein is synthesized with the reactive groups present at the chosen sites. Chemical modification of these residues with a photoswitchable molecule yields a photoresponsive enzyme.

This approach was used for controlling the ATPase activity of kinesin,[264] an ATP fueled motor that is responsible for many cellular processes, including transport, cell division, and signal transduction. Two loops in the protein, depicted L11 and L12, are considered to be responsible for motility (Figure 63). Five amino acid residues (Figure 63a, highlighted in white), located within these loops, were separately mutated to cysteines, resulting in five mutants modified with azobenzene derivative **95** (Figure 57).

The results obtained upon incorporation of photoswitches into L11 depended strongly on the choice of the introduction site. Proteins modified in position 252 lost ATPase activity, which was explained by the fact that the neck region in the vicinity A252 of L11 is important for ATP binding and signal transduction. Modification of position 247, which is farther away from this site, did not affect the native ATPase activity; however, no significant changes upon irradiation were detected. Promising results were obtained upon modification of residue 249, as the resulting bioconjugate showed a reversible photoregulation of activity. The modification of loop L12

dx.doi.org/10.1021/cr300179f | *Chem. Rev.* 2013, 113, 6114−6178

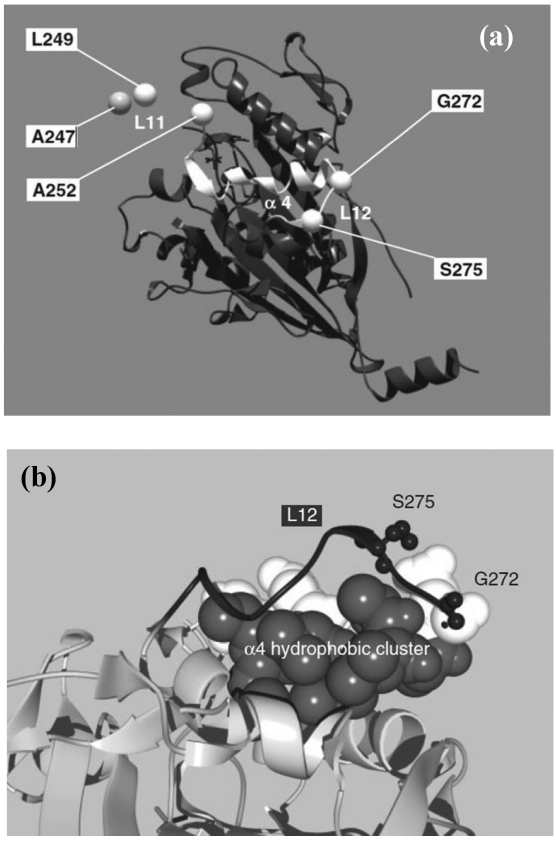

Figure 63. (a) Fragment of kinesin structure addressed by mutagenesis; (b) Loop L12 of kinesin. Reproduced with permission from ref 264. Copyright 2007 Oxford University Press.

yielded a variant modified in position 272, which showed no change in activity upon irradiation, and a variant modified in position 275, for which roughly 50% photocontrol could be measured, expressed as a difference in activity between the two states.

A detailed explanation of the mechanism of photoswitching could not be provided for loop L11, due to a lack of structural information. For the mutations located in L12, it was suggested that changes in activity were caused by a change in hydrophobicity of the azobenzene unit in the *trans* and *cis* states. The more polar *cis* photoisomer points away from the α4 hydrophobic cluster (Figure 63b), and in this respect, it more resembles the side chain of serine, which is present in position 275 in the wild-type protein. On the other hand, the more hydrophobic *trans* state can interact with the α4 cluster, inducing the distortion of L12. This hypothesis was confirmed by the activity profile, as the *cis* form was less active than the wild-type yet more active than the *trans* form. Preliminary experiments based on the introduction of spiropyran switches were reported to be successful,[264] further confirming the influence of polarity changes of the photoswitch in the two photostates rather than simply changes in sterics and geometry.

Pingoud and co-workers also employed this methodology for the preparation of modified restriction enzyme R.PvuII.[265] PvuII is a homodimeric protein (Figure 64) that has in each subunit a catalytic triad formed from D58, E68, and K70. After the introduction of pairs of cysteine residues by genetic modification, the enzyme was cross-linked with photoswitchable, bifunctional compound **96** (Figure 57), which was later dubbed a "molecular spring". In the crude mixture, the

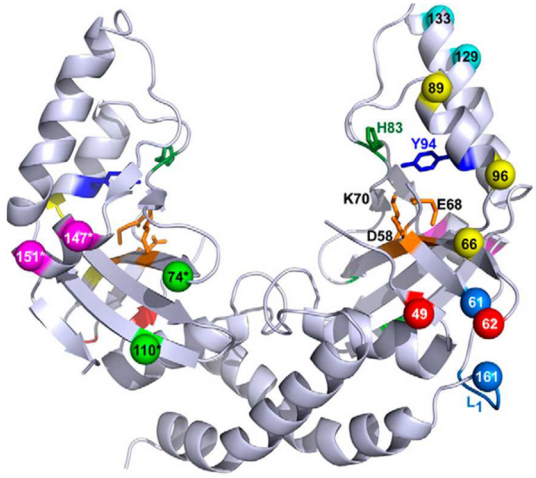

Figure 64. Structure of R.PvuII. Residues shown in orange (D58, E68, and K70) form the active site. Highlighted residues were used for cross-linking with a bifunctional azobenzene photochromic unit **96** (see text). Reproduced with permission from ref 265. Copyright 2010 National Academy of Sciences, USA.

existence of partially modified or non-cross-linked proteins was detected. Therefore, the proteins were subjected to purification by a series of chromatographic steps.

Extensive optimization of the modification sites was presented. Over 30 variants of PvuII with pairs of cysteine residues introduced in selected places were tested for levels of photoresponsiveness after modification with a bridging azobenzene unit. These variants included proteins with one or two *azo*-linkers per enzyme. Additional mutations of residues in the active site (H83 and Y94, Figure 64) and in the linker region (L1, Figure 64) were also introduced. The best variants showed a 16-fold change in activity upon photoswitching, and the effects were shown to be reversible. Cross-linking cysteine residues introduced close to the active site (positions 49 and 62, Figure 64) as well as the introduction of an additional mutation Y94F proved to be the most effective to achieve photocontrol of enzyme activity. Kinetic analysis of these variants has shown small changes in binding affinity (K_M) and considerable change in k_{cat} upon irradiation, an effect that can be explained by the modification of the active site conformation.[265]

As an alternative to the "molecular spring", which is useful for smaller proteins, a "molecular gate" approach was proposed recently for the photocontrol of the activity of a larger, homodimeric restriction enzyme R.SsoII. This approach exploits the fact that in many enzymes the active site is buried behind an entrance or tunnel through which the substrates/products diffuse. The "molecular gate" strategy relies on the incorporation of molecular photoswitches at such an entrance to the active site of an enzyme (Figure 65a) in an attempt to change the binding of the substrate upon irradiation.[266]

Site-selective introduction of molecular photoswitches **99** and **100** (Figure 65b) was achieved by introducing cysteine mutations into selected positions and subsequent modification using maleimide modified switches. Two mutations (C33S and C60S, Figure 65c) had to be introduced to prevent the modification of naturally occurring cysteines with photoswitches. This is an intrinsic problem for the strategy described in this section, as the activated photochromic units cannot be expected to react only with the active amino acid side chains

dx.doi.org/10.1021/cr300179f | *Chem. Rev.* 2013, 113, 6114–6178

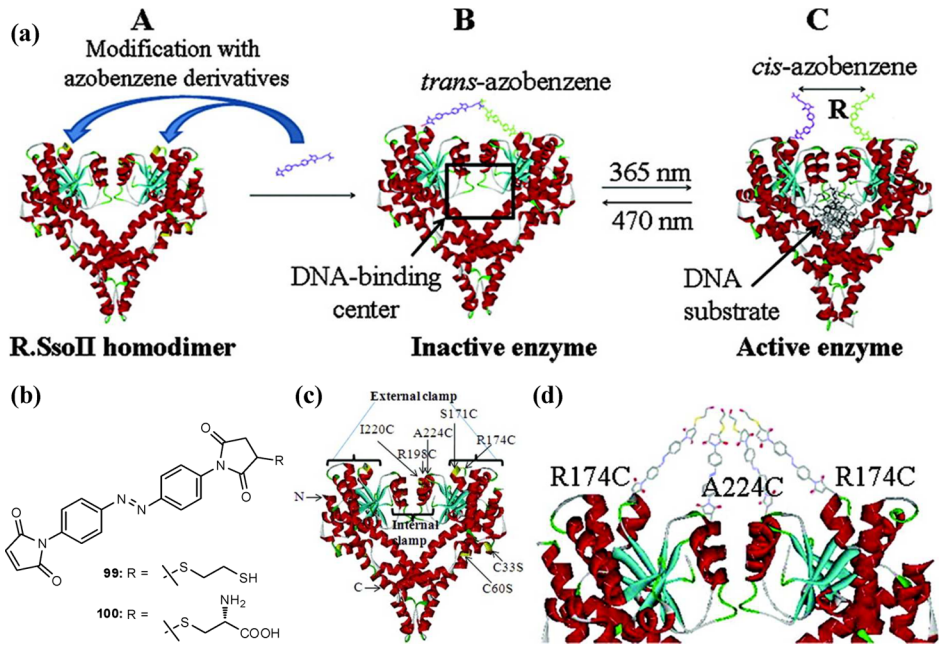

Figure 65. (a) "Molecular gate" approach for the photocontrol of restriction enzyme R.SsoII. (b) Molecular photoswitches used for the photoregulation of R.SsoII activity. (c) Mutations introduced for the site-selective incorporation of molecular photoswitches. (d) Model of the R174C/A224C mutant modified with **100**. Reprinted with permission from ref 266. Copyright 2011 American Chemical Society.

introduced by mutagenesis but will also modify the active residues that occur naturally on the surface of the protein.

Five sites were chosen for Cys mutation (Figure 65c), and a library of 11 mutants was prepared, including five single-point mutants and six combined variants. The assay, based upon the hydrolysis of a model DNA substrate, revealed that introduction of Cys residues close to the active site had a detrimental effect on the activity. Modification of seven of the most active mutants with compound **99** proceeded with up to 95% yield, and the highest level of photocontrol (2.4 ± 0.4), expressed as a rate of the activity of the nonirradiated and irradiated enzymes, was found for the R174C/A224C mutant (Figure 65d). Kinetic analysis for this mutant revealed that it had a 4-fold higher K_M as compared to the wild-type, while the V_{max} was comparable. This observation is in agreement with the "molecular gate" model presented in Figure 65a. In the next step, the mutant S171C was coupled to the molecular photoswitch **100** with a cysteine-derived amino acid terminus, which was able to form chelates with Ni^{2+} and Co^{2+}, thereby stabilizing the closure of the gate. The level of photocontrol increased from the value of 1.1 ± 0.1 to 2.2 ± 0.2 when 1 mM $NiCl_2$ was added, providing an initial confirmation of the "molecular gate" model.[266]

These examples show the possibilities offered by the introduction of a reactive amino acid side chain into the structure of a peptide/protein and its subsequent modification with a photoresponsive compound. It enables both the optimization of the switch anchoring position and, possibly, the structure of the photoswitch. It is limited, however, by the occurrence of natural reactive side chains on the surface of the wild-type protein, which can in principle also be modified during the bioconjugation, giving rise to unexpected results.

4.5.3. Introduction of Photoswitchable Amino Acids during *in Vivo* or *in Vitro* Synthesis of the Enzyme. Two methods have been used for the biosynthetic incorporation of photoswitchable amino acids into proteins (Figure 60c): the nonsense-suppression method (Figure 66a) and the frame-shift suppression method (Figure 66b). The nonsense-suppression

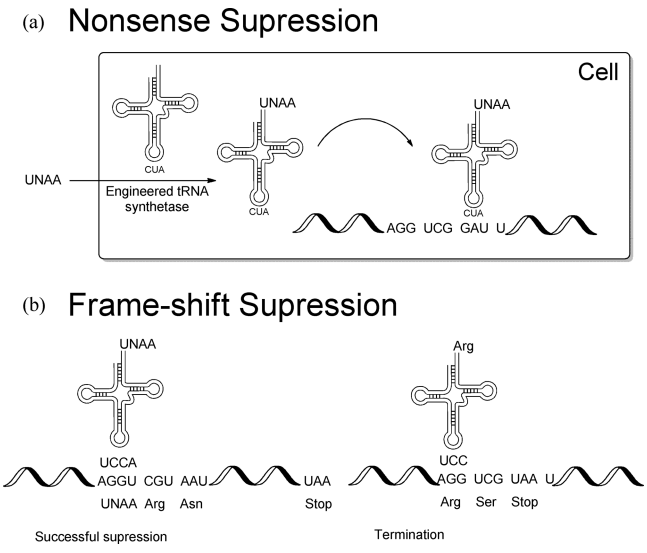

Figure 66. Strategies used for the biosynthetic incorporation of photoswitchable amino acids into proteins. (a) Nonsense-suppression method. (b) Frame-shift suppression method (Adapted with permission from ref 268. Copyright 1996 American Chemical Society). UNAA—unnatural amino acid. See text for detailed description.

method (Figure 66a), established by Schultz,[267] relies on the use of orthogonal tRNA-aminoacyl−tRNA synthetase pairs for the suppression of the amber nonsense codon. The tRNA synthetase, which is engineered in such a way that it is able to acylate the tRNA with a unnatural amino acid, is expressed within the host cell. The cells are grown in the medium that contains the unnatural amino acid. Upon entering the cell, the amino acid is ligated to tRNA, which can act as a nonsense suppressor, allowing for the synthesis of a protein with

dx.doi.org/10.1021/cr300179f | Chem. Rev. 2013, 113, 6114−6178

unnatural amino acid incorporated at the position where normally the nonsense codon is present.

The frame-shift suppression method, pioneered by the group of Sisido,[268] uses a four letter codon tRNA, aminoacylated with the unnatural amino acid, to compete with the natural, three letter tRNA during the *in vitro* protein synthesis. Upon successful use of the modified tRNA, the synthesis of the protein is continued. If the natural tRNA is used by the translation machinery of the cell, the stop codon is activated and the biosynthesis stops (Figure 66b).

The frame-shift suppression methodology was first used for the preparation of photoresponsive horseradish peroxidase (E.C. 1.11.1.7),[269] an enzyme widely used in biochemistry for signal amplification. Sixteen variants of the enzyme were prepared, with photoswitchable amino acid **97** (Figure 61) introduced in various positions. Only four of the variants retained up to 10% of peroxidase activity. This was explained by unfavorable influence of compound **97** on protein folding after introduction. One of these enzymes, modified in position 179 with the photochromic amino acid **97**, showed complete (on−off), reversible photoswitching. This was attributed to the close proximity of position 179 to the substrate binding site,[269] although no K_M values were presented to support this assumption.

The frame-shift suppression method also enabled the preparation of modified restriction enzyme *Bam*HI (E.C. 3.1.21.4) with a different strategy used for the selection of the introduction site.[270] *Bam*HI is a protein that is catalytically active only in its dimeric state. This state is stabilized by the formation of a salt bridge on the interface between two α-helices that originate from the two monomers (Figure 67).

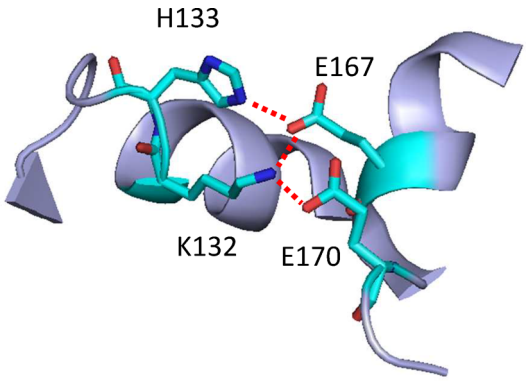

Figure 67. Fragment of *Bam*HI with the salt bridge that stabilizes the dimeric structure highlighted in color. Adapted from coordinate data (1BHM)[271] of *Bacillus amyloliquefaciens Bam*HI from the protein databank, using PyMOL software.

Three variants of *Bam*HI were prepared, in which the photoswitchable amino acid **97** was introduced at the dimer interface in place of residues 132, 167, and 170. Incorporation was determined to be 52%, 64%, and 43%, respectively. One of the mutants, modified in position 132, showed a very high (above 30-fold difference in enzyme activity) degree of photoregulation, as its activity was almost completely suppressed when the azobenzene moiety was in the *trans* state and almost completely recovered upon UV irradiation. This result was explained by lower steric hindrance for the dimer formation process when the photoswitch was in the *cis* state. The other two mutants, modified in positions 167 and 170, were inactive, attributed to misfolding of the enzyme. Finally, a correlation between the activity recovery and the irradiation time was shown as a method to control enzymatic activity. Unfortunately, the increase in activity upon UV irradiation was irreversible, as the dimeric protein did not lose its activity upon irradiation with visible light (436 nm).

In a follow up study, the group of Majima introduced amino acid **98** (Figure 61), an analog of **97**, into position 132 of *Bam*HI.[272] Compound **98** has an additional carboxyl group in the aromatic ring, which is ionized under the assay conditions, and was expected to induce a local structural change in the enzyme. Comparison of the light-mediated activity recovery in mutants containing amino acids **97** and **98** revealed that the presence of the carboxyl anion in the photoswitch promoted the initial activation of the enzyme. This was rationalized by the difference in steric interactions or by changes in the structure of the interfacial region of the enzyme.

Site-selective introduction of photoswitchable amino acids during *in vivo* or *in vitro* synthesis of enzymes is a powerful method, which allows for the optimization of the position within the enzyme in which the switch operates.[270] It is free from limitations of the previously described methods that rely on the introduction and subsequent functionalization of a reactive amino acid side chain, because there is no possibility of undesired functionalization of residues important for enzymatic activity. However, the optimization of photoswitch structure and properties using this methodology is difficult, as it requires the development of new tRNA synthetase mutants (in the nonsense suppression method) or preparation of aminoacylated tRNA molecules (in the frameshift suppression method).

4.6. Incorporation of Natural Photoactive Domains

This method relies on the *in vivo* production of a chimeric protein, which comprises the catalytically active part and the natural photoactive domain, e.g. the light-oxygen-voltage (LOV) sensitive domain of the photoactive yellow protein.[273−277] Light-induced changes in the conformation of the LOV domain influence the activity of the enzymatic component of the chimeric protein. This purely biochemical approach lies beyond the scope of this review and is only briefly mentioned here. It has been recently used for the photocontrol of such enzymes as dihydrofolate reductase (E.C. 1.5.1.3),[278,279] kinases,[280,281] and GTPases,[282] among others. It has also been used for the photocontrol of DNA binding by proteins.[283,284]

4.7. Concluding Remarks

The preparation of light-responsive biocatalysts remains a major challenge which requires an interdisciplinary approach, and as of yet no generic, widely applicable methodology has been designed to achieve this goal. Different strategies have been employed, focusing either on the important role of precise positioning, i.e. the introduction site,[261,264,269] or on the properties of the photochromic compound.[272] It has been shown that the sites in the biocatalyst structure, which can successfully be addressed toward high activity photoregulation, include the immediate surrounding of the active site,[252,255,256,263,265] the dimer interface,[270,272] and the allosteric site.[249] The optimization of the attachment point is important, as even small differences in the positioning of the photoswitch may lead to substantial differences in photocontrol[264,265] or result in misfolding of the enzyme.[270] Very good results were obtained with switches that were able to bridge two reactive sites in one enzyme.[265]

The properties (structure, functional groups, hydrophobic/hydrophilic nature) of the molecular photoswitch introduced into the biocatalyst also play a crucial role. It has been shown that changes both in geometry[270] and in polarity[264] upon irradiation can be responsible for photocontrol of enzyme activity. Even small changes in the structure of the photochromic molecule may have strong impact on the efficiency of photocontrol.[272]

While both the introduction site and the structure of the photoswitch are key to success, most of the methods used for the incorporation of molecular photoswitches into enzymes allow for convenient optimization of only one of these features. Site optimization can be performed using *in vitro* or *in vivo* biosynthesis of the protein (section 4.5.3), while the structure of the photoswitch can be easily altered in an approach where the photochromic unit is randomly incorporated into the enzyme (section 4.4). The method of introduction and subsequent functionalization of reactive amino acid side chains (section 4.5.2) seems to be the most generic with respect to optimization studies.

In general, the following important observations can be drawn from the studies reported in the literature. The incorporation of a molecular photoswitch into the structure of a protein may result in the loss of enzymatic activity[269] and a change in the PSS of the photoswitch.[256] Most methods used for the bioconjugation result in the formation of heterogeneous mixtures[48,249,251] in which enzymes with different levels/positions of introduced photochromic units are present. This implies the use of laborious purification steps.[265] The photoswitching effect can be caused by the changes in both substrate binding (K_M)[47,48,251,252] and reaction rate (k_{cat})[241,249,250,265] or by changes in both binding and rate,[263] and it can depend on the polarity of the medium.[253]

To date, few successful examples of photoresponsive enzymes exist in the literature.[244,255,265,269] In some cases, a complete, on−off control of activity has been reported, although the enzyme activity was drastically reduced by the incorporation of the molecular photoswitch.[269] Nevertheless, a generic methodology is still to be developed, and most of the potential applications have not yet been tested and confirmed, leaving a breadth of space for novel approaches.

5. PHOTOMODULATION OF LIGAND BINDING BY INCORPORATION OF MOLECULAR SWITCHES INTO SOLUBLE PROTEINS

The incorporation of molecular photoswitches into proteins has not only been used for the control of enzymatic activity. The following section focuses on the photoregulation of protein interactions with ligands.

The first reports on the alteration of protein affinity to small molecules were focused on modification of concavalin A, which is a lectin, i.e. sugar-binding protein. Random modification of concavalin A with thiophenefulgide derivative **91** (Figure 57) allowed for the photochemical control of the affinity toward a model ligand, 4-nitrophenyl α-D-mannopyranoside (Table 11).[285]

The loading degree, determined by UV−vis spectroscopy, proved to have a crucial influence on the efficiency of photocontrol. When all 12 lysine residues in the protein were modified with photoswitches, no difference in ligand binding was observed upon irradiation. At the average modification of 9 and 6 lysines, the photoswitching effect was detectable and the affinity could be repeatedly changed in time (Table 11).

Table 11. Affinity of Concavalin A, Modified with Thiophenefulgide Derivative 91, toward 4-Nitrophenyl α-D-Mannopyranoside[285]

	K_A x 10^4 (M^{-1})	
avg loading	opened	closed
0	2.2	2.2
6	1.64	2
9	0.78	1.21
12	0.64	0.64

The group of Willner studied the kinetics of binding of concavalin A, modified with spiropyran derivative **92** (Figure 57), in monosaccharide-functionalized self-assembled monolayers.[286] The derivatives of three different sugars, α-D-mannopyranose (**101**), α-D-glucopyranose (**102**), and β-D-glucopyranose (**103**), were covalently bound to monolayers on polished gold electrodes (Figure 68).

The electrodes were immersed into a buffer that contained $Fe(CN)_6^{4-}$ as an electroactive component. Upon binding of the protein to the electrodes, a time-dependent decrease in the amperometric response of the cyclic voltammogram was observed, which was attributed to the insulation of the electrode by the protein.[286] This phenomenon allowed for studying the kinetics of binding. The results are summarized in Table 12.

A high level of photocontrol was observed for monolayers modified with compounds **101** and **102**, i.e. monosacharides that associate to a specific binding site in the protein. In a control experiment, compound **103** was used, which does not exhibit specific binding to concavalin A, and the measured level of photocontrol was negligible. On the basis of these data, the photostimulated binding was explained by the perturbation of the protein binding site.

This effect was further confirmed by the studies of the conformational dynamics of modified concavalin A, using time-resolved light scattering.[287,288] It was shown that the protein undergoes a "shrinkage" upon isomerization of the photoswitch. At high loading of the photochromic compound, when on average 8 of the 12 lysine residues were modified with **92**, a rapid shrinkage of concavalin A was observed ($\tau_{1/2}$ = 60 μs) upon irradiation. It was followed by a slower ($\tau_{1/2}$ = 250 μs) conformational change leading to the formation of a more compact structure.

Hoffman and co-workers have studied the possibility of obtaining light regulated control over streptavidin−biotin interactions with potential applications for photoregulation of affinity separations.[289] Site-selective incorporation of photoresponsive polymers (Figure 69a) into the structure of the protein was achieved by the preparation of an E116C mutant of streptavidin (Figure 69b). Further modification of the reactive side chain of the introduced Cys was performed using a vinyl sulfone terminus in the polymer. The efficiency of conjugation was estimated to be 12−20%.

The DMAA and DMAAm polymers (see Figure 69) used in this study express opposite solubility in different photochromic states. While DMAA is soluble under UV irradiation and insoluble in visible light, DMAAm shows better solubility under visible light and precipitates upon UV irradiation. These features of both polymers were exploited in the binding behavior of their bioconjugates (Figure 70). The interaction with biotin could be reversibly changed by UV irradiation from about 33% to 80% of the native binding in the case of DMAA

dx.doi.org/10.1021/cr300179f | *Chem. Rev.* 2013, 113, 6114−6178

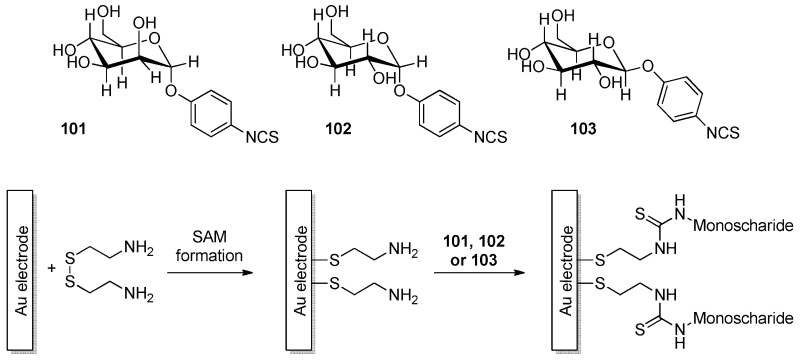

Figure 68. Formation of sugar-decorated, self-assembled monolayers on gold electrodes.[286]

Table 12. Time Constants for Concavalin A Binding to Monosaccharide-Functionalized Self-Assembled Monolayers on Gold Electrodes[286]

	time constants $\tau_{1/2}$ (s)		
		concavalin A modified with **92**	
monosacharide	concavalin A	closed	opened
101	40	60	160
102	85	220	670
103	100	100	110

(SA-DMAA curve, Figure 70) and from 90% to about 50% for DMAAm (SA-DMAAm curve, Figure 70). It has also been confirmed,that the presence of unconjugated polymer had no influence on the photoresponse (SA+DMAA(m) curves, Figure 70) and that the unmodified E116C mutant was also not photoresponsive with respect to biotin binding (SA(E116C) curve, Figure 70).

What distinguishes the photoresponsive polymer-based approach from the use of small photoswitchable molecules is the fact that the thermal reisomerization of the photochromic units in the polymer is not simultaneously accompanied by the changes in the overall structure of the polymer. The polymer reorganization happens very slowly, on the time scale of days. This results in much higher thermal stability of the photo-irradiated state. It has also been shown that when a single azobenzene unit was introduced into streptavidin E116C, using activated derivative **95** (Figure 57), no photocontrol of binding was observed. This research presents an important alternative to small photoswitchable molecules as photocontrol elements.

The photocontrol of cAMP binding to *E. coli* catabolite activator protein, CAP, has been studied by Schultz and co-

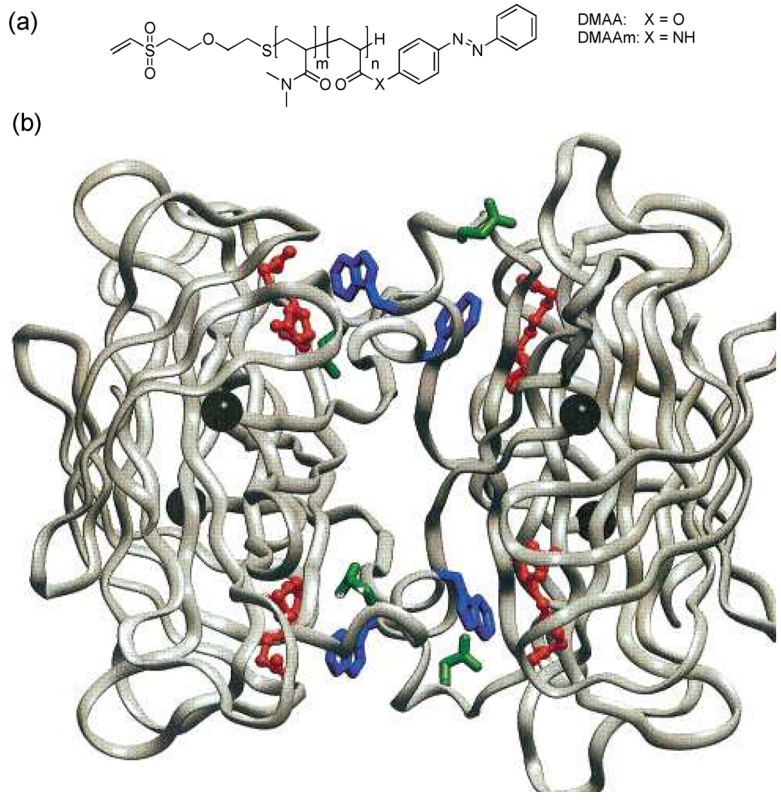

Figure 69. Elements used in the preparation of photocontrolled streptavidin. (a) Photoresponsive polymer. (b) The tetrameric structure of streptavidin. Mutated residue 116 is highlighted in green. The biotin binding site is marked by a black sphere. Reprinted with permission from ref 289. Copyright 2002 American Chemical Society.

dx.doi.org/10.1021/cr300179f | *Chem. Rev.* 2013, 113, 6114–6178

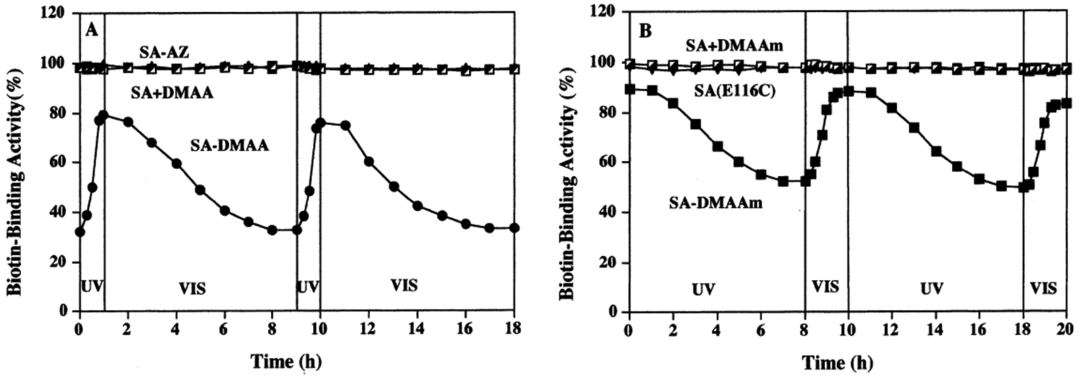

Figure 70. Light-induced changes of biotin binding affinity by streptavidin modified with photoresponsive polymers. DMAA, *N,N*-dimethylacrylamide-*co*-4-phenylazophenyl acrylate; DMAAm, *N,N*-dimethylacrylamide-*co*-4-phenylazophenyl acrylamide. Reprinted with permission from ref 289. Copyright 2002 American Chemical Society.

workers.[290] CAP is a dimeric transcriptional activator that upon binding of cAMP interacts strongly with its promoter, resulting in enhanced transcription and regulation of a number of operons in *E. coli*. Using the nonsense suppression method (see section 4.5.3), photoswitchable amino acid **97** (Figure 61) was introduced into position 71 of CAP, which lies in close proximity with the residues that are responsible for the binding interactions with cAMP.

While the photosatationary state of the incorporated azobenzene was estimated to be only about 50%, a 4-fold drop in binding to a Lac promoter was observed upon irradiation (Table 13). This surprisingly high level of photocontrol has been attributed to the fact that the protein is a dimer, which results in roughly 75% of dimers having at least one photoisomerized molecular switch in their structure.

Table 13. Photocontrolled Binding Affinities of CAP to cAMP[290]

CAP variant	binding constant K_b
wt	16×10^6 M^{-1}
I7197	4×10^6 M^{-1}
I7197 irradiated	1×10^6 M^{-1}

In a recent study, the group of Maruta has shown the photocontrol of calmodulin interacting with a target peptide.[291] Calmodulin is a Ca^{2+}-binding protein that plays a crucial role in calcium-dependent processes. Therefore, the regulation of its binding to target proteins might offer a valuable tool for the photoregulation of important events in the cell, such as apoptosis and metabolism. The protein has four Ca^{2+}-binding sites (so-called "EF-hands"): two in the *N*-terminal domain and two in the *C*-terminal domain (Figure 71).

The site-selective incorporation of photoswitches was obtained by the preparation of cysteine mutants and their modification with azobenzene derivative **95** (Figure 57).[291] Seven different mutation points were used in order to optimize the attachment site (Figure 71). They were chosen on the basis of the assumption that the photoswitch introduction site should be slightly away from the area that interacts directly with the target peptide in order not to completely abolish the binding. Three points (A57, N60, and D64) were focused around the N-terminal portion, which is responsible for the Ca^{2+}-dependent regulation of physiological CaM function. Four other mutagenesis sites (M124, E127, A128, and M144) were located in the C-terminal portion, which is responsible for the interaction with the model target peptide. For the latter role, the M13 peptide was chosen, which is a fragment of skeletal muscle myosin light chain kinase. To facilitate the analysis, it was conjugated to yellow fluorescent protein.

Efficient photocontrol was observed in the cases of three incorporation sites (Figure 71) located both in the N-terminal Ca^{2+}-binding site (positions 60 and 64) and in the peptide binding site (position 124). While the level of photocontrol was relatively low (about 3-fold change in binding affinity upon photoswitching), this study presents an interesting approach to the choice of photoswitch attachment points.

The photocontrol of ligand binding to proteins provides outstanding possibilities, as these recognition events are at the basis of many important biological processes. Therefore, in this area a substantial increase of activity can be expected in the coming years. Thus far, complete photocontrol of binding has not been reported, and the largest changes in affinity upon irradiation were around 4-fold.[290,291] An interesting approach[289] for the preparation of photoswitchable biomolecules was also reported, in which the protein of interest was modified with a copolymer comprising regular and photoactive units. This resulted in a much higher thermostability of the photostationary state and showed promise in the applications in which the protein's function had to be turned on or off for a longer period of time.

6. MOLECULAR PHOTOSWITCHES IN RECEPTORS AND CHANNELS

Controlling receptor and channel function with light has been of interest to researchers for several decades and has led to a variety of photocontrolled systems.[4,5,293−298] By incorporating molecular photoswitches into cellular receptors and transmembrane channels, it is possible to spatially and temporally control cellular signaling and function using light. Switching cellular functions on and off, by the use of an external stimulus that does not interfere with normal cell functioning, allows studying cellular processes in a unique manner. Furthermore, one can imagine that by engineering photoswitchable endogenous receptors and channels, a new generation of treatment options for various diseases could become available.

To date, most receptors addressed with photoswitchable molecules are ligand-gated ion channels. In order to obtain information about their functionality, it is important to measure changes in current through the ion channel or across the membrane. The method of choice is usually the patch clamp

dx.doi.org/10.1021/cr300179f | *Chem. Rev.* 2013, 113, 6114−6178

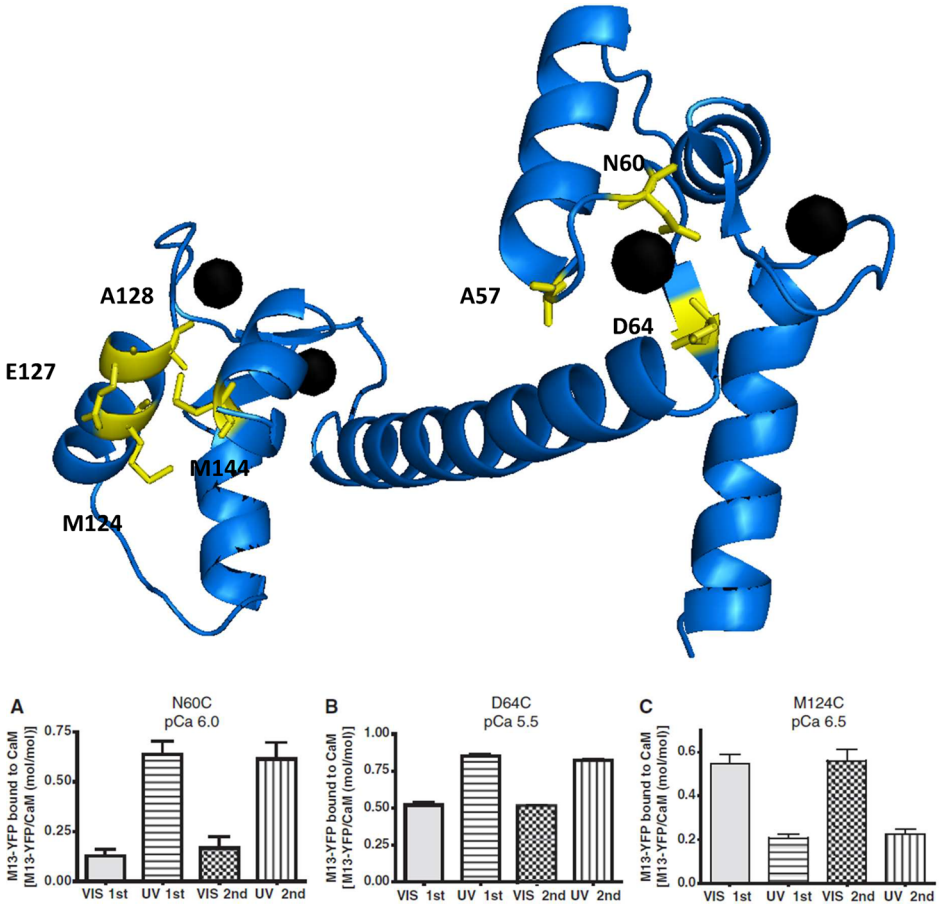

Figure 71. Upper panel: Chosen mutation sites in calmodulin (in yellow). Bound Ca^{2+} atoms are shown in black. Adapted from coordinate data (1CLL)[292] of *Homo sapiens* CaM from the protein databank, using PyMOL software. Lower panel: results obtained for chosen mutants, showing the highest level of photocontrol for the mutant in which the cysteine was introduced in position 60. Reprinted with permission from ref 291. Copyright 2009 Oxford University Press.

technique.[299,300] In short, a thin glass pipet, which functions as an electrode, is sealed onto the surface of a cell-membrane. This part of the cell-membrane surface, or patch, contains one or multiple ion channels of interest. The pipet is filled with a conductive solution in contact with a recording electrode. This electrode is connected to a low-noise current amplifier, enabling recording of the current across the membrane (see Figure 79 for an example of an electrophysiological recording of current over time). A cell can also be current clamped, which keeps the current constant and allows the voltage to be measured instead of the current. Multiple variations of the patch clamp technique exist, depending on the requirements of the study.[299]

6.1. Nicotinic Acetylcholine Receptor

The first steps toward a photocontrolled receptor were performed in the late 1960s with studies on the nicotinic acetylcholine (nACh) receptor. Acetylcholine (ACh) functions as a neurotransmitter in the human body and plays an important role in the central nervous system. Physiological functions, such as pain processing, sleep, anxiety, and cognitive function, are affected by acetylcholine.[301] There are two main receptor types on which ACh acts: the muscarinic ACh receptor and the nACh receptor.[301−303] The nACh receptors are believed to be pentameric, ligand-gated ion channels found in various tissues of the human body.[301] Upon binding of acetylcholine, the nACh ion channel opens, allowing sodium and potassium ions to flow through the channel and causing a depolarization, i.e. a change in the cell's membrane potential. This process can, for example, lead to muscle contraction.[304]

The discovery by Karlin et al. that disulfide bonds in the nACh receptor are easily reduced and thereby form sulfhydryl groups that can react with electrophilic partners led to the design and synthesis of covalently bound (conjugated) nACh receptor agonists.[305,306] These compounds contain a fragment with known affinity for the binding site of the nACh receptor and an electrophilic anchor, allowing the ligand to irreversibly conjugate with the receptor near the binding site. These studies were conducted around the same time Erlanger et al. reported two photoswitchable inhibitors (**53** and **55**, Figure 46) of the nACh receptor.[224] These inhibitors were derivatives of the known nACh receptor agonists, carbamylcholine and phenyltrimethylammonium ion, and they bore a photoswitchable azobenzene moiety.

The biological activity of compounds **53** and **55** was tested on monocellular electroplax of *Electrophorus electricus*. The membrane of these cells is known to depolarize following exposure to compounds that interact with the ACh receptor. This process could be measured with intracellular electrodes.[224,307,308] The *trans* isomers of **53** and **55** were stronger nACh receptor inhibitors than the *cis* isomers. By switching between the *trans* and *cis* states of these inhibitors, it was possible to regulate the cell-membrane depolarization with light (see section 4.1).

dx.doi.org/10.1021/cr300179f | *Chem. Rev.* 2013, 113, 6114−6178

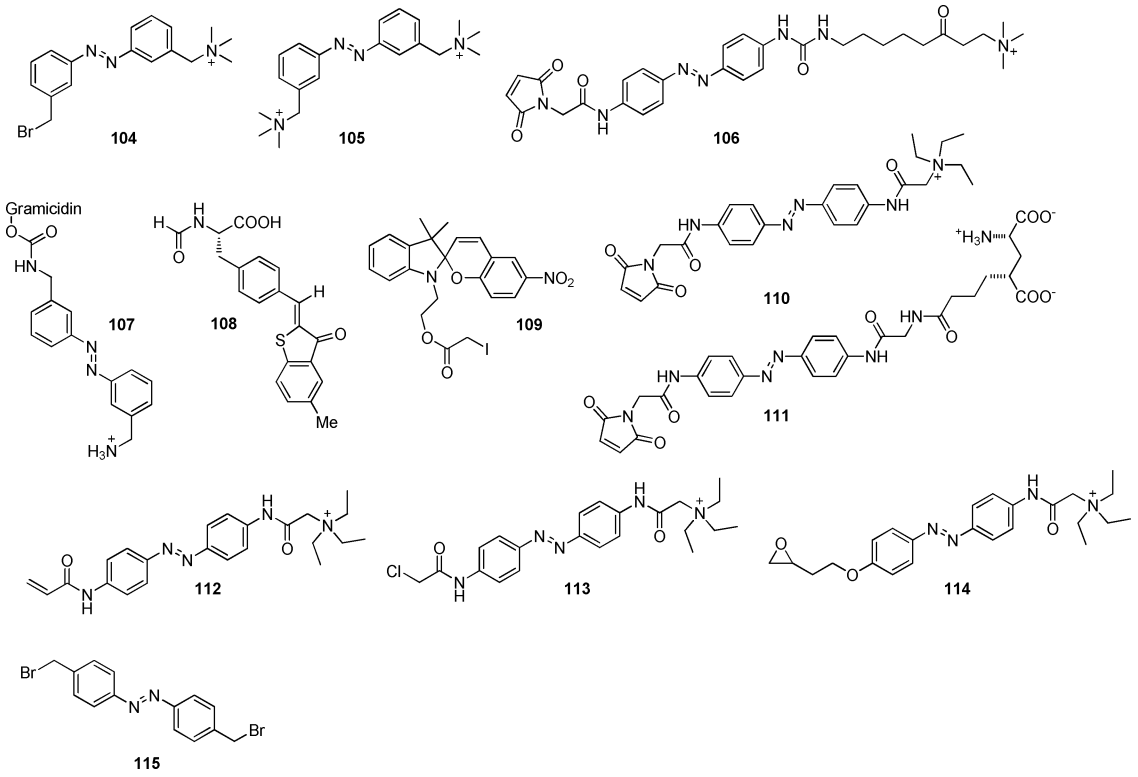

Figure 72. Compounds used for engineering photoswitchable receptors and ion channels.[62,309,318,319,325,332,353,355]

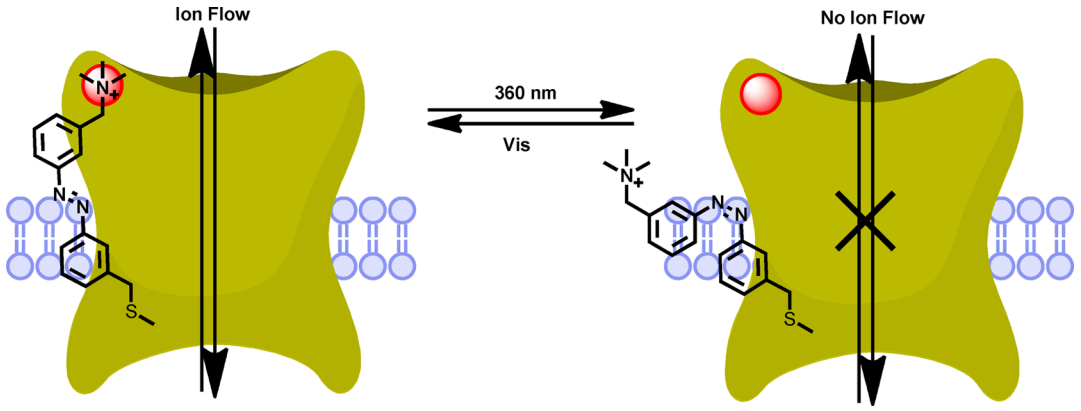

Figure 73. Photoswitchable nACh receptor.[309] When **104** was in its *trans* form, the trimethylammonium (TMA) group interacted with one of the nACh receptor binding sites (red sphere), causing the ion channel to change its conformation and allowing ion flow. *cis*–*trans* isomerization of **104**, induced by irradiation at λ = 360 nm, weakened the interaction of the TMA group with the binding pocket of the receptor, which resulted in the closing of the channel.

Although the above-described results showed the functioning of photoswitchable inhibitors, combining this concept with covalently bound agonists led to the first photoactivated receptor.[309] Compound **104** (Figure 72) consists of a photoswitchable azobenzene, functionalized with a bromide at one end and a trimethylammonium (TMA) group at the other end. The TMA group is a known ligand for the nACh receptor binding pocket.[309] Before reduction of the disulfide bonds in the nACh receptor, the uncoupled *trans* isomer of **104** (5×10^{-7} M) caused a depolarization of 3 mV. After reduction, **104** could be conjugated with the receptor and covalently bound **104** caused a depolarization of 5 mV. Also, the depolarization of the membrane by carbamylcholine[304] was completely inhibited by the covalently bound **104**. The observed effect of conjugated **104** was explained by the TMA group of the *trans* isomer interacting with the binding site, causing channel opening, followed by depolarization of the membrane. When the ligand was isomerized to the *cis* form using light, the TMA group was no longer able to bind the active site; therefore, no depolarization was detected (Figure 73).

This was the first time that a photoswitchable, engineered receptor was reported, and the usefulness of this technique for studying receptor function was shown over the next decade.[310−312] As the ligand was conjugated with the receptor, the interaction between ligand and receptor was independent of ligand and binding pocket encounter events. This enabled the study of pharmacodynamics in a unique way.[310,311] For example, Lester et al. investigated the transition between an open- and closed-nACh receptor.[310] Two hypotheses for the rate-limiting step were initially suggested: (i) the binding and

dx.doi.org/10.1021/cr300179f | *Chem. Rev.* 2013, 113, 6114−6178

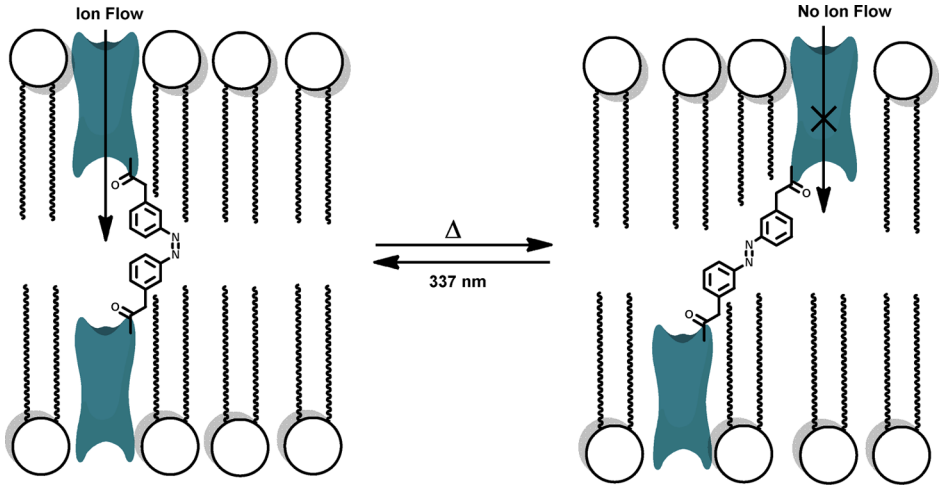

Figure 74. Proposed mechanism for the action of a photoswitchable gramicidin A channel. Two gramicidin A monomers coupled at both ends of an azobenzene moiety were expected to form one long pore through a lipid bilayer when the azobenzene was in its *cis* form, allowing ion flow. By increasing the temperature, the *trans* form was favored and the two monomers were not properly aligned, inhibiting ion flow. Adapted with permission from ref 320. Copyright 1991 Elsevier B.V.

dissociation of the agonist at the active site of the receptor and (ii) a conformational change in the receptor when the agonist was bound. It was found that the conductance induced by the conjugated receptor agonist **104** was comparable to the one induced by reversibly bound agonists. From this observation it was assumed that the rate-limiting step was not the encounter of agonist and receptor binding site, since this should have been faster for the covalently bound agonist. However, the authors could not unequivocally establish what the rate-limiting step was.

Another example of an application of a photocontrolled nACh receptor was reported by Chabala and Lester.[312] When one or more ligands bind to the nACh receptor, the channel opens and closes for a certain amount of time.[313] All of these single opening events contribute to the total conductance measured. The authors characterized the lifetime and conductance of these single opening periods using **104**. They found that the major increase in conductance resulted from nACh channel openings with a lifetime of ∼5 ms, which contributed to 80% of the total conductance.

These two examples of photocontrol of a receptor improved the understanding of receptor function. Furthermore, not only the covalently bound ligands but also the nonconjugated photoswitchable ligands were shown to be useful for nACh receptor research.[314−316] It was later found[315] that the *trans* isomer of **105** is a highly potent ACh receptor activator with an activity that is 50-fold higher than that of acetylcholine. However, the *cis* isomer has less than 1% of the activity of the *trans* isomer. This led to the conclusion that the binding of a ligand to the ACh receptor binding site required multiple intermolecular interactions that were previously unknown. To test this, derivatives of **105** with slightly different molecular structures were synthesized.[315] When comparing the activities of these derivatives, the molecular features that were important for a ligand in order to bind to the nACh receptor binding site were elucidated (*vide infra*).[315] This information gave new structural insight into the nACh receptor binding site. It was concluded that the ACh receptor has a planar hydrophobic region in its binding site that interacts with both hydrophobic and electron-donating functional groups. Furthermore, it was proposed that the ACh receptor binding site possesses two anionic regions. This study shows how photoswitchable compounds can not only elicit spatial and temporal control but also help with fundamental research on the nature of receptors.

Recently, a successful engineering of a photocontrolled nACh receptor was achieved using a more widely applicable method,[317] applied earlier to create a photocontrollable Shaker Channel[318] and ionotropic glutamate receptor[319] (see sections 6.4 and 6.5, respectively). The method is similar to the approach exploited by Erlanger et al.[309] in that an azobenzene photoswitch was used with at one side an agonist (trimethylammonium group) and at the other side a maleimide moiety that can covalently bind to the receptor protein (**106**, Figure 72). Maleimides react selectively with cysteine residues, covalently anchoring the photoswitch to the receptor. Cysteine residues can be genetically introduced into receptor proteins, which renders this method widely applicable. When a suitable site for cysteine introduction is chosen, the agonist attached to the photoswitch can interact with the receptor binding pocket in one photoisomeric form of the molecule. However, when the compound is photoisomerized, the agonist is not in the proximity of the binding pocket and cannot interact with it. In the case of the nACh receptor, three suitable mutation sites were selected, including the E61 of the β4 subunit of the heteropentameric neuronal nACh receptor.[317] This mutant receptor was expressed in *Xenopus* oocytes and screened for activity using voltage-clamp recordings. Following the incubation with **106**, exposure to 380 nm light produced an inward current of 6.8 ± 1.3% of the saturating cholinergic current. This effect could be reversed by irradiation with 500 nm light, after which the receptor still responded normally to acetylcholine. Oocytes expressing mutated nACh receptors with introduced cysteines at the two other selected sites showed similar results.

6.2. Gramicidin A

A different approach for using light to control ion channel function was exploited in the early 1990s.[320] Gramicidin A is an antibiotic peptide that is synthesized by *Bacillus brevis* and is supposed to dimerize in amphiphilic environments, such as lipid vesicles and membranes, to form a pore-like structure.[321]

dx.doi.org/10.1021/cr300179f | *Chem. Rev.* 2013, 113, 6114−6178

Monovalent cationic ions and water molecules are able to pass through these pores.[322] Gramicidin A channels are of interest for transmembrane research because of their size, their availability, and their susceptibility for chemical modification.[323,324]

Two gramicidin A monomers were linked with an azobenzene switch in such a way that when the switch was in its *cis* form, the two monomers form one long pore spanning the lipid membrane (Figure 74), allowing ion transport.[320] It was hypothesized that when the azobenzene moiety was switched to its *trans* form, the monomers should no longer be able to align, limiting ion transport (Figure 74). It was possible to modulate the conductance of these ion channels with light, which was measured using electrophysiological recordings.

The *trans* isomer showed a conductance of about 9 pA at a membrane potential of 200 mV, where it was expected to show no conductance at all.[320] On the other hand, irradiation with light at wavelengths between 320 and 400 nm, which favored isomerization to the *cis* isomer, led to channels with "flickering" behavior. An open time of about 40 ms and a closed time of 13 ms were measured. During the open time, the channels showed a conductance of 14 pA at a membrane potential of 200 mV, which is comparable to the conductance of a normal gramicidin A channel. The attempts at explaining the unexpected results using a single model were unsuccessful.[320] However, these studies did prove the possibility of photomodulating channel conductance.

A different approach for photocontrolling the opening and closing of gramicidin A channels was exploited a few years later.[325] It was discovered that coupling an alkylamine to the *C*-terminal end of a gramicidin A *via* a carbamate linkage (Figure 75) could block the cation flux across the membrane.[327] This blockage was shown to be dependent on the length of the linker (Figure 76), where the use of longer alkyl chains resulted in decreased channel blockage.[325] Introducing an azobenzene photoswitch into this linker (**107**, Figure 72) enabled the change of linker length by switching between the *cis* and *trans* forms upon irradiation with light (Figure 76), and channel opening and closing could be photocontrolled.[325] A conductance of 14.9 pA at a potential of 200 mV was measured using single channel recordings in a lipid bilayer when both azobenzenes at the entrance and the exit of the channel were in their *trans* state. Irradiation with 337 nm light resulted in isomerization to 85% of the *cis* isomer, and a maximum conductance of 12.8 pA was measured. Here, four different levels of conductance were observed, corresponding with *trans*/*trans*, *trans*(in)/*cis*(out), *cis*(in)/*trans*(out), and *cis*/*cis*. The changes in conductance between the different levels were 1.1, 2.6, and 3.5 pA, respectively. Additionally, the opening and closing of the channels was shown to be reversible.

A third attempt at creating a photoswitchable gramicidin A channel was exploited using a photoswitchable amino acid, substituted into the gramicidin A peptide (for the introduction of photoswitchable amino acids into proteins, see also sections 4.4 and 4.5).[62] A hemithioindigo-derived switch was ligated to an amino acid, giving rise to compound **108** (Figure 72). Subsequently, the amino acid was incorporated into the gramicidin A peptide at position one, replacing valine. Irradiation with 406 nm light resulted in *Z* to *E* isomerization, with a photostationary state of 72% *E*. Irradiation with 480 nm light produced ~100% of the *Z* isomer. The dipole moment was calculated to be 2.8 D for the *Z* isomer and 1.2 D for the *E* isomer. Furthermore, it was believed that the distance between

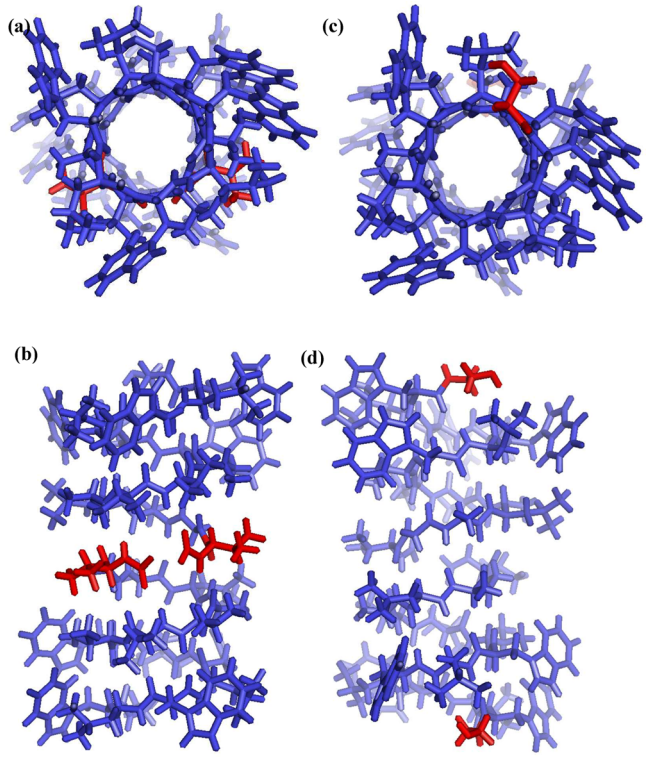

Figure 75. Structure of gramicidin A dimer and attachment/modification points shown in red. (a and b) Top and side view of gramicidin A dimer with the N-terminal end highlighted in red as attachment point of the azobenzene switch as described by Stankovic et al.[320] This is the same position as the amino acid valine, which was replaced by a hemithioindigo-based amino acid by Lougheed et al.[62] (c and d) Top and side views of gramicidin A dimer with the C-terminal ends highlighted in red. This position was used by Lien et al.[325] to attach their azobenzene group by a carbamate linkage. Adapted from coordinate data (1MAG)[326] of Brevibacillus brevis gramicidin A from the protein databank, using PyMOL software.

the cation in the pore and the carbonyl oxygen (negative dipole) of **108** influenced the energy of dipole−ion interaction (Figure 77). In the *Z* form, this distance was 12.5−13.5 Å, and for the *E* form, this distance was 8.5−11.8 Å.[62] From these data, it was predicted that the channel would have a higher conductance with the switch in the *E* form. Next, the modified gramicidin peptide was added to membranes of diphytanoylphosphatidylcholine/decane and single channel currents were recorded. As with the previous photoswitchable gramicidin A example, four different conducting states were observed corresponding to *E*/*E*, *E*/*Z*, *Z*/*E*, and *Z*/*Z* isomers. When using Na^+ as the cation and a voltage of 200 mV, a current of 1.33 pA was measured for the *Z*/*Z* configuration, 1.75 pA for *E*/*E*, and 1.50 pA for both of the intermediate states. When Cs^+ was used, the relative differences in conducting states decreased to 6.0 pA, 6.5 pA, and 7.0 pA for the *Z*/*Z*, *E*/*E*, and intermediate configurations, respectively.[62]

The studies with gramicidin A proved that it is relatively easy to manipulate photoswitchable peptide channels.[62,320,325,327] Furthermore, it was feasible to exploit various approaches, all resulting in photocontrol over gramicidin A channel opening and closing. Some of them even were shown to be highly sensitive, which was apparent from the observation of three or four conducting levels corresponding to the *E* and *Z* forms of the various photoswitches.[62,325]

dx.doi.org/10.1021/cr300179f | *Chem. Rev.* 2013, 113, 6114−6178

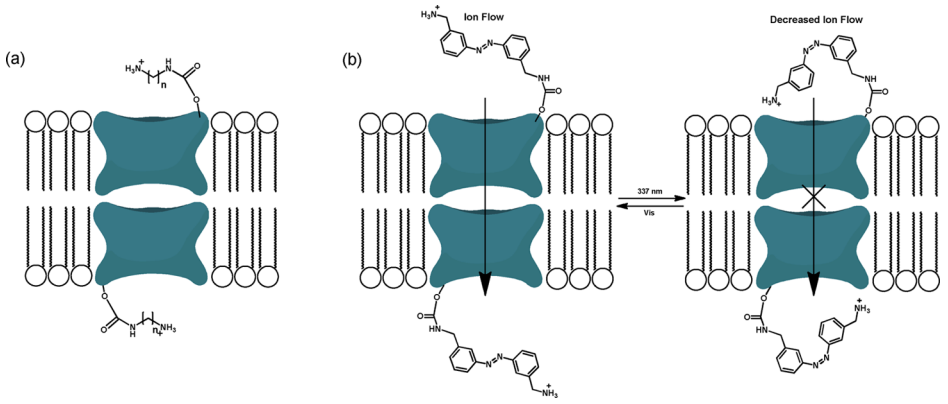

Figure 76. (a) Modified gramicidin used to study the influence of linker length on channel blockage.[325] (b) A photoswitchable gramicidin A channel.[325] An azobenzene tether with a cationic group at the end was attached to the entry and the exit of a gramicidin A channel. When the azobenzene was in its *trans* form, the channel was unblocked and ion flow was possible. Irradiation at λ = 337 nm induced the isomerization of the azobenzene to its *cis* form, which resulted in blocking of the channel, and ion flow was reduced. The channel could be unblocked by irradiating the azobenzene switch with visible light.

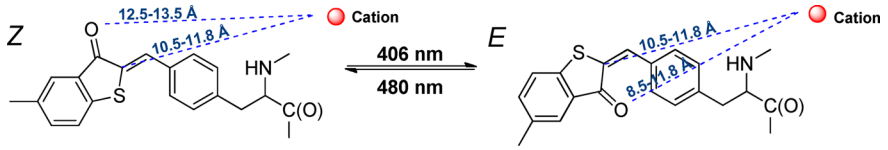

Figure 77. Change in distance between a cation in the middle of a gramicidin A channel and negative dipole of a hemithioindigo amino acid upon switching. The distance between the cation and carbonyl oxygen changed, while the distance between the cation and double bond carbon in the thioindoxyl ring remained constant. This change in distance was believed to influence the energy between a cation and the dipole. Adapted with permission from ref 62. Copyright 2004 Royal Society of Chemistry.

Follow-up experiments could focus on the use of these channels in more biologically relevant environments, such as cells. For example, it could be possible to incorporate these photoswitchable channels in a bacterial cell membrane by simply adding these molecules to the bacteria's surrounding environment, allowing the potential for bacterial cell death to be controlled by light. This approach would result in photoswitchable antibiotic agents.

6.3. Mechanosensitive Channel of Large Conductance

The mechanosensitive channel of large conductance (MscL) helps bacteria adapt to changes in osmotic pressure.[328−330] The channel opens in response to mechanical force on the cell membrane caused by an influx of water. It consists of five helices that contract *via* hydrophobic interactions. These interactions can be disrupted by polar groups that attract water and lead to hydration of the pore.[331] To engineer a photosensitive MscL, first the glycine at position 22 of the channel was mutated to a cysteine (Figure 78).[332] Then an uncharged spiropyran core modified with an iodoacetate moiety, **109** (Figure 72), was reacted with this cysteine. When the spiropyran moiety was exposed to 366 nm light, its ring-opening resulted in a charged zwitterionic merocyanine structure (Figure 78). This charged molecule disrupted the hydrophobic interactions in the channel, causing it to open. When the photoactive protein was embedded in a lipid membrane, patch clamp recordings showed that the channel could be opened and closed by changing the wavelength of light used for irradiation. When exposed to 366 nm light, currents of 20 pA were measured at a set potential of 20 mV, indicating the opening of the channel. Subsequent exposure to visible light significantly reduced the channel opening events, and the currents were decreased to almost 0 pA (Figure 79).

The fact that the structure and functioning of this channel was well described made it simpler to predict how it could be mutated and made photoswitchable. Although the number of channels that can be controlled *via* manipulation of hydrophobic effects may be limited, the proof of concept is a valuable step. When these photoswitchable channels were incorporated in vesicles or capsules, content release could be externally controlled, making this concept highly interesting for application in (drug) delivery systems.[332,334]

6.4. Shaker Channel

In 2004 a photoswitchable ion channel was reported by Kramer, Trauner, and co-workers,[318] developed using a method similar to the one used to obtain a photoswitchable nACh receptor.[309] In this case,[318] the ion channel of interest was the voltage-dependent Shaker K^+ channel. This channel responds to a change in membrane potential and opens when the potential reaches a certain positive threshold.[335] After this activation, the channel enters a state of inactivity in which it is nonconducting and cannot be activated again by depolarization.[336] The Shaker K^+ ion channel can be blocked by tetraethylammonium (TEA) ions.[337] To make the blocking of this channel photoresponsive, a quaternary ammonium moiety was coupled to an azobenzene group. To conjugate this molecule with the channel, a maleimide group was coupled to the other end of the azobenzene moiety (**110**, Figure 72). The maleimide was used to selectively bind to cysteines present on the surface of a Shaker channel. The distance between glutamic acid residue 422 in the channel protein and the channel's exit corresponded to the length of the photoswitchable molecule in its *trans* form. Thus, this glutamic acid was chosen for mutation to a cysteine for a ligation site for the maleimide group of **110**. When the maleimide was covalently bound to the cysteine, the

dx.doi.org/10.1021/cr300179f | *Chem. Rev.* 2013, 113, 6114−6178

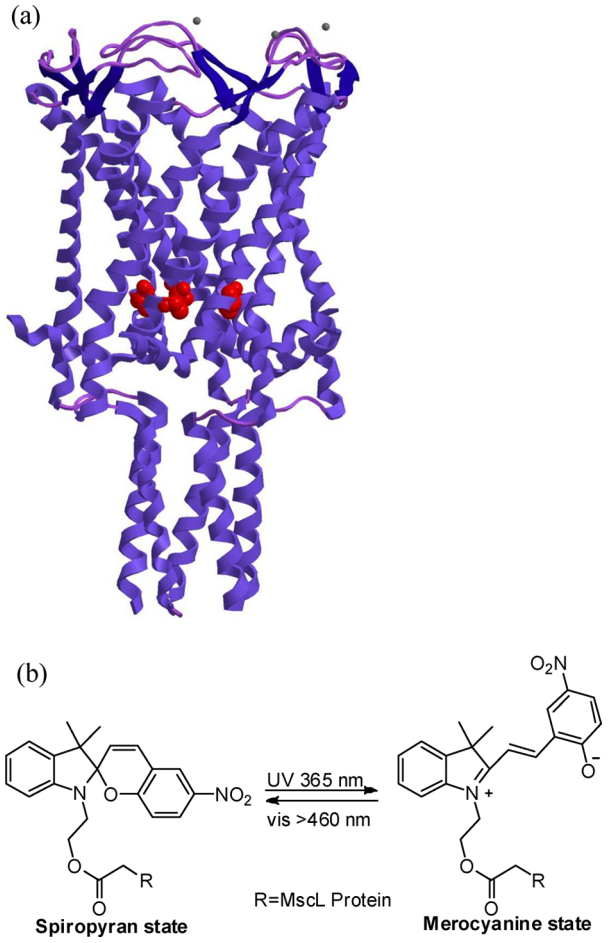

Figure 78. (a) Structure of the MscL protein. The attachment site of the photoswitch[332] is shown in red. Adapted from coordinate data (2OAR)[333] from the protein databank, using PyMOL software. (b) Photoswitching between an uncharged spiropyran state and a charged zwitterionic merocyanine state.[332] In the merocyanine state, the charges disrupted the hydrophobic interactions in the inside of the channel, which caused the channel to open. When switched back upon irradiation with visible light, the merocyanine state returns to the uncharged spiropyran state, which restored the hydrophobic interactions and closed the channel. Adapted with permission from ref 332. Copyright 2005 National Academy of Sciences.

TEA group of **110** was within proximity to block the Shaker channel with the photoswitch in the *trans* form (Figure 80a). However, when the azobenzene was switched to the *cis* form, the length of the photoswitchable molecule was insufficient for the TEA group to block the channel (Figure 80a). Experiments, performed on mutated *Xenopus laevis* oocytes and cultured hippocampal neurons, revealed that during exposure to UV light the channel was open and conducting, and a current of ~1 nA was measured using patch clamp recordings on an oocyte expressing the mutated Shaker channel (Figure 80b). When, instead of exposure to UV light, visible light was used, the current dropped dramatically to ~100 pA, indicating that the channel was blocked. These cycles could be repeated several times. When the light-activated channels were expressed in hippocampal pyramidal neurons,[318] similar results were observed, indicating photocontrol of neuronal excitability was achieved.

From a bioengineering perspective, these experiments are a major step forward compared to the photomodulation of gramicidin A and MscL channels. While these photoswitchable systems clearly proved the concept and feasibility of photoswitchable receptors and channels, the Shaker channel experiments were taken to a next level, since the method was tested on living cells instead of artificial lipid bilayers and vesicles. With this, photocontrol over cellular communication became an even more realistic possibility.

6.5. Ionotropic Glutamate Receptor

After developing a photoswitchable Shaker channel, Trauner and co-workers changed their focus to the ionotropic glutamate receptor (iGluR).[319] The glutamate receptor (GluR) plays an important role in neuronal communication in the brain.[338] Different subtypes of GluRs have been described, i.e. ionotropic as well as metabotropic.[339] Its ligand, L-glutamate, is the major excitatory neurotransmitter in the mammalian central nervous system.[340] The GluRs are also involved in the pathophysiology of brain functioning.[341]

A similar approach as with the Shaker channel[318] was exploited. Namely, a tethered agonist was synthesized consisting of an azobenzene with an electrophilic maleimide at one end and glutamate (acting as an agonist) at the other end (compound **111**, Figure 72).[319] A well established cell line, HEK293, which is easy to grow and transfect,[342] was used to study the activity of this tethered agonist **111**.

iGluR were mutated at the 439 position to bear a cysteine group to which the maleimide could bind. After attachment of **111**, iGluR was successfully turned on and off by irradiating the cells with different wavelengths of light. The wavelength range from 300 to 500 nm was scanned, and at 380 nm the greatest conductance of 900 pA was measured at a voltage of −60 mV, indicating that this was the optimum wavelength for opening the channel. The optimum wavelength for closing the channel was found by irradiating the opened form with light of wavelengths ranging from 400 to 600 nm. At 500 nm the smallest conductance of almost 0 pA was measured, and this was chosen as the optimum wavelength for closing the channel.

A major improvement over the methodology presented for the Shaker channel[318] consists of using a ligand that binds to the binding site of the receptor and does not block the channel itself. In other words, the receptor could be allosterically controlled.

One might consider, for instance, addressing metabotropic receptors[343] as well. G protein coupled receptors (GPCRs) are a class of transmembrane receptors that activate signal transduction upon binding of a ligand.[344] Interestingly, a widely used model for studying GPCRs is rhodopsin, a photoreceptor found in the retina of vertebrates.[345] Rhodopsin is covalently attached to a photoswitchable compound, retinal. Exposure to light causes a *cis* to *trans* isomerization of retinal, which leads to conformational changes within rhodopsin initiating signal transduction.[344] It might be possible to address other GPCRs using photoswitchable tethered agonists allowing photocontrol of signal transduction.

In follow-up studies with **111**,[24,346−349] Isacoff, Trauner, and co-workers studied the mechanisms by which **111** was conjugated to iGluR.[24] It was assumed that the maleimide moiety could not bind to the cysteine at the same time as the glutamate moiety of *trans*-**111** was interacting with the binding site of the receptor. For this, the distance between the two groups was too large. However, *cis*-**111** did have the right distance between the two groups, allowing them to interact at the same time. Taking advantage of this would enable selective

dx.doi.org/10.1021/cr300179f | *Chem. Rev.* 2013, 113, 6114−6178

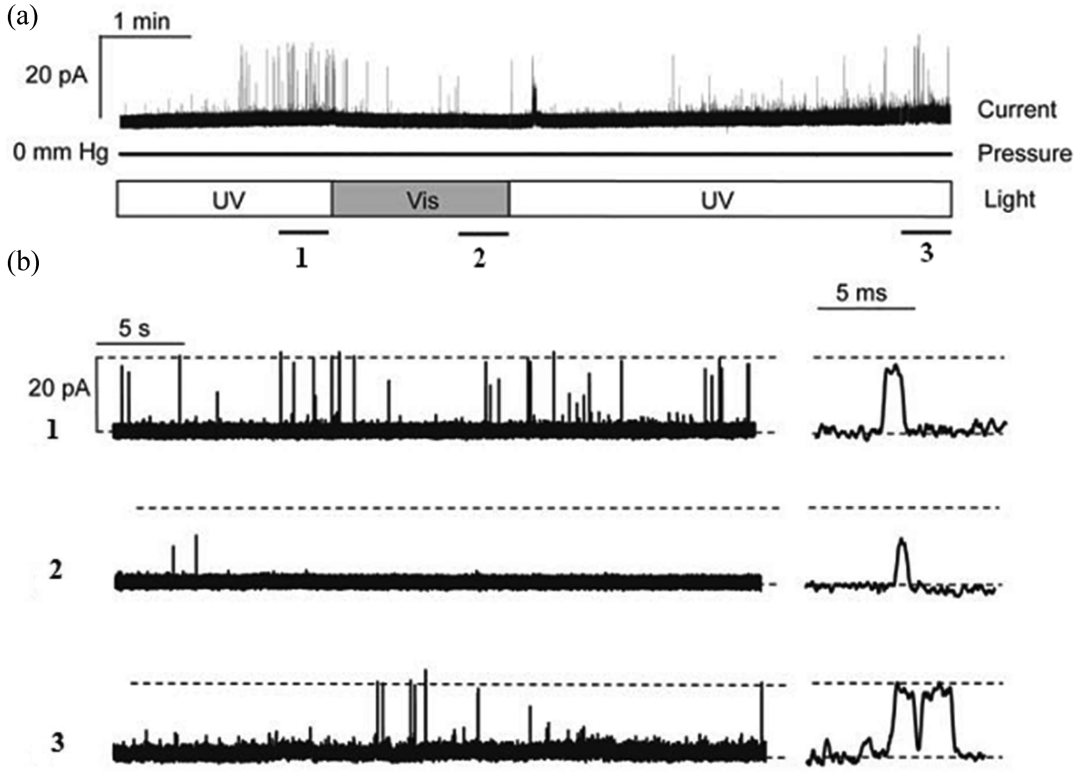

Figure 79. Electrophysiological recordings of the modified MscL channel exposed to UV and visible light. (a) The current was measured at 20 mV, and current peaks correlated with channel openings. (b) Close up of the electrophysiological recordings from part a. Figures 1, 2, and 3 correspond to the area designated in part a. Reproduced with permission from ref 332. Copyright 2005 AAAS.

conjugation of one of the photoisomers of **111** with the mutated iGluR by affinity labeling.

This phenomenon was studied using calcium imaging.[24] In this technique, a fluorescent calcium indicator gives a signal when calcium concentration is high, which was the case when the calcium permeable iGluR is open. Therefore, a high signal corresponds with a high number of open iGluR channels, expected to be triggered by **111**. Incubating HEK293 cells transfected with the mutated iGluR with **111**, under visible light irradiation, resulted in a weak signal of 10.7%. A more than 3-fold higher signal of 36.1% was measured when the cells were incubated with **111** under UV irradiating conditions, favoring the *cis* form of the switch. To prove the affinity labeling, a control experiment was performed, in which the cells were incubated with *cis*-**111** and competing concentrations of free glutamate. Subsequent calcium imaging produced a 3-fold lower signal as compared to the receptor incubated without free glutamate, indicating that in the latter case affinity labeling occurs.

Additionally, when only a small part of a cell culture was irradiated with light of a wavelength that favored the *cis* form and the rest of the cells were irradiated with light of a wavelength that favors the *trans* form, only the former could conjugate with **111** by affinity labeling (Figure 81). This resulted in a high concentration of conjugated **111** in only a small, spatially designated part of the cell culture. This experiment showed it was possible to spatially control photoswitchable agonist conjugation. This method could possibly allow controlling the conjugation of different photoswitchable agonists in a single cell culture. Further experiments could be performed to study the behavior of cells in one culture conjugated to different photoswitchable agonists and to gauge how light controls the intercellular communication.

Another follow-up study focused on the usage of **111** *in vivo*.[346] Experiments were performed on zebrafish.[346] Normally, zebrafish respond to mechanical pressure by moving away. First, the gene for mutated iGluR bearing the cysteine residue was introduced in embryonic zebrafish. When the mutated fish were incubated with **111**, normal behavior was observed. Following irradiation with UV light favoring the *cis* form of **111**, 28% of the fish did not elicit a touch response. When these fish were subsequently irradiated with light favoring the *trans* form of **111**, 81% of the nonresponding fish regained a normal touch response. These results indicate that **111** was capable of reversibly interfering with neuronal signaling *in vivo*. Furthermore, **111** gave no evidence of toxicity, and delivery of this compound to the active site was relatively easy.[346]

More recently, a hybrid glutamate receptor, developed from a mammalian and a prokaryotic glutamate receptor, was reported to be addressable with light using the same strategy as with the natural occurring iGluR.[347] This shows that not only naturally occurring receptors can be altered with photoswitchable compounds, but that it is possible to expand the scope by designing and engineering new hybrid receptors that can be chemically modified to become photoresponsive.

It is believed that in some diseases which result in blindness the photoreceptors lose their function while the retinal neurons remain alive.[350] Adeno-associated viral vectors (AAV), which have proven to be capable of introducing genes *in vivo*,[351] were used for expressing mutated iGluR receptors in blind *rd1* mice retinal ganglion cells (RGCs),[352] which are known to lack photoreceptors. Visually evoked field recordings (VEPs) were taken from the primary visual cortex of wild-type mice and *rd1*

dx.doi.org/10.1021/cr300179f | *Chem. Rev.* 2013, 113, 6114–6178

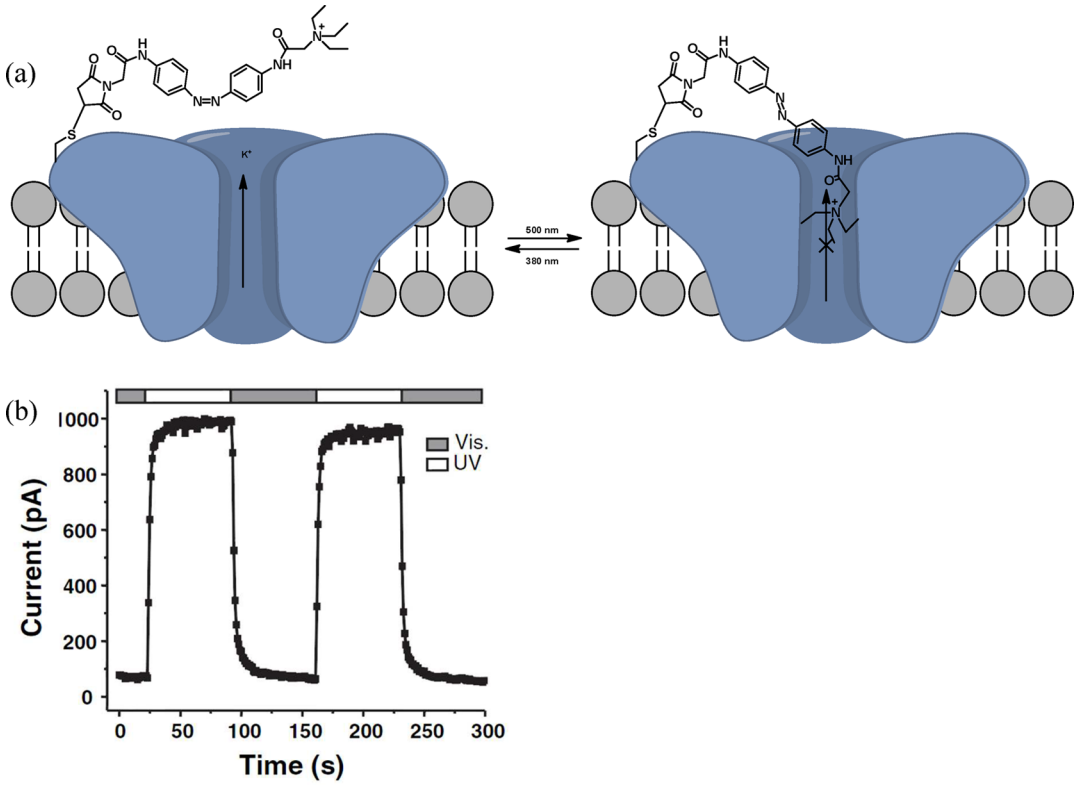

Figure 80. (a) Photoswitchable Shaker Channel. The channel was open when the azobenzene was in its *cis* form. However, when the azobenzene was switched to the *trans* form, the TEA group blocked the exit of the channel. Adapted with permission from ref 318. (b) Patch clamp recording of an oocyte treated with 100 μM **85** for 30 min. When exposed to UV light (λ = 380 nm), a current of approximately 1 nA was measured. Under visible light (λ = 500 nm), a channel current of 100 pA was measured, indicating the channel was blocked. Reprinted with permission from ref 318. Copyright 2004 Nature Publishing Group.

mice expressing the mutated iGluR, in the presence and absence of **111**. VEPs were used as a measure for light responsiveness. Electrodes were placed just below the surface of the cortex, contralateral to the stimulated eye, and the response to light was recorded as VEPs. VEPs were restored to 50% in *rd1* mice incubated with **111** compared to wild-type mice when exposed to 380 nm light (Figure 82a).[352]

Furthermore, iGluR, in combination with **111**, was capable of restoring the pupillary reflex. This reflex makes the pupil contract when exposed to light. iGluR and **111** restored almost 60% of the pupillary response in triple knockout mice that lack phototransduction and papillary reflexes (Figure 82b).[352]

This work shows the great potential molecular photoswitches have for usage in the biomedical field, and they might be used in the future to treat illnesses. Furthermore, it clearly proves the importance of interdisciplinary research in order to make achievements like this possible.

6.6. Endogenous Ion Channels

While the methods developed for the photocontrol of the iGluRs are highly promising,[319,346,348,349,352] their *in vivo* use is limited by the need to mutate the receptors to introduce a cysteine site to which the molecular photoswitch binds. To overcome this problem, Kramer, Trauner, and co-workers introduced a method based on photoswitches that ligated with naturally occurring nucleophilic amino acids of voltage-gated K^+ channels, thereby avoiding the need to mutate the receptor first.[353] These photoisomerizable small molecules were regarded as photoswitchable affinity labels (PALs) (see also section 4.4).

The photoswitchable ligands used by Trauner and co-workers[353] consisted of a photochrome functionalized with a quartenary ammonium group, that blocks K^+ channels, at one end and an electrophilic group at the other end. The electrophiles acrylamide (**112**, Figure 72), chloroacetamide (**113**, Figure 72), and an epoxide (**114**, Figure 72) were tested. These electrophilic groups were chosen to react with nucleophilic amino acids present in the natural receptor, unlike the maleimide moiety in **111**, which relied on an artificially introduced cysteine for conjugation. In cultured neurons, *trans*-**112** blocked 72% of the voltage-gated K^+ currents. Exposure to 380 nm light relieved channel blockage, and 117% of the current was recovered as compared to pretreatment. Similar results were observed with **113**, while **114** appeared to be toxic.

To test whether this method could be applicable in tissues, rat cerebellar slices were subjected to treatment with compound **112**.[353] This research aimed to address the concerns focused on the wavelength of the light used to switch the photoswitchable ligands, as UV light may not be able to penetrate the tissue deep enough to reach the switch. Furthermore, photoswitchable ligands may not have been able to reach the active site. However, **112** could block and unblock K^+ channels in cerebellar slices when irradiated with 500 and 360 nm light, respectively. Later it was suggested that, in contrast to the assumption that guided the design of PALs, compound **112** does not covalently bind to the receptor protein, but that it remains in proximity of the binding site by association with the plasma membrane.[354] This could provide an alternative explanation for the long lasting channel blockage of **112**.

dx.doi.org/10.1021/cr300179f | *Chem. Rev.* 2013, 113, 6114–6178

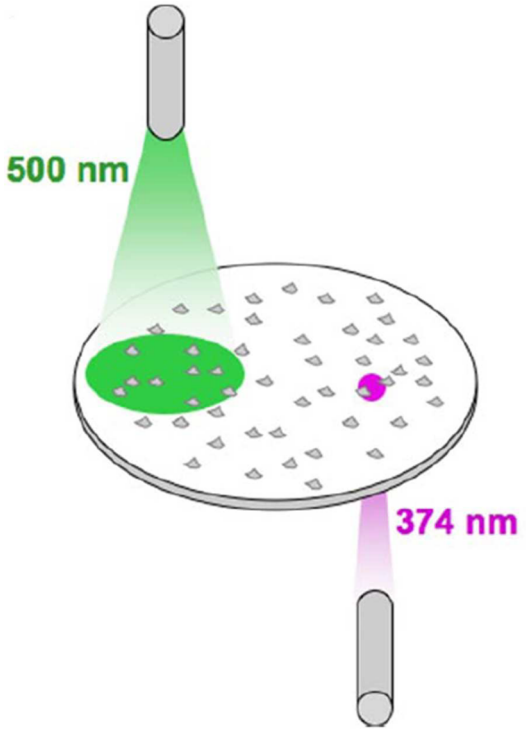

Figure 81. Controlling **111** conjugation by patterned illumination. By irradiating only a part of a cell culture while incubating with **111**, it was possible to control conjugation in different parts of a culture by taking advantage of affinity labeling. Reproduced with permission from ref 24. Copyright 2007 National Academy of Sciences, USA.

Penetrating isolated tissue is still different from penetrating tissues in a human body, because light has to travel further to reach the site of action. However, the use of photoswitchable affinity labeling to address the function of endogenous channels represents a large leap in this field, because genetic manipulation of cells is no longer a requirement. Therefore, this method can be exploited on endogenous cells and possibly even living organisms.

6.7. SecYEG

Recently, Driessen, Feringa, and co-workers reported a photocontrolled protein transport channel, SecYEG.[355] In bacteria, some of the proteins produced in the cell need to be transported to the periplasm or even outside the cell. An important route that facilitates this secretory process is the Sec pathway.[356] Three integral membrane proteins, SecY, SecE, and SecG, form a channel through which preproteins can be transported.[356,357] SecA, which is an ATPase, recognizes proteins that need to be translocated and uses ATP hydrolysis to perform this process.[356] The pore width of SecYEG is important relative to the size of proteins that are allowed to use this system for translocation. The size of this pore has recently been probed by using spherical molecules of different sizes conjugated to preproteins.[358] It was found that when the opening of a lateral gate present in SecY was limited by introducing a disulfide bridge or a chemical cross-link of 5 Å or less, the SecYEG complex lost its translocation function. When the size of this linker was increased, translocation was sustained.[359] The authors hypothesized that by using an azobenzene switch the size of the linker could be altered by photostimulation, dictating the opening and closing of that channel.[355] Inner-membrane vesicles expressing SecY conjugated with **115** (Figure 72) were assessed with a translocation assay using a fluorescent preprotein. The translocation of the preprotein was similar for the **115** conjugated in the *trans* form and nonconjugated SecY subunits and showed around 13−16% efficiency.[355] However, irradiation with UV light, favoring the *cis* form, resulted in a 3- to 5-fold decrease in translocation efficiency. Furthermore, opening and closing the channel was shown to be reversible upon irradiation with visible and UV light.[355]

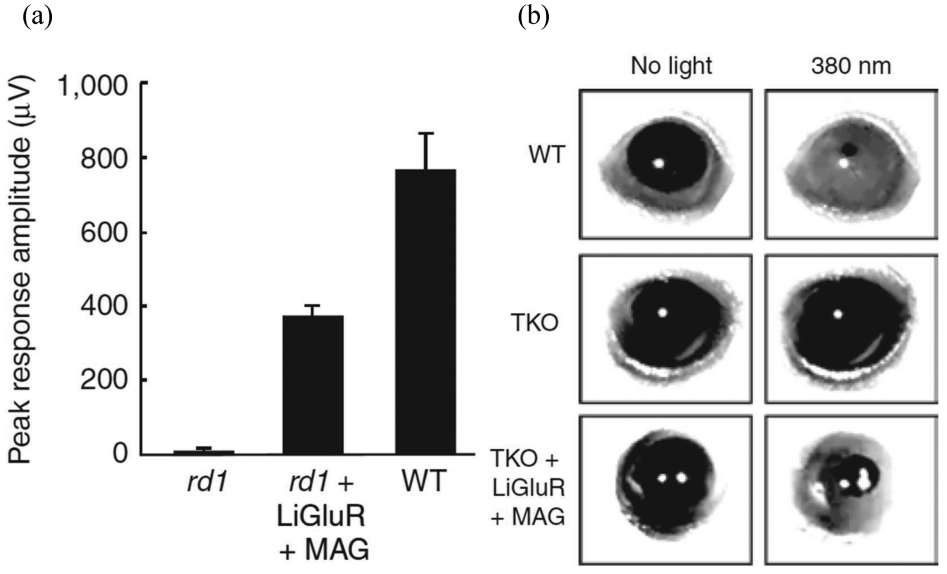

Figure 82. (a) Peak response amplitude in different groups. *Rd1* mice showed almost no response. *Rd1* mice expressing mutated iGluR and incubated with MAG (**111**) showed a peak response of 371.75 ± 35.70 μV compared to 766.00 ± 100.51 μV for the wild-type group (WT). (b) Pupil contraction in wild-type (WT), triple knockout (TKO), and triple knockout mice expressing mutated iGluR and incubated with MAG (**111**). The latter group had 60% contraction compared to the WT group after exposure to 380 nm light. Reprinted with permission from ref 352. Copyright 2011 Nature Publishing Group.

dx.doi.org/10.1021/cr300179f | *Chem. Rev.* 2013, 113, 6114−6178

Most receptors addressed with photoswitches were able to control movement of ions over a membrane. Photoswitchable SecYEG is unique in that it allows photocontrol over transportation of preproteins. This unique function shows the potential of photocontrolled transport of not only small ions but also much larger molecules.

6.8. Concluding Remarks

In the past decade, considerable progress has been made in the field of photocontrolled receptors and ion channels. Various approaches have been exploited and were shown to be successful in controlling ion channel and receptor functioning with light. The first experiments *in vivo* were executed and resulted in photocontrol of channel functioning in mammals. Another great achievement in the field has been addressing endogenous receptors.

Although still in an early stage of development, these large leaps in photocontrol of biological systems allow noninvasive interference with many biological functions and numerous exciting possibilities lie ahead. When the photoswitches are tuned in such a way that the different receptors can be turned on with different wavelengths of light, it will be possible to independently turn various cellular processes on and off. This could ultimately result in total control over cell function with the use of light, enabling the study of cell signaling in a unique manner.

Most photocontrolled receptors and ion channels described to date are found in cell membranes. Addressing intracellular receptors could offer new targets and possibilities. Using the approach of a tethered agonist requires the uptake of this molecule by the cell, which may not be trivial. Therefore, methods will need to be developed that allow the photoswitchable receptor ligands to be taken up by the cell.

A major hurdle that needs further work continues to be the transition from *in vitro* to *in vivo* application. To become of any interest for drug development and pharmacotherapy, it is necessary that this research area proves itself *in vivo*. For that, more endogenous receptors will need to be addressed. For this to be successful, the photoswitch should first reach the active site. While this was shown to work in organ slices[353] and zebrafish,[346,347] it will be difficult to achieve this in mammals, although preliminary applications in tissues have proven to be promising.[353] Next, the photoswitch has to conjugate with the endogenous receptor. An even greater challenge is to achieve control of photoswitching by irradiating with the right wavelength within the body. It was shown to be possible to irradiate photoswitches in zebrafish and organ slices of several millimeters, but it is clearly more challenging to penetrate higher eukaryotes, such as mice, with light, in order to control photoswitching *in vivo*. Most of the photoswitches described here are responsive to light of a wavelength between 300 and 500 nm. These wavelengths are too short to penetrate tissue deep enough to reach the photoswitches at the site of action.[360] This is one of the major concerns when trying to make photoswitchable compounds useful for *in vivo* application. By changing the substituents of the photoswitch, switching wavelengths can be tuned,[205,361] but designing effective photoswitches that can operate at wavelengths, such as infrared, that can penetrate mammalian tissue, remains a major challenge.

7. SUMMARY AND OUTLOOK

The ability to modulate structure and function in response to energy input and external signals is an essential feature of a biological system, which allows it to, for example, sense, move, adapt, and replicate. In the broader context of synthetic and chemical biology, while exploring the use of small molecule approaches to manipulate biological function, the incorporation of molecular switches as responsive elements offers tremendous opportunities for noninvasive control. As outlined above, the opportunities are numerous with respect to both biological targets and molecular switches, while this rapidly emerging field also has bright prospects to design a wealth of biohybrid materials with intrinsic adaptive behavior. Although scientists have mastered the construction of discrete objects of nanometer dimensions, it has been very difficult to develop molecular systems and devices that can adapt their structure, function, or activity in response to environmental triggers in a way anywhere close to what we see in Nature's highly integrated and complex dynamic systems. Nevertheless, reversible tuning of peptide structure using synthetic molecular switches has recently culminated in the control of processes by light in the living cell.

Photochemical switches, in particular those based on azobenzenes, have been highly successful in modulating, for example, DNA, peptides and proteins, transmembrane receptors, and transporters. The development of azobenzenes, switchable in both directions with visible light,[26,33] and the confirmation of photochromic behavior and metabolic stability of azobenzenes in living organisms[32−34] are major recent advances. Methodology is now available for solid phase synthesis of oligonucleotides which include photochromic units. This allows modular approaches for the preparation of light-responsive nucleic acid oligomers and systematic evaluation of their "addressable" properties, including hybridization and information transfer. The most relevant structures in proteins, i.e. α-helix, β-sheet, and β-hairpin, can now confidently be induced or distorted upon irradiation of a photoswitch incorporated in the peptide. The synthetic approaches also retain the modularity inherent in amino acid-based systems, allowing for the chromophore to be introduced at a number of specific positions which elicit a range of structural effects. In recent years, several methods for the incorporation of photoswitches into proteins have been established. The introduction of a reactive amino acid (e.g., thiol, amine) into a chosen site by mutagenesis and subsequent modification of the residue by anchoring an activated photoswitch offers high modularity in the approach regarding the introduction site and the nature of the photoswitch. These basic studies toward responsive biohybrid systems have recently initiated the application of photoswitches for manipulating processes in cells. These include a photoswitchable peptide for influencing the amplitude of shortening of the sarcomere length in skeletal muscle fibers from Flexor digitorum brevis (FDB) of mice.[32] Furthermore, photocontrol of AP1 transcription factor activity in HEK293T cells was achieved using a light-switchable peptide, while a photoswitchable iGluR receptor was used to influence calcium flux in HEK293 cells.[24] The great prospect of these approaches for controlling processes in living organisms is perhaps best illustrated by the recent use of photoswitchable iGluR receptor to partially restore light responsiveness in retinal ganglion cells of rd1 mice.[352]

dx.doi.org/10.1021/cr300179f | *Chem. Rev.* 2013, 113, 6114−6178

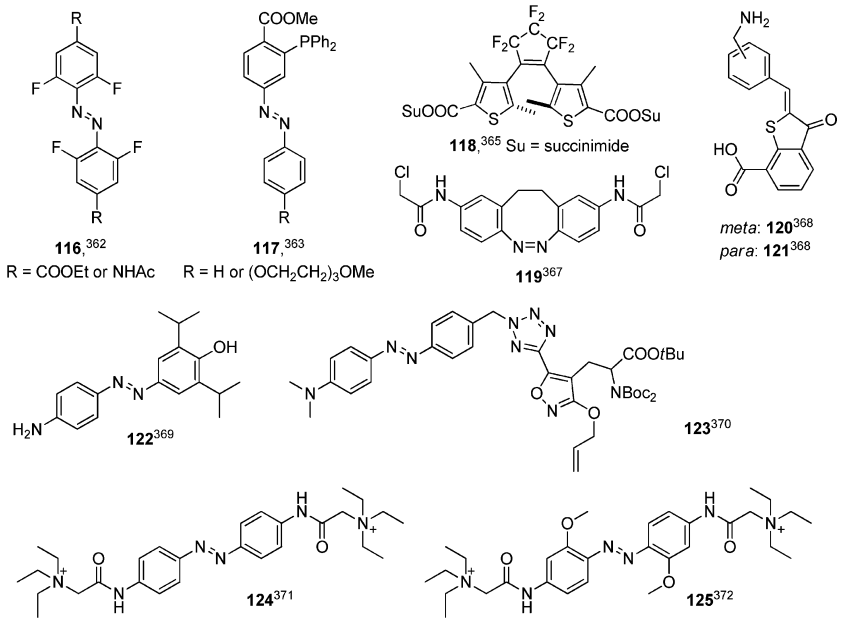

Figure 83. Recently introduced structures of molecular photoswitches relevant for the photocontrol of biological processes.

Beyond the study of *in vivo* peptide, protein, and oligonucleotide function, the ultimate goal of the approaches discussed here, based on the incorporation of molecular switches, is to manipulate the biological function in a reversible manner in systems ranging from living cells to whole organisms. This presents numerous challenges, which will have to be met in the coming years. First, our current toolbox needs expansion toward novel classes of switches, in particular those photoresponsive molecules that operate in the near-IR, for better tissue penetration. Second, the issue of crossing the biological membranes by the photoresponsive compound or biomolecules will have to be solved, and first steps toward this goal have been made with the confirmed incorporation of a photoresponsive peptide into the cells of skeletal muscle fibers[32] and rat tissues.[353] Third, the issues of metabolic stability and toxicity of xenobiotic photoswitches and photoswitch-modified biomolecules will have to be addressed. Considerable advances were achieved recently toward the *in vivo* approaches based on azobenzene switches,[32−34] but these developments are still at an early stage, and more studies are eagerly awaited.

By no means is the field of responsive biomolecules limited to the incorporation of photoswitches, as, for example, magnetic responsiveness, small molecule effectuators, or catalytic functions also offer opportunities to address biological function. A major advantage of light is, of course, spatial-temporal control, the possibility of tuning wavelengths, and the ability to couple the switching function to fluorescence detection. In particular, multiple switching with on−off control of multiple fluorescence reporters is highly challenging but possesses exciting prospects in the context of dynamic control of integrated metabolic pathways or protein networks in cells. In addition, the use of photoswitchable nucleic acids *in vivo* to allow translation, transcription, and replication to be activated and deactivated by light in a fully reversible manner seems to have high potential to allow one to interfere with cellular processes.

To reach a high level of control, the precise incorporation of the photoswitch in the target biomacromolecule is essential. This is often a formidable task, as is evident from the challenge to achieve complete on/off photochemical control of enzyme function without considerable loss of its activity. The development of a more general and easy methodology for the site selective incorporation of molecular photoswitches into proteins that would allow for convenient optimization of the introduction site as well as the magnitude of the responsive effect will greatly stimulate further breakthroughs in this field. Once we understand better how to address in a fully reversible manner protein structure and function in its native environment, the more distant future holds promise for the control of a range of cellular functions, including neurobiological, sensory, motoric, or metabolic processes. The ability to switch selectively on−off one or more pathways in cellular networks or reversibly control membrane receptor functions might be particularly helpful in the process of drug discovery. The development of photoswitchable biosystems offers not only the delight of merging the power of synthetic chemistry with the beauty of biomacromolecule function, but also the intellectual challenge to interfere with biological processes and the ultimate prospect to treat malfunction of the living system by precise control at the molecular level.

8. UPDATE

While this manuscript was under review and revision, a number of important contributions to the field were published, which are summarized below.

8.1. Molecular Photoswitches

8.1.1. The groups of Brouwer and Hecht have reported an azobenzene structure **116** (Figure 83),[362] in which fluorine atoms are introduced in all four *ortho* positions. Optimization of spectral properties, by incorporation of electron-donating and electron-withdrawing groups, resulted in photoswitches which can be addressed with visible light and which possess a highly thermostable *cis* isomer, with a half-life of about 700 days at 25 °C.

8.1.2. The group of Feringa has introduced a novel azobenzene architecture **117** (Figure 83), in which a ligation tag responsible for the Staudinger−Bertozzi ligation was

dx.doi.org/10.1021/cr300179f | *Chem. Rev.* 2013, 113, 6114−6178

introduced into the structure of the photochrome.[363] Products obtained after the reaction with model azides showed up to 95% of *cis* isomer in the UV-irradiated samples. Ligation of **117** to azide groups, site-selectively introduced into a model enzyme,[363] confirms the possibility of using the presented methodology to optimize the photocontrol of protein function by changing both the photoswitch structure and attachment point.

8.2. Photocontrol of Nucleic Acids

The diarylethene-modified nucleotide **13** (Figure 7), reported previously from the group of Jaeschke,[84] has been incorporated into oligonucleotides.[364] With these new photoresponsive structures a partial photocontrol of transcription has been presented.[364]

8.3. Photoswitchable Peptides

8.3.1. The group of Inouye has used a diarylethene-based photoswitch to regulate the helicity of a DNA-binding peptide, by cross-linking ornithine residues with compound **118** (Figure 83).[365] When the switch was in the open form, the peptides folded into stable α-helices and interacted strongly with target DNA strands. UV irradiation resulted in the photocyclization of diarylethene, destabilization of the α-helices, and weaker interactions with DNA.

8.3.2. The groups of Hoppmann and Beyermann have used the AMPB azobenzene (Figure 22) as a backbone-modifier (Figure 18b) introduced into the structure of the 42-residue, linear amyloid β-peptide, relevant in the development of Alzheimer's disease.[366] While the neuronal toxicity of the hybrid was found to be almost independent of the photostate of the switch, the influence of the photoirradiation on the distribution of amyloid peptide oligomers was confirmed.[366] The latter provides important insight into the role of oligomers, resolubilized from plaques, on the death of the cell.

8.3.3. Woolley and co-workers used a bridged azobenzene **119**, based on a structure introduced earler by Siewertsen et al.,[26] for a bidirectional control of peptide conformation, using the cysteine cross-linking strategy (Figure 18c).[367] In this class of azobenzenes, there is a large separation (~85 nm) between the n−π^* absorption bands of the photoisomers, which allows for the selective isomerization between the *trans* (less table) and *cis* (more stable) isomers. Indeed, the authors report[367] an impressive >400-fold change in the population of the *cis* isomer upon irradiation with green (λ = 500−550 nm) light. Irradiation with violet light produced 70% of the *trans* state. Reversible photochromism of the **119**-bridged model peptide could be confirmed in >100 cycles of irradiation. The stability in the presence of reduced glutathione was also studied and revealed that the strained *trans* isomer undergoes a slow bleaching process.

8.3.4. Hemithioindigo switches **120** and **121** (Figure 83) were introduced into the backbone of model linear and cyclic peptides (Figure 18b), and their photoisomerization was subsequently studied by ultrafast spectroscopy in visible and IR ranges.[368] For the smaller, linear peptide, modified with compound **121**, the photoisomerization was slower than for the isolated switch but was closely followed by the changes in the peptide conformation. The larger, cyclic, β-hairpin forming peptide underwent a much slower change in conformation, which did not match the time scale of the isomerization of the photochromic units.[368] These results are in agreement with the previous studies on azobenzene-bridged cyclic peptides.[23]

8.4. Photocontrol of Receptors and Channels

8.4.1. The groups of Sigel and Trauner used a small photoswitchable propofol derivative **122** (Figure 83) to modulate $GABA_A$ receptors.[369] This photochromic potentiator was able to alter the strength of GABA-induced currents upon light irradiation. Furthermore, the anesthetic effect of **122** was shown on albino *Xenopus laevis* tadpoles, which could be anesthetized by **122** and revived after UV light irradiation.

8.4.2. Trauner and co-workers developed a photochromic agonist of AMPA receptors.[370] Azobenzene-based agonist **123** (Figure 83) was a derivative of AMPA and could trigger neuronal firing, which was silenced after irradiation with blue-green light.

8.4.3. The groups of Kramer and Trauner reported the photocontrol of nociception.[371] The designed compound **124** (Figure 83) could selectively enter pain-sensing neurons and block voltage-gated ion channels. Switching **124** to the *cis* isomer with 380 nm light completely removed the blockage.[371] In a follow-up publication,[372] Trauner and co-workers investigated the possibility of tuning the spectral properties of **124**. For this purpose, compound **125** (Figure 83), an *ortho*,*ortho*′-dimethoxy analog of **124**, was synthesized. The absorption maximum was red-shifted, and compound *trans*-**125** could be converted into the *cis* isomer with visible light.[372]

8.4.4. A follow-up study on a previously reported paper[352] was conducted by the group of Kramer.[373] It was shown that compound **112** (Figure 72) could restore light-sensitivity and behavioral responses in blind mice.

AUTHOR INFORMATION

Corresponding Author

*E-mail: b.l.feringa@rug.nl.

Present Addresses

[†]J.M.B.: University of California, Irvine, 5003 Reines Hall, Irvine, CA 92697.
[‡]H.A.V.K.: Universiteit Leiden, Leiden Institute of Chemistry (Gorlaeus Laboratories), Einsteinweg 55, 2333 CC, Leiden, The Netherlands.

Notes

The authors declare no competing financial interest.

Biographies

Wiktor Szymański received his Ph.D. degree from The Warsaw University of Technology, Poland, in 2008, under the supervision of Prof. Ryszard Ostaszewski. Since then, he has been working with Prof. Ben L. Feringa and Prof. Dick B. Janssen at the University of

Groningen on the use of biotransformations in organic chemistry and the construction of photoactive bioconjugates.

After graduating from the Boston College cum laude, John Beierle was awarded a Fulbright Fellowship to study molecular machines at the Université Louis Pasteur in Strasbourg, France. His Ph.D. research followed at the Scripps Research Institute as a NESSF Fellow, focusing on reversible bond formation and biomolecular recognition. As an NSF-IRFP Fellow at Groningen, he has focused on nanoscale self-assembly and photosensitive materials. He now focuses on bionanotechnology at UC Irvine using polymer nanoparticles to manipulate protein folding.

Hans A. V. Kistemaker received his B.Sc. and M.Sc. degrees in organic chemistry from the University of Groningen under the guidance of Prof. Ben L. Feringa with a specialization in the synthesis of molecular motors and self-assembled monolayers. He is currently a Ph.D. student in bio-organic chemistry at Leiden University in the research group of Prof. Hermen S. Overkleeft and Prof. Gijs van der Marel. His work focuses on the synthesis of mono- and poly-ADPribosylated peptides and proteins in order to determine their biological relevance.

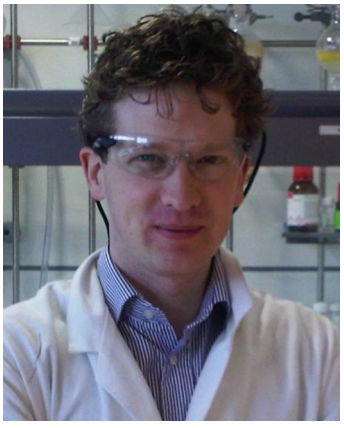

Willem Velema studied Pharmacy at the University of Groningen and obtained his B.Sc. in 2007. He received his M.Sc. in 2010 after conducting his master thesis on cell handling in microfluidic systems in the laboratory of Professor Elisabeth M. J. Verpoorte. He is currently pursuing his Ph.D. at the Stratingh Institute for Chemistry in Groningen under the supervision of Professor Ben L. Feringa. His recent research focuses on the use of molecular photoswitches in biological relevant molecules.

Ben L. Feringa obtained his Ph.D. degree in 1978 at the University of Groningen in The Netherlands under the guidance of Professor Hans Wynberg. After working as a research scientist at Shell, he was appointed full professor at the University of Groningen in 1988 and named the distinguished Jacobus H. van't Hoff Professor of Molecular Sciences in 2004. He was elected a foreign honorary member of the American Academy of Arts and Sciences and a member of the Royal Netherlands Academy of Sciences. His research interests include stereochemistry, organic synthesis, asymmetric catalysis, molecular switches and motors, self-assembly, and nanosystems.

ACKNOWLEDGMENTS

We thank Prof. Asanuma for the structure in Figure 8b. B.L.F. acknowledges financial support through an ERC Advanced Investigator Grant (227897). J.M.B. also thanks the U.S. National Science Foundation for an International Research Postdoctoral Fellowship (OISE-0853019). The research has received funding from the Ministry of Education, Culture and Science (Gravity program 024.001.035).

REFERENCES

(1) Willner, I.; Rubin, S. *Angew. Chem., Int. Ed.* **1996**, *35*, 367.
(2) Mayer, G.; Heckel, A. *Angew. Chem., Int. Ed.* **2006**, *45*, 4900.
(3) Dugave, C.; Demange, L. *Chem. Rev.* **2003**, *103*, 2475.
(4) Gorostiza, P.; Isacoff, E. Y. *Science* **2008**, *322*, 395.

(5) Fehrentz, T.; Schönberger, M.; Trauner, D. *Angew. Chem., Int. Ed.* **2011**, *50*, 12182.
(6) Deiters, A. *ChemBioChem* **2010**, *11*, 47.
(7) Beharry, A. A.; Woolley, G. A. *Chem. Soc. Rev.* **2011**, *40*, 4422.
(8) Sameiro, M.; Goncalves, T. *Chem. Rev.* **2009**, *109*, 190.
(9) Newman, R. H.; Fosbrink, M. D.; Zhang, J. *Chem. Rev.* **2011**, *111*, 3614.
(10) Sletten, E. M.; Bertozzi, C. R. *Acc. Chem. Res.* **2011**, *44*, 666.
(11) Curley, K.; Lawrence, D. S. *Pharmacol. Ther.* **1999**, *82*, 347.
(12) Shigeri, Y.; Tatsu, Y.; Yumoto, N. *Pharmacol. Ther.* **2001**, *91*, 85.
(13) Lemke, E. A. *ChemBioChem* **2010**, *11*, 1825.
(14) Mendes, P. M. *Chem. Soc. Rev.* **2008**, *37*, 2512.
(15) Robertus, J.; Browne, W. R.; Feringa, B. L. *Chem. Soc. Rev.* **2010**, *39*, 354.
(16) Liu, R.; Asato, A. *Proc. Natl. Acad. Sci. U. S. A.* **1985**, *82*, 259.
(17) Berg, J. M.; Tymoczko, J. L.; Stryer, L. *Biochemistry*, 5th ed.; W. H. Freeman: New York, 2002.
(18) Hamon, F.; Djedaini-Pilard, F.; Barbot, F.; Len, C. *Tetrahedron* **2010**, *66*, 2538.
(19) Hamon, F.; Djedaini-Pilard, F.; Barbot, F.; Len, C. *Tetrahedron* **2009**, *65*, 10105.
(20) Briquet, L.; Vercauteren, D. P.; Perpète, E. A.; Jacquemin, D. *Chem. Phys. Lett.* **2006**, *417*, 190.
(21) Briquet, L.; Vercauteren, D. P.; Andre, J.-M.; Perpète, E. A.; Jacquemin, D. *Chem. Phys. Lett.* **2007**, *435*, 257.
(22) Cattaneo, P.; Persico, M. *Phys. Chem. Chem. Phys.* **1999**, *1*, 4739.
(23) Renner, C.; Moroder, L. *ChemBioChem* **2006**, *7*, 869.
(24) Gorostiza, P.; Volgraf, M.; Numano, R.; Szobota, S.; Trauner, D.; Isacoff, E. Y. *Proc. Natl. Acad. Sci. U. S. A.* **2007**, *104*, 10865.
(25) Zhang, F. Z.; Zarrine-Afsar, A.; Al-Abdul-Wahid, M. S.; Prosser, R. S.; Davidson, A. R.; Woolley, G. A. *J. Am. Chem. Soc.* **2009**, *131*, 2283.
(26) Siewertsen, R.; Neumann, H.; Buchheim-Stehn, B.; Herges, R.; Naether, C.; Renth, F.; Temps, F. *J. Am. Chem. Soc.* **2009**, *131*, 15594.
(27) Beharry, A. A.; Sadovski, O.; Woolley, G. A. *J. Am. Chem. Soc.* **2011**, *133*, 19684.
(28) Bandara, H. M. D.; Burdette, S. C. *Chem. Soc. Rev.* **2012**, *41*, 1809.
(29) Nishimura, N.; Sueyoshi, T.; Yamanaka, H.; Imai, E.; Yamamoto, S.; Hasegawa, S. *Bull. Chem. Soc. Jpn.* **1976**, *49*, 1381.
(30) Bortolus, P.; Monti, S. *J. Phys. Chem.* **1979**, *83*, 648.
(31) Boulegue, C.; Loweneck, M.; Renner, C.; Moroder, L. *ChemBioChem* **2007**, *8*, 591.
(32) Hoppmann, C.; Schmieder, P.; Domaing, P.; Vogelreiter, G.; Eichhorst, J.; Wiesner, B.; Morano, I.; Rück-Braun, K.; Beyermann, M. *Angew. Chem., Int. Ed.* **2011**, *50*, 7699.
(33) Beharry, A. A.; Wong, L.; Tropepe, V.; Woolley, G. A. *Angew. Chem., Int. Ed.* **2011**, *50*, 1325.
(34) Wachtveitl, J.; Zumbusch, A. *ChemBioChem* **2011**, *12*, 1169.
(35) Mendonça, C. R.; Balogh, D. T.; De Boni, L.; dos Santos, J. D. S.; Zucolotto, V.; Oliveira, O. N., Jr. In Optically Induced Processes in Azopolymers. Feringa, B. L., Browne, W. R., Eds.; *Molecular Switches*, 2nd ed.; Wiley-VCH: Weinheim, 2011; Chapter 12.
(36) Waldeck, D. H. *Chem. Rev.* **1991**, *91*, 415.
(37) Han, W. G.; Lovell, T.; Liu, T. Q.; Noodleman, L. *ChemPhysChem* **2002**, *3*, 167.
(38) Cammenga, H. K.; Emel'yanenko, V. N.; Verevkin, S. P. *Ind. Eng. Chem. Res.* **2009**, *48*, 10120.
(39) Minkin, V. I. In Photoswitchable Molecular Systems Based on Spiropyrans and Spirooxazines. Feringa, B. L., Browne, W. R., Eds.; *Molecular Switches*, 2nd ed.; Wiley-VCH: Weinheim, 2011; Chapter 2.
(40) Berkovic, G.; Krongauz, V.; Weiss, V. *Chem. Rev.* **2000**, *100*, 1741.
(41) Lukyanov, B. S.; Lukyanova, M. B. *Chem. Heterocycl. Compd.* **2005**, *41*, 281.
(42) Levitus, M.; Glasser, G.; Neher, D.; Aramendía, P. F. *Chem. Phys. Lett.* **1997**, *277*, 118.
(43) Bletz, M.; Pfeifer-Fukumura, U.; Kolb, U.; Baumann, W. *J. Phys. Chem. A* **2002**, *106*, 2232.
(44) Chibisov, A. K.; Görner, H. *J. Phys. Chem. A* **1997**, *101*, 4305.
(45) Flannery, J. B. *J. Am. Chem. Soc.* **1968**, *90*, 5660.
(46) Wetzler, D. E.; Aramendía, P. F.; Japas, M. L.; Fernández-Prini, R. *Phys. Chem. Chem. Phys.* **1999**, *1*, 4955.
(47) Aizawa, M.; Namba, K.; Suzuki, S. *Arch. Biochem. Biophys.* **1977**, *180*, 41.
(48) Namba, K.; Suzuki, S. *Chem. Lett.* **1975**, *4*, 947.
(49) Sakata, T.; Yan, Y. L.; Marriott, G. *Proc. Natl. Acad. Sci. U. S. A.* **2005**, *102*, 4759.
(50) Irie, M. *Chem. Rev.* **2000**, *100*, 1685.
(51) Warford, C. C.; Lemieux, V.; Branda, N. R. Multifunctional Diarylethenes. Feringa, B. L., Browne, W. R., Eds.; *Molecular Switches*, 2nd ed.; Wiley-VCH: Weinheim, 2011; Chapter 1.
(52) Kellogg, R. M.; Groen, M. B.; Wynberg, H. *J. Org. Chem.* **1967**, *32*, 3093.
(53) Nakamura, S.; Irie, M. *J. Org. Chem.* **1988**, *53*, 6136.
(54) Gilat, S. L.; Kawai, S. H.; Lehn, J. M. *Chem.—Eur. J.* **1995**, *1*, 275.
(55) Yokoyama, Y.; Gushiken, T.; Ubukata, T. In Fulgides and Related Compounds. Feringa, B. L., Browne, W. R., Eds.; *Molecular Switches*, 2nd ed.; Wiley-VCH: Weinheim, 2011; Chapter 3.
(56) Santiago, A.; Becker, R. S. *J. Am. Chem. Soc.* **1968**, *90*, 3654.
(57) Yokoyama, Y. *Chem. Rev.* **2000**, *100*, 1717.
(58) Heller, H. G.; Oliver, S. *J. Chem. Soc., Perkin Trans. 1* **1981**, 197.
(59) Darcy, P. J.; Heller, H. G.; Strydom, P. J.; Whittall, J. *J. Chem. Soc., Perkin Trans. 1* **1981**, 202.
(60) Ilge, H. D.; Colditz, R. *J. Mol. Struct.* **1990**, *218*, 39.
(61) Yokoyama, Y.; Ogawa, K.; Iwai, T.; Shimazaki, K.; Kajihara, Y.; Goto, T.; Yokoyama, Y.; Kurita, Y. *Bull. Chem. Soc. Jpn.* **1996**, *69*, 1605.
(62) Lougheed, T.; Borisenko, V.; Hennig, T.; Rück-Braun, K.; Woolley, G. A. *Org. Biomol. Chem.* **2004**, *2*, 2798.
(63) Yamaguchi, T.; Seki, T.; Tamaki, T.; Ichimura, K. *Bull. Chem. Soc. Jpn.* **1992**, *65*, 649.
(64) Cordes, T.; Weinrich, D.; Kempa, S.; Riesselmann, K.; Herre, S.; Hoppmann, C.; Rück-Braun, K.; Zinth, W. *Chem. Phys. Lett.* **2006**, *428*, 167.
(65) Cordes, T.; Schadendorf, T.; Rück-Braun, K.; Zinth, W. *Chem. Phys. Lett.* **2008**, *455*, 197.
(66) Tang, X.; Dmochowski, I. J. *Mol. Biosyst.* **2007**, *3*, 100.
(67) Wagenknecht, H. *Nat. Prod. Rep.* **2006**, *23*, 973.
(68) Letsinger, R. L.; Wu, T. F. *J. Am. Chem. Soc.* **1994**, *116*, 811.
(69) Letsinger, R. L.; Wu, T. F. *J. Am. Chem. Soc.* **1995**, *117*, 7323.
(70) Lewis, F. D.; Liu, X. Y. *J. Am. Chem. Soc.* **1999**, *121*, 11928.
(71) Lewis, F. D.; Wu, Y. S.; Liu, X. Y. *J. Am. Chem. Soc.* **2002**, *124*, 12165.
(72) Yamana, K.; Yoshikawa, A.; Nakano, H. *Tetrahedron Lett.* **1996**, *37*, 637.
(73) Yamana, K.; Yoshikawa, A.; Noda, R.; Nakano, H. *Nucleosides Nucleotides Nucleic Acids* **1998**, *17*, 233.
(74) Yamana, K.; Kan, K.; Nakano, H. *Bioorg. Med. Chem.* **1999**, *7*, 2977.
(75) Wang, Q.; Yi, L.; Liu, L.; Zhou, C.; Xi, Z. *Tetrahedron Lett.* **2008**, *49*, 5087.
(76) Wu, L.; Koumoto, K.; Sugimoto, N. *Chem. Commun.* **2009**, *14*, 1915.
(77) Lewis, F.; Liu, X.; Wu, Y.; Miller, S.; Wasielewski, M.; Letsinger, R.; Sanishvili, R.; Joachimiak, A.; Tereshko, V.; Egli, M. *J. Am. Chem. Soc.* **1999**, *121*, 9905.
(78) Patnaik, S.; Kumar, P.; Garg, B. S.; Gandhi, R. P.; Gupta, K. C. *Bioorg. Med. Chem.* **2007**, *15*, 7840.
(79) Keiper, S.; Vyle, J. S. *Angew. Chem., Int. Ed.* **2006**, *45*, 3306.
(80) Ogasawara, S.; Maeda, M. *Angew. Chem., Int. Ed.* **2008**, *47*, 8839.
(81) Ogasawara, S.; Saito, I.; Maeda, M. *Tetrahedron Lett.* **2008**, *49*, 2479.
(82) Lena, S.; Neviani, P.; Masiero, S.; Pieraccini, S.; Spada, G. P. *Angew. Chem., Int. Ed.* **2010**, *49*, 3657.
(83) Ogasawara, S.; Maeda, M. *Angew. Chem., Int. Ed.* **2009**, *48*, 6671.
(84) Singer, M.; Jaeschke, A. *J. Am. Chem. Soc.* **2010**, *132*, 8372.

(85) Kashida, H.; Liang, X.; Asanuma, H. *Curr. Org. Chem.* **2009**, *13*, 1065.
(86) Asanuma, H.; Ito, T.; Komiyama, M. *Tetrahedron Lett.* **1998**, *39*, 9015.
(87) Asanuma, H.; Shirasuka, K.; Yoshida, T.; Takarada, T.; Liang, X. G.; Komiyama, M. *Chem. Lett.* **2001**, *30*, 108.
(88) Asanuma, H.; Ito, T.; Yoshida, T.; Liang, X. G.; Komiyama, M. *Angew. Chem., Int. Ed.* **1999**, *38*, 2393.
(89) Liang, X. G.; Asanuma, H.; Kashida, H.; Takasu, A.; Sakamoto, T.; Kawai, G.; Komiyama, M. *J. Am. Chem. Soc.* **2003**, *125*, 16408.
(90) Asanuma, H.; Liang, X. G.; Yoshida, T.; Komiyama, M. *ChemBioChem* **2001**, *2*, 39.
(91) Moser, H. E.; Dervan, P. B. *Science* **1987**, *238*, 645.
(92) Duca, M.; Vekhoff, P.; Oussedik, K.; Halby, L.; Arimondo, P. B. *Nucleic Acids Res.* **2008**, *36*, 5123.
(93) Asanuma, H.; Liang, X. G.; Yoshida, T.; Yamazawa, A.; Komiyama, M. *Angew. Chem., Int. Ed.* **2000**, *39*, 1316.
(94) Liang, X. G.; Asanuma, H.; Komiyama, M. *J. Am. Chem. Soc.* **2002**, *124*, 1877.
(95) Yamazawa, A.; Liang, X. G.; Asanuma, H.; Komiyama, M. *Angew. Chem., Int. Ed.* **2000**, *39*, 2356.
(96) Liu, Y.; Sen, D. *J. Mol. Biol.* **2004**, *341*, 887.
(97) Asanuma, H.; Takarada, T.; Yoshida, T.; Tamaru, D.; Liang, X. G.; Komiyama, M. *Angew. Chem., Int. Ed.* **2001**, *40*, 2671.
(98) Asanuma, H.; Liang, X.; Nishioka, H.; Matsunaga, D.; Liu, M.; Komiyama, M. *Nat. Protocols* **2007**, *2*, 203.
(99) Asanuma, H.; Matsunaga, D.; Komiyama, M. *Nucleic Acids Symp. Ser.* **2005**, *49*, 35.
(100) Nishioka, H.; Liang, X.; Kashida, H.; Asanuma, H. *Chem. Commun.* **2007**, *42*, 4354.
(101) Matsunaga, D.; Asanuma, H.; Komiyama, M. *J. Am. Chem. Soc.* **2004**, *126*, 11452.
(102) Liu, M. Z.; Asanuma, H.; Komiyama, M. *J. Am. Chem. Soc.* **2006**, *128*, 1009.
(103) Kim, Y.; Phillips, J. A.; Liu, H.; Kang, H.; Tan, W. *Proc. Natl. Acad. Sci. U. S. A.* **2009**, *106*, 6489.
(104) Liang, X.; Takenaka, N.; Nishioka, H.; Asanuma, H. *Chem.—Asian J.* **2008**, *3*, 553.
(105) Liang, X.; Nishioka, H.; Takenaka, N.; Asanuma, H. *ChemBioChem* **2008**, *9*, 702.
(106) Liang, X.; Mochizuki, T.; Asanuma, H. *Small* **2009**, *5*, 1761.
(107) Zhou, M.; Liang, X.; Mochizuki, T.; Asanuma, H. *Angew. Chem., Int. Ed.* **2010**, *49*, 2167.
(108) Tanaka, F.; Mochizuki, T.; Liang, X.; Asanuma, H.; Tanaka, S.; Suzuki, K.; Kitamura, S.; Nishikawa, A.; Ui-Tei, K.; Hagiya, M. *Nano Lett.* **2010**, *10*, 3560.
(109) Stafforst, T.; Hilvert, D. *Angew. Chem., Int. Ed.* **2010**, *49*, 9998.
(110) Andersson, J.; Li, S.; Lincoln, P.; Andreasson, J. *J. Am. Chem. Soc.* **2008**, *130*, 11836.
(111) Dohno, C.; Uno, S.; Nakatani, K. *J. Am. Chem. Soc.* **2007**, *129*, 11898.
(112) Uno, S.; Dohno, C.; Oku, M.; Nakatani, K. *Nucleic Acids Symp. Ser.* **2007**, *51*, 173.
(113) Dohno, C.; Nakatani, K. *Chem. Soc. Rev.* **2011**, *40*, 5729.
(114) Peng, T.; Dohno, C.; Nakatani, K. *Angew. Chem., Int. Ed.* **2006**, *45*, 5623.
(115) Dohno, C.; Uno, S.; Sakai, S.; Oku, M.; Nakatani, K. *Bioorg. Med. Chem.* **2009**, *17*, 2536.
(116) Ciardelli, F.; Bronco, S.; Pieroni, P.; Pucci, A. In Photoswitchable Polypeptides. Feringa, B. L., Browne, W. R., Eds.; *Molecular Switches*, 2nd ed.; Wiley-VCH: Weinheim, 2011; Chapter 10.
(117) Goodman, M.; Kossoy, A. *J. Am. Chem. Soc.* **1966**, *88*, 5010.
(118) Goodman, M.; Falxa, M. L. *J. Am. Chem. Soc.* **1967**, *89*, 3863.
(119) Benedetti, E.; Goodman, M. *Biochemistry* **1968**, *7*, 4242.
(120) Benedetti, E.; Kossoy, A.; Falxa, M. L.; Goodman, M. *Biochemistry* **1968**, *7*, 4234.
(121) Goodman, M.; Benedetti, E. *Biochemistry* **1968**, *7*, 4226.
(122) Pieroni, O.; Houben, J. L.; Fissi, A.; Costantino, P. *J. Am. Chem. Soc.* **1980**, *102*, 5913.
(123) Pieroni, O.; Fissi, A. *J. Photochem. Photobiol. B* **1992**, *12*, 125.
(124) Pieroni, O.; Fabbri, D.; Fissi, A.; Ciardelli, F. *Makromol. Chem., Rapid Commun.* **1988**, *9*, 637.
(125) Ciardelli, F.; Fabbri, D.; Pieroni, O.; Fissi, A. *J. Am. Chem. Soc.* **1989**, *111*, 3470.
(126) Fissi, A.; Pieroni, O.; Angelini, N.; Lenci, F. *Macromolecules* **1999**, *32*, 7116.
(127) Pieroni, O.; Fissi, A.; Viegi, A.; Fabbri, D.; Ciardelli, F. *J. Am. Chem. Soc.* **1992**, *114*, 2734.
(128) Fissi, A.; Pieroni, O.; Balestreri, E.; Amato, C. *Macromolecules* **1996**, *29*, 4680.
(129) Fissi, A.; Pieroni, O.; Ruggeri, G.; Ciardelli, F. *Macromolecules* **1995**, *28*, 302.
(130) Ueno, A.; Takahashi, K.; Anzai, J.; Osa, T. *Chem. Lett.* **1981**, *10*, 113.
(131) Ueno, A.; Takahashi, K.; Anzai, J. I.; Osa, T. *J. Am. Chem. Soc.* **1981**, *103*, 6410.
(132) Stanfield, R. L.; Wilson, I. A. *Curr. Opin. Struct. Biol.* **1995**, *5*, 103.
(133) Stites, W. E. *Chem. Rev.* **1997**, *97*, 1233.
(134) Ulysse, L.; Cubillos, J.; Chmielewski, J. *J. Am. Chem. Soc.* **1995**, *117*, 8466.
(135) Ulysse, L. G.; Chmielewski, J. *Chem. Biol. Drug Des.* **2006**, *67*, 127.
(136) Reichlin, S. *N. Engl. J. Med.* **1983**, *309*, 1495.
(137) Behrendt, R.; Renner, C.; Schenk, M.; Wang, F. Q.; Wachtveitl, J.; Oesterhelt, D.; Moroder, L. *Angew. Chem., Int. Ed.* **1999**, *38*, 2771.
(138) Behrendt, R.; Schenk, M.; Musiol, H. J.; Moroder, L. *J. Pept. Sci.* **1999**, *5*, 519.
(139) Mustacich, D.; Powis, G. *Biochem. J.* **2000**, *346*, 1.
(140) Renner, C.; Behrendt, R.; Sporlein, S.; Wachtveitl, J.; Moroder, L. *Biopolymers* **2000**, *54*, 489.
(141) Renner, C.; Cramer, J.; Behrendt, R.; Moroder, L. *Biopolymers* **2000**, *54*, 501.
(142) Renner, C.; Behrendt, R.; Heim, N.; Moroder, L. *Biopolymers* **2002**, *63*, 382.
(143) Cattani-Scholz, A.; Renner, C.; Cabrele, C.; Behrendt, R.; Oesterhelt, D.; Moroder, L. *Angew. Chem., Int. Ed.* **2002**, *41*, 289.
(144) Wilkinson, B.; Gilbert, H. F. *Biochim. Biophys. Acta: Proteins Proteomics* **2004**, *1699*, 35.
(145) Cabrele, C.; Cattani-Scholz, A.; Renner, C.; Behrendt, R.; Oesterhelt, D.; Moroder, L. *Eur. J. Org. Chem.* **2002**, 2144.
(146) Loweneck, M.; Milbradt, A. G.; Root, C.; Satzger, H.; Zinth, W.; Moroder, L.; Renner, C. *Biophys. J.* **2006**, *90*, 2099.
(147) Renner, C.; Kusebauch, U.; Loweneck, M.; Milbradt, A. G.; Moroder, L. *J. Pept. Res.* **2005**, *65*, 4.
(148) Sporlein, S.; Carstens, H.; Satzger, H.; Renner, C.; Behrendt, R.; Moroder, L.; Tavan, P.; Zinth, W.; Wachtveitl, J. *Proc. Natl. Acad. Sci. U. S. A.* **2002**, *99*, 7998.
(149) Wachtveitl, J.; Sporlein, S.; Satzger, H.; Fonrobert, B.; Renner, C.; Behrendt, R.; Oesterhelt, D.; Moroder, L.; Zinth, W. *Biophys. J.* **2004**, *86*, 2350.
(150) Satzger, H.; Root, C.; Renner, C.; Behrendt, R.; Moroder, L.; Wachtveitl, J.; Zinth, W. *Chem. Phys. Lett.* **2004**, *396*, 191.
(151) Bredenbeck, J.; Helbing, J.; Sieg, A.; Schrader, T.; Zinth, W.; Renner, C.; Behrendt, R.; Moroder, L.; Wachtveitl, J.; Hamm, P. *Proc. Natl. Acad. Sci. U. S. A.* **2003**, *100*, 10580.
(152) Bredenbeck, J.; Helbing, J.; Sieg, A.; Schrader, T.; Zinth, W.; Renner, C.; Behrendt, R.; Moroder, L.; Wachtveitl, J.; Hamm, P. *Proc. Natl. Acad. Sci. U. S. A.* **2003**, *100*, 6452.
(153) Koller, F. O.; Reho, R.; Schrader, T. E.; Moroder, L.; Wachtveitl, J.; Zinth, W. *J. Phys. Chem. B* **2007**, *111*, 10481.
(154) Denschlag, R.; Schreier, W. J.; Rieff, B.; Schrader, T. E.; Koller, F. O.; Moroder, L.; Zinth, W.; Tavan, P. *Phys. Chem. Chem. Phys.* **2010**, *12*, 6204.
(155) Pfister, R.; Ihalainen, J.; Hamm, P.; Kolano, C. *Org. Biomol. Chem.* **2008**, *6*, 3508.
(156) Schutt, M.; Krupka, S. S.; Milbradt, A. G.; Deindl, S.; Sinner, E. K.; Oesterhelt, D.; Renner, C.; Moroder, L. *Chem. Biol.* **2003**, *10*, 487.

(157) Ruoslahti, E. *Annu. Rev. Cell Dev. Biol.* **1996**, *12*, 697.
(158) Milbradt, A. G.; Loweneck, M.; Krupka, S. S.; Reif, M.; Sinner, E. K.; Moroder, L.; Renner, C. *Biopolymers* **2005**, *77*, 304.
(159) Hoppmann, C.; Seedorff, S.; Richter, A.; Fabian, H.; Schmieder, P.; Rück-Braun, K.; Beyermann, M. *Angew. Chem., Int. Ed.* **2009**, *48*, 6636.
(160) Fanning, A. S.; Anderson, J. M. *Curr. Biol.* **1996**, *6*, 1385.
(161) Hillier, B. J.; Christopherson, K. S.; Prehoda, K. E.; Bredt, D. S.; Lim, W. A. *Science* **1999**, *284*, 812.
(162) Gajiwala, K. S.; Chen, H.; Cornille, F.; Roques, B. P.; Reith, W.; Mach, B.; Burley, S. K. *Nature* **2000**, *403*, 916.
(163) Robinson, J. A. *Acc. Chem. Res.* **2008**, *41*, 1278.
(164) Vollmer, M. S.; Clark, T. D.; Steinem, C.; Ghadiri, M. R. *Angew. Chem., Int. Ed.* **1999**, *38*, 1598.
(165) Krautler, V.; Aemissegger, A.; Hunenberger, P. H.; Hilvert, D.; Hansson, T.; van Gunsteren, W. F. *J. Am. Chem. Soc.* **2005**, *127*, 4935.
(166) Aemissegger, A.; Krautler, V.; van Gunsteren, W. F.; Hilvert, D. *J. Am. Chem. Soc.* **2005**, *127*, 2929.
(167) Espinosa, J. F.; Gellman, S. H. *Angew. Chem., Int. Ed.* **2000**, *39*, 2330.
(168) Jurt, S.; Aemissegger, A.; Guntert, P.; Zerbe, O.; Hilvert, D. *Angew. Chem., Int. Ed.* **2006**, *45*, 6297.
(169) Cochran, A. G.; Skelton, N. J.; Starovasnik, M. A. *Proc. Natl. Acad. Sci. U. S. A.* **2001**, *98*, 5578.
(170) Dong, S. L.; Loweneck, M.; Schrader, T. E.; Schreier, W. J.; Zinth, W.; Moroder, L.; Renner, C. *Chem.—Eur. J.* **2006**, *12*, 1114.
(171) Schrader, T. E.; Schreier, W. J.; Cordes, T.; Koller, F. O.; Babitzki, G.; Denschlag, R.; Renner, C.; Loeweneckt, M.; Dong, S.; Moroder, L.; Tavan, P.; Zinth, W. *Proc. Natl. Acad. Sci. U. S. A.* **2007**, *104*, 15729.
(172) Erdelyi, M.; Varedian, M.; Skold, C.; Niklasson, I. B.; Nurbo, J.; Persson, A.; Bergquist, J.; Gogoll, A. *Org. Biomol. Chem.* **2008**, *6*, 4356.
(173) Erdelyi, M.; Karlen, A.; Gogoll, A. *Chem.—Eur. J* **2006**, *12*, 403.
(174) Hernandez, N. *Genes Dev.* **1993**, *7*, 1291.
(175) Varedian, M.; Erdelyi, M.; Persson, A.; Gogoll, A. *J. Pept. Sci.* **2009**, *15*, 107.
(176) Lindgren, N. J. V.; Varedian, M.; Gogoll, A. *Chem.—Eur. J.* **2009**, *15*, 501.
(177) Caamaño, A. M.; Vázquez, M. E.; Martínez-Costas, J.; Castedo, L.; Mascareñas, J. L. *Angew. Chem., Int. Ed.* **2000**, *39*, 3104.
(178) Woolley, G. A.; Jaikaran, A. S. I.; Berezovski, M.; Calarco, J. P.; Krylov, S. N.; Smart, O. S.; Kumita, J. R. *Biochemistry* **2006**, *45*, 6075.
(179) Harada, M.; Sisido, M.; Hirose, J.; Nakanishi, M. *FEBS Lett.* **1991**, *286*, 6.
(180) Parisot, J.; Kurz, K.; Hilbrig, F.; Freitag, R. *J. Sep. Sci.* **2009**, *32*, 1613.
(181) Nomura, A.; Okamoto, A. *Chem. Commun.* **2009**, *14*, 1906.
(182) Wolfe, S.; Nekludova, L.; Pabo, C. *Annu. Rev. Biophys. Biomol. Struct.* **2000**, *29*, 183.
(183) Klug, A. *Annu. Rev. Biochem.* **2010**, *79*, 213.
(184) Hayashi, G.; Hagihara, M.; Dohno, C.; Nakatani, K. *Nucleic Acids Symp. Ser.* **2007**, *51*, 93.
(185) Hayashi, G.; Hagihara, M.; Nakatani, K. *Chem.—Eur. J.* **2009**, *15*, 424.
(186) Sinicropi, A.; Bernini, C.; Basosi, R.; Olivucci, M. *Photochem. Photobiol. Sci.* **2009**, *8*, 1639.
(187) Cordes, T.; Elsner, C.; Herzog, T. T.; Hoppmann, C.; Schadendorf, T.; Summerer, W.; Rück-Braun, K.; Zinth, W. *Chem. Phys.* **2009**, *358*, 103.
(188) Pabo, C. O.; Sauer, R. T. *Annu. Rev. Biochem.* **1984**, *53*, 293.
(189) Landschulz, W. H.; Johnson, P. F.; Mcknight, S. L. *Science* **1988**, *240*, 1759.
(190) Kumita, J. R.; Smart, O. S.; Woolley, G. A. *Proc. Natl. Acad. Sci. U. S. A.* **2000**, *97*, 3803.
(191) Kumita, J. R.; Flint, D. G.; Smart, O. S.; Woolley, G. A. *Protein Eng.* **2002**, *15*, 561.
(192) Borisenko, V.; Woolley, G. A. *J. Photochem. Photobiol. A* **2005**, *173*, 21.
(193) Flint, D. G.; Kumita, J. R.; Smart, O. S.; Woolley, G. A. *Chem. Biol.* **2002**, *9*, 391.
(194) Burns, D. C.; Flint, D. G.; Kumita, J. R.; Feldman, H. J.; Serrano, L.; Zhang, Z. H.; Smart, O. S.; Woolley, G. A. *Biochemistry* **2004**, *43*, 15329.
(195) Chen, E. F.; Kumita, J. R.; Woolley, G. A.; Kliger, D. S. *J. Am. Chem. Soc.* **2003**, *125*, 12443.
(196) Bredenbeck, J.; Helbing, J.; Kumita, J. R.; Woolley, G. A.; Hamm, P. *Proc. Natl. Acad. Sci. U. S. A.* **2005**, *102*, 2379.
(197) Ihalainen, J. A.; Bredenbeck, J.; Pfister, R.; Helbing, J.; Chi, L.; van Stokkum, I. H. M.; Woolley, G. A.; Hamm, P. *Proc. Natl. Acad. Sci. U. S. A.* **2007**, *104*, 5383.
(198) Ihalainen, J. A.; Paoli, B.; Muff, S.; Backus, E. H. G.; Bredenbeck, J.; Woolley, G. A.; Caflisch, A.; Hamm, P. *Proc. Natl. Acad. Sci. U. S. A.* **2008**, *105*, 9588.
(199) Backus, E. H. G.; Bloem, R.; Donaldson, P. M.; Ihalainen, J. A.; Pfister, R.; Paoli, B.; Caflisch, A.; Hamm, P. *J. Phys. Chem. B* **2010**, *114*, 3735.
(200) Zhang, Z. H.; Burns, D. C.; Kumita, J. R.; Smart, O. S.; Woolley, G. A. *Bioconjugate Chem.* **2003**, *14*, 824.
(201) Zhang, F. Z.; Sadovski, O.; Woolley, G. A. *ChemBioChem* **2008**, *9*, 2147.
(202) Pozhidaeva, N.; Cormier, M. E.; Chaudhari, A.; Woolley, G. A. *Bioconjugate Chem* **2004**, *15*, 1297.
(203) Chi, L.; Sadovski, O.; Woolley, G. A. *Bioconjugate Chem.* **2006**, *17*, 670.
(204) Beharry, A. A.; Sadovski, O.; Woolley, G. A. *Org. Biomol. Chem.* **2008**, *6*, 4323.
(205) Sadovski, O.; Beharry, A.; Zhang, F.; Woolley, G. *Angew. Chem., Int. Ed.* **2009**, *48*, 1484.
(206) Samanta, S.; Woolley, G. A. *ChemBioChem* **2011**, *12*, 1712.
(207) Kusebauch, U.; Cadamuro, S. A.; Musiol, H. J.; Moroder, L.; Renner, C. *Chem.—Eur. J.* **2007**, *13*, 2966.
(208) Kusebauch, U.; Cadamuro, S. A.; Musiol, H. J.; Lenz, M. O.; Wachtveitl, J.; Moroder, L.; Renner, C. *Angew. Chem., Int. Ed.* **2006**, *45*, 7015.
(209) Guerrero, L.; Smart, O. S.; Woolley, G. A.; Allemann, R. K. *J. Am. Chem. Soc.* **2005**, *127*, 15624.
(210) Guerrero, L.; Smart, O. S.; Weston, C. J.; Burns, D. C.; Woolley, G. A.; Allemann, R. K. *Angew. Chem., Int. Ed.* **2005**, *44*, 7778.
(211) Kumita, J. R.; Flint, D. G.; Woolley, G. A.; Smart, O. S. *Faraday Discuss.* **2003**, *122*, 89.
(212) Zhang, F.; Timm, K.; Arndt, K.; Woolley, G. *Angew. Chem., Int. Ed.* **2010**, *49*, 3943.
(213) Kneissl, S.; Loveridge, E. J.; Williams, C.; Crump, M. P.; Allemann, R. K. *ChemBioChem* **2008**, *9*, 3046.
(214) Hoppmann, C.; Schmieder, P.; Heinrich, N.; Beyermann, M. *ChemBioChem* **2011**, *12*, 2555.
(215) Bale, T.; Vale, W. *Annu. Rev. Pharmacol. Toxicol.* **2004**, *44*, 525.
(216) Rivado-Casas, L.; Sampedro, D.; Campos, P. J.; Fusi, S.; Zanirato, V.; Olivucci, M. *J. Org. Chem.* **2009**, *74*, 4666.
(217) Varfolomeyev, S. D.; Kazanskaya, N. F.; Eremeev, N. L. *BioSystems* **1996**, *39*, 35.
(218) Willner, I. *Acc. Chem. Res.* **1997**, *30*, 347.
(219) Martinek, K.; Berezin, I. V. *Photochem. Photobiol.* **1979**, *29*, 637.
(220) Willner, I.; Rubin, S. *React. Polym.* **1993**, *21*, 177.
(221) Bieth, J.; Vratsanos, S. M.; Wassermann, N.; Erlanger, B. F. *Proc. Natl. Acad. Sci. U. S. A.* **1969**, *64*, 1103.
(222) Wilson, I. B.; Alexander, J. *J. Biol. Chem.* **1962**, *237*, 1323.
(223) Bieth, J.; Erlanger, B. F.; Wasserma., N.; Vratsano., Sm *Proc. Natl. Acad. Sci. U. S. A.* **1970**, *66*, 850.
(224) Deal, W. J.; Erlanger, B. F.; Nachmansohn, D. *Proc. Natl. Acad. Sci. U. S. A.* **1969**, *64*, 1230.
(225) Hohsaka, T.; Kawashima, K.; Sisido, M. *J. Am. Chem. Soc.* **1994**, *116*, 413.
(226) Westmark, P. R.; Kelly, J. P.; Smith, B. D. *J. Am. Chem. Soc.* **1993**, *115*, 3416.
(227) Harvey, A. J.; Abell, A. D. *Tetrahedron* **2000**, *56*, 9763.

(228) Pearson, D.; Abell, A. D. *Org. Biomol. Chem.* **2006**, *4*, 3618.
(229) Pearson, D.; Alexander, N.; Abell, A. D. *Chem.—Eur. J.* **2008**, *14*, 7358.
(230) Abell, A. D.; Jones, M. A.; Neffe, A. T.; Aitken, S. G.; Cain, T. P.; Payne, R. J.; McNabb, S. B.; Coxon, J. M.; Stuart, B. G.; Pearson, D.; Lee, H. Y. -.; Morton, J. D. *J. Med. Chem.* **2007**, *50*, 2916.
(231) Pearson, D.; Abell, A. D. *Chem.—Eur. J.* **2010**, *16*, 6983.
(232) Pearson, D.; Downard, A. J.; Muscroft-Taylor, A.; Abell, A. D. *J. Am. Chem. Soc.* **2007**, *129*, 14862.
(233) Robertson, L. J. G.; Morton, J. D.; Yamaguchi, M.; Bickerstaffe, R.; Shearer, T. R.; Azuma, M. *Invest. Ophthalmol. Vis. Sci.* **2005**, *46*, 4634.
(234) Fujita, D.; Murai, M.; Nishioka, T.; Miyoshi, H. *Biochemistry* **2006**, *45*, 6581.
(235) Ichimaru, N.; Murai, M.; Abe, M.; Hamada, T.; Yamada, Y.; Makino, S.; Nishioka, T.; Makabe, H.; Makino, A.; Kobayashi, T.; Miyoshi, H. *Biochemistry* **2005**, *44*, 816.
(236) Vomasta, D.; Hogner, C.; Branda, N. R.; Konig, B. *Angew. Chem., Int. Ed.* **2008**, *47*, 7644.
(237) Vomasta, D.; Innocenti, A.; Konig, B.; Supuran, C. T. *Bioorg. Med. Chem. Lett.* **2009**, *19*, 1283.
(238) Banerjee, A. L.; Eiler, D.; Roy, B. C.; Jia, X.; Haldar, M. K.; Mallik, S.; Srivastava, D. K. *Biochemistry* **2005**, *44*, 3211.
(239) Kuil, J.; van Wandelen, L. T. M.; de Mol, N. J.; Liskamp, R. M. J. *Bioorg. Med. Chem.* **2008**, *16*, 1393.
(240) Kuil, J.; van Wandelen, L. T. M.; de Mol, N. J.; Liskamp, R. M. J. *J. Pept. Sci.* **2009**, *15*, 685.
(241) Karube, I.; Nakamoto, Y.; Suzuki, S. *Biochim. Biophys. Acta* **1976**, *445*, 774.
(242) Nakamoto, Y.; Karube, I.; Suzuki, S. *J. Ferment. Technol.* **1975**, *53*, 595.
(243) Willner, I.; Rubin, S.; Zor, T. *J. Am. Chem. Soc.* **1991**, *113*, 4013.
(244) Willner, I.; Rubin, S.; Shatzmiller, R.; Zor, T. *J. Am. Chem. Soc.* **1993**, *115*, 8690.
(245) Mirarefi, P.; Lee, C. T., Jr. *Biochim. Biophys. Acta, Proteins Proteomics* **2010**, *1804*, 106.
(246) Wang, S.; Lee, C. T., Jr. *Biochemistry* **2007**, *46*, 14557.
(247) Lee, C. T.; Smith, K. A.; Hatton, T. A. *Biochemistry* **2005**, *44*, 524.
(248) Wang, S.; Lee, C. T., Jr. *J. Phys. Chem. B* **2006**, *110*, 16117.
(249) Erlanger, B. F.; Wassermann, N. H.; Cooper, A. G.; Monk, R. J. *Eur. J. Biochem.* **1976**, *61*, 287.
(250) Karube, I.; Nakamoto, Y.; Namba, K.; Suzuki, S. *Biochim. Biophys. Acta* **1976**, *429*, 975.
(251) Aizawa, M.; Namba, K.; Suzuki, S. *Arch. Biochem. Biophys.* **1977**, *182*, 305.
(252) Willner, I.; Rubin, S.; Riklin, A. *J. Am. Chem. Soc.* **1991**, *113*, 3321.
(253) Willner, I.; Liondagan, M.; Rubin, S.; Wonner, J.; Effenberger, F.; Bauerle, P. *Photochem. Photobiol.* **1994**, *59*, 491.
(254) Willner, I.; Lion-Dagan, M.; Marx-Tibbon, S.; Katz, E. *J. Am. Chem. Soc.* **1995**, *117*, 6581.
(255) Weston, D. G.; Kirkham, J.; Cullen, D. C. *Biochim. Biophys. Acta, Gen. Subj.* **1999**, *1428*, 463.
(256) Harvey, J. H.; Trauner, D. *ChemBioChem* **2008**, *9*, 191.
(257) Ueda, T.; Murayama, K.; Yamamoto, T.; Kimura, S.; Imanishi, Y. *J. Chem. Soc., Perkin Trans. 1* **1994**, 225.
(258) van Dam-Mieras, M. C. E.; Slotboom, A. J.; Pieterson, W. A.; Haas, G. H. D. *Biochemistry* **1975**, *14*, 5387.
(259) Imperiali, B.; Roy, R. S. *J. Am. Chem. Soc.* **1994**, *116*, 12083.
(260) Chatani, E.; Hayashi, R.; Moriyama, H.; Ueki, T. *Protein Sci.* **2002**, *11*, 72.
(261) Liu, D.; Karanicolas, J.; Yu, C.; Zhang, Z. H.; Woolley, G. A. *Bioorg. Med. Chem. Lett.* **1997**, *7*, 2677.
(262) Hamachi, I.; Hiraoka, T.; Yamada, Y.; Shinkai, S. *Chem. Lett.* **1998**, *27*, 537.
(263) James, D. A.; Burns, D. C.; Woolley, G. A. *Protein Eng.* **2001**, *14*, 983.
(264) Yamada, M. D.; Nakajima, Y.; Maeda, H.; Maruta, S. *J. Biochem.* **2007**, *142*, 691.
(265) Schierling, B.; Noel, A. J.; Wende, W.; Hien, L. T.; Volkov, E.; Kubareva, E.; Oretskaya, T.; Kokkinidis, M.; Rompp, A.; Spengler, B.; Pingoud, A. *Proc. Natl. Acad. Sci. U. S. A.* **2010**, *107*, 1361.
(266) Hien, L. T.; Zatsepin, T. S.; Schierling, B.; Volkov, E. M.; Wende, W.; Pingoud, A.; Kubareva, E. A.; Oretskaya, T. S. *Bioconjugate Chem.* **2011**, *22*, 1366.
(267) Wang, L.; Brock, A.; Herberich, B.; Schultz, P. G. *Science* **2001**, *292*, 498.
(268) Hohsaka, T.; Ashizuka, Y.; Murakami, H.; Sisido, M. *J. Am. Chem. Soc.* **1996**, *118*, 9778.
(269) Muranaka, N.; Hohsaka, T.; Sisido, M. *FEBS Lett.* **2002**, *510*, 10.
(270) Nakayama, K.; Endo, M.; Majima, T. *Chem. Commun.* **2004**, *21*, 2386.
(271) Newman, M.; Strzelecka, T.; Dorner, L.; Schildkraut, I.; Aggarwal, A. *Science* **1995**, *269*, 656.
(272) Nakayama, K.; Endo, M.; Majima, T. *Bioconjugate Chem.* **2005**, *16*, 1360.
(273) Krauss, U.; Lee, J.; Benkovic, S. J.; Jaeger, K. E. *Microb. Biotechnol.* **2010**, *3*, 15.
(274) Ostermeier, M. *Curr. Opin. Struct. Biol.* **2009**, *19*, 442.
(275) Golynskiy, M. V.; Koay, M. S.; Vinkenborg, J. L.; Merkx, M. *ChemBioChem* **2011**, *12*, 353.
(276) Krauss, U.; Drepper, T.; Jaeger, K. *Chem.—Eur. J.* **2011**, *17*, 2552.
(277) Pastrana, E. *Nat. Methods* **2011**, *8*, 24.
(278) Lee, J.; Natarajan, M.; Nashine, V. C.; Socolich, M.; Vo, T.; Russ, W. P.; Benkovic, S. J.; Ranganathan, R. *Science* **2008**, *322*, 438.
(279) Berg, T. *Angew. Chem., Int. Ed.* **2009**, *48*, 3218.
(280) Yao, X.; Rosen, M. K.; Gardner, K. H. *Nat. Chem. Biol.* **2008**, *4*, 491.
(281) Möglich, A.; Ayers, R. A.; Moffat, K. *J. Mol. Biol.* **2009**, *385*, 1433.
(282) Wu, Y. I.; Frey, D.; Lungu, O. I.; Jaehrig, A.; Schlichting, I.; Kuhlman, B.; Hahn, K. M. *Nature* **2009**, *461*, 104.
(283) Morgan, S. A.; Al-Abdul-Wahid, S.; Woolley, G. A. *J. Mol. Biol.* **2010**, *399*, 94.
(284) Morgan, S. A.; Woolley, G. A. *Photochem. Photobiol. Sci.* **2010**, *9*, 1320.
(285) Willner, I.; Rubin, S.; Wonner, J.; Effenberger, F.; Bäuerle, P. *J. Am. Chem. Soc.* **1992**, *114*, 3150.
(286) Willner, I.; Rubin, S.; Cohen, Y. *J. Am. Chem. Soc.* **1993**, *115*, 4937.
(287) Zahavy, E.; Rubin, S.; Willner, I. *J. Chem. Soc., Chem. Commun.* **1993**, *23*, 1753.
(288) Zahavy, E.; Rubin, S.; Willner, I. *Mol. Cryst. Liq. Cryst. Sci. Technol., Sect A: Mol. Cryst. Liq. Cryst.* **1994**, *246*, 195.
(289) Shimoboji, T.; Ding, Z. L.; Stayton, P. S.; Hoffman, A. S. *Bioconjugate Chem.* **2002**, *13*, 915.
(290) Bose, M.; Groff, D.; Xie, J. M.; Brustad, E.; Schultz, P. G. *J. Am. Chem. Soc.* **2006**, *128*, 388.
(291) Shishido, H.; Yamada, M. D.; Kondo, K.; Maruta, S. *J. Biochem.* **2009**, *146*, 581.
(292) Chattopadhyaya, R.; Meador, W. E.; Means, A. R.; Quiocho, F. A. *J. Mol. Biol.* **1992**, *228*, 1177.
(293) Thompson, S. M.; Kao, J. P. Y.; Kramer, R. H.; Poskanzer, K. E.; Silver, R. A.; Digregorio, D.; Wang, S. S. H. *J. Neurosci.* **2005**, *25*, 10358.
(294) Banghart, M. R.; Volgraf, M.; Trauner, D. *Biochemistry* **2006**, *45*, 15129.
(295) Gorostiza, P.; Isacoff, E. *Mol. Biosyst.* **2007**, *3*, 686.
(296) Gorostiza, P.; Isacoff, E. Y. *Physiology* **2008**, *23*, 238.
(297) Szobota, S.; Isacoff, E. Y. *Annu. Rev. Biophys.* **2010**, *39*, 329.
(298) Volgraf, M.; Banghart, M.; Trauner, D. In Switchable Proteins and Channels. Feringa, B. L., Browne, W. R., Eds.; *Molecular Switches*, 2nd ed.; Wiley-VCH: Weinheim, 2011; Chapter 15.
(299) Sakmann, B.; Neher, E. *Annu. Rev. Physiol.* **1984**, *46*, 455.

(300) Liem, L. K.; Simard, J. M.; Song, Y. M.; Tewari, K. *Neurosurgery* **1995**, *36*, 382.
(301) Gotti, C.; Clementi, F. *Prog. Neurobiol.* **2004**, *74*, 363.
(302) Karczmar, A. G. *Neuropsychopharmacology* **1993**, *9*, 181.
(303) Hulme, E. C.; Birdsall, N. J. M.; Buckley, N. J. *Annu. Rev. Pharmacol. Toxicol.* **1990**, *30*, 633.
(304) Devillersthiery, A.; Galzi, J. L.; Eisele, J. L.; Bertrand, S.; Bertrand, D.; Changeux, J. P. *J. Membr. Biol.* **1993**, *136*, 97.
(305) Karlin, A.; Winnik, M. *Proc. Natl. Acad. Sci. U. S. A.* **1968**, *60*, 668.
(306) Silman, I.; Karlin, A. *Science* **1969**, *164*, 1420.
(307) Schoffeniels, E.; Nachmansohn, D. *Biochim. Biophys. Acta* **1957**, *26*, 1.
(308) Higman, H. B.; Podleski, T. R.; Bartels, E. *Biochim. Biophys. Acta* **1964**, *79*, 138.
(309) Bartels, E.; Wassermann, N. H.; Erlanger, B. F. *Proc. Natl. Acad. Sci. U. S. A.* **1971**, *68*, 1820.
(310) Lester, H. A.; Krouse, M. E.; Nass, M. M.; Wassermann, N. H.; Erlanger, B. F. *J. Gen. Physiol.* **1980**, *75*, 207.
(311) Lester, H. A.; Nass, M. M.; Krouse, M. E.; Nerbonne, J. M.; Wassermann, N. H.; Erlanger, B. F. *Ann. N. Y. Acad. Sci.* **1980**, *346*, 475.
(312) Chabala, L. D.; Lester, H. A. *J. Physiol.-London* **1986**, *379*, 83.
(313) Colquhoun, D.; Sakmann, B. *Nature* **1981**, *294*, 464.
(314) Lester, H. A.; Chang, H. W. *Nature* **1977**, *266*, 373.
(315) Wassermann, N. H.; Bartels, E.; Erlanger, B. F. *Proc. Natl. Acad. Sci. U. S. A.* **1979**, *76*, 256.
(316) Nargeot, J.; Lester, H. A.; Birdsall, N. J. M.; Stockton, J.; Wassermann, N. H.; Erlanger, B. F. *J. Gen. Physiol.* **1982**, *79*, 657.
(317) Tochitsky, I.; Banghart, M. R.; Mourot, A.; Yao, J. Z.; Gaub, B.; Kramer, R. H.; Trauner, D. *Nat. Chem.* **2012**, *4*, 105.
(318) Banghart, M.; Borges, K.; Isacoff, E.; Trauner, D.; Kramer, R. H. *Nat. Neurosci.* **2004**, *7*, 1381.
(319) Volgraf, M.; Gorostiza, P.; Numano, R.; Kramer, R. H.; Isacoff, E. Y.; Trauner, D. *Nat. Chem. Biol.* **2006**, *2*, 47.
(320) Stankovic, C. J.; Heinemann, S. H.; Schreiber, S. L. *Biochim. Biophys. Acta* **1991**, *1061*, 163.
(321) Koeppe, R. E.; Andersen, O. S. *Annu. Rev. Biophys. Biomol. Struct.* **1996**, *25*, 231.
(322) Andersen, O. S. *Annu. Rev. Physiol.* **1984**, *46*, 531.
(323) Kelkar, D. A.; Chattopadhyay, A. *Biochim. Biophys. Acta: Biomembr.* **2007**, *1768*, 2011.
(324) Finkelstein, A.; Andersen, O. S. *J. Membr. Biol.* **1981**, *59*, 155.
(325) Lien, L.; Jaikaran, D. C. J.; Zhang, Z. H.; Woolley, G. A. *J. Am. Chem. Soc.* **1996**, *118*, 12222.
(326) Ketchem, R. R.; Lee, K. C.; Huo, S.; Cross, T. A. *J. Biomol. NMR* **1996**, *8*, 1.
(327) Woolley, G. A.; Jaikaran, A. S. I.; Zhang, Z. H.; Peng, S. Y. *J. Am. Chem. Soc.* **1995**, *117*, 4448.
(328) Levina, N.; Totemeyer, S.; Stokes, N. R.; Louis, P.; Jones, M. A.; Booth, I. R. *EMBO J.* **1999**, *18*, 1730.
(329) Blount, P.; Iscla, I.; Moe, P. C.; Li, Y. Z. *Curr. Top. Membr.* **2007**, *58*, 201.
(330) Sukharev, S. I.; Blount, P.; Martinac, B.; Kung, C. *Annu. Rev. Physiol.* **1997**, *59*, 633.
(331) Yoshimura, K.; Batiza, A.; Kung, C. *Biophys. J.* **2001**, *80*, 2198.
(332) Kocer, A.; Walko, M.; Meijberg, W.; Feringa, B. L. *Science* **2005**, *309*, 755.
(333) Steinbacher, S.; Bass, R.; Strop, P.; Rees, D. C. *Curr. Top. Membr.* **2007**, *58*, 1.
(334) Kocer, A.; Walko, M.; Feringa, B. L. *Nat. Protoc.* **2007**, *2*, 1426.
(335) Hoshi, T.; Zagotta, W. N.; Aldrich, R. W. *Science* **1990**, *250*, 533.
(336) Demo, S. D.; Yellen, G. *Neuron* **1991**, *7*, 743.
(337) Mackinnon, R.; Yellen, G. *Science* **1990**, *250*, 276.
(338) Lujan, R.; Shigemoto, R.; Lopez-Bendito, G. *Neuroscience* **2005**, *130*, 567.
(339) Michaelis, E. K. *Prog. Neurobiol.* **1998**, *54*, 369.
(340) Kew, J. N. C.; Kemp, J. A. *Psychopharmacology* **2005**, *179*, 4.
(341) Ozawa, S.; Kamiya, H.; Tsuzuki, K. *Prog. Neurobiol.* **1998**, *54*, 581.
(342) Graham, F. L.; Smiley, J.; Russell, W. C.; Nairn, R. *J. Gen. Virol.* **1977**, *36*, 59.
(343) Schoepp, D.; Bockaert, J.; Sladeczek, F. *Trends Pharmacol. Sci.* **1990**, *11*, 508.
(344) Strader, C. D.; Fong, T. M.; Tota, M. R.; Underwood, D.; Dixon, R. A. F. *Annu. Rev. Biochem.* **1994**, *63*, 101.
(345) Hargrave, P. A.; McDowell, J. H. *FASEB J.* **1992**, *6*, 2323.
(346) Szobota, S.; Gorostiza, P.; Del Bene, F.; Wyart, C.; Fortin, D. L.; Kolstad, K. D.; Tulyathan, O.; Volgraf, M.; Numano, R.; Aaron, H. L.; Scott, E. K.; Kramer, R. H.; Flannery, J.; Baier, H.; Trauner, D.; Isacoff, E. Y. *Neuron* **2007**, *54*, 535.
(347) Janovjak, H.; Szobota, S.; Wyart, C.; Trauner, D.; Isacoff, E. Y. *Nat. Neurosci.* **2010**, *13*, 1027.
(348) Numano, R.; Szobota, S.; Lau, A. Y.; Gorostiza, P.; Volgraf, M.; Roux, B.; Trauner, D.; Isacoff, E. Y. *Proc. Natl. Acad. Sci. U. S. A.* **2009**, *106*, 6814.
(349) Wang, S.; Szobota, S.; Wang, Y.; Volgraf, M.; Liu, Z.; Sun, C.; Trauner, D.; Isacoff, E. Y.; Zhang, X. *Nano Lett.* **2007**, *7*, 3859.
(350) Mazzoni, F.; Novelli, E.; Strettoi, E. *J. Neurosci.* **2008**, *28*, 14282.
(351) Simonelli, F.; Maguire, A. M.; Testa, F.; Pierce, E. A.; Mingozzi, F.; Bennicelli, J. L.; Rossi, S.; Marshall, K.; Banfi, S.; Surace, E. M.; Sun, J.; Redmond, T. M.; Zhu, X.; Shindler, K. S.; Ying, G.; Ziviello, C.; Acerra, C.; Wright, J. F.; McDonnell, J. W.; High, K. A.; Bennett, J.; Auricchio, A. *Mol. Ther.* **2010**, *18*, 643.
(352) Caporale, N.; Kolstad, K. D.; Lee, T.; Tochitsky, I.; Dalkara, D.; Trauner, D.; Kramer, R.; Dan, Y.; Isacoff, E. Y.; Flannery, J. G. *Mol. Ther.* **2011**, *19*, 1212.
(353) Fortin, D. L.; Banghart, M. R.; Dunn, T. W.; Borges, K.; Awagenaar, D.; Gaudry, Q.; Karakossian, M. H.; Otis, T. S.; Kristan, W. B.; Trauner, D.; Kramer, R. H. *Nat. Methods* **2008**, *5*, 331.
(354) Banghart, M.; Mourot, A.; Fortin, D.; Yao, J.; Kramer, R.; Trauner, D. *Angew. Chem., Int. Ed.* **2009**, *48*, 9097.
(355) Bonardi, F.; London, G.; Nouwen, N.; Feringa, B.; Driessen, A. J. M. *Angew. Chem., Int. Ed.* **2010**, *49*, 7234.
(356) Veenendaal, A. K. J.; van der Does, C.; Driessen, A. M. *Biochim. Biophys. Acta, Mol. Cell Res.* **2004**, *1694*, 81.
(357) Driessen, A. J. M.; Nouwen, N. *Annu. Rev. Biochem.* **2008**, *77*, 643.
(358) Bonardi, F.; Halza, E.; Walko, M.; Du Plessis, F.; Nouwen, N.; Feringa, B. L.; Driessen, A. J. M. *Proc. Natl. Acad. Sci. U. S. A.* **2011**, *108*, 7775.
(359) du Plessis, D. J. F.; Berrelkamp, G.; Nouwen, N.; Driessen, A. J. M. *J. Biol. Chem.* **2009**, *284*, 15805.
(360) Stolik, S.; Delgado, J. A.; Perez, A.; Anasagasti, L. *J. Photochem. Photobiol. B* **2000**, *57*, 90.
(361) Mourot, A.; Kienzler, M. A.; Banghart, M. R.; Fehrentz, T.; Huber, F. M. E.; Stein, M.; Kramer, R. H.; Trauner, D. *ACS Chem. Neurosci.* **2011**, *2*, 536.
(362) Bléger, D.; Schwarz, J.; Brouwer, A. M.; Hecht, S. *J. Am. Chem. Soc.* **2012**, *134*, 20597.
(363) Szymanski, W.; Wu, B.; Poloni, C.; Janssen, D. B.; Feringa, B. L. *Angew. Chem., Int. Ed.* **2013**, *52*, 2068.
(364) Cahová, H.; Jaschke, A. *Angew. Chem., Int. Ed.* **2013**, *52*, 3186.
(365) Fujimoto, K.; Kajino, M.; Sakaguchi, I.; Inouye, M. *Chem.—Eur. J.* **2012**, *18*, 9834.
(366) Hoppmann, C.; Barucker, C.; Lorenz, D.; Multhaup, G.; Beyermann, M. *ChemBioChem* **2012**, *13*, 2657.
(367) Samanta, S.; Qin, C.; Lough, A. J.; Woolley, G. A. *Angew. Chem., Int. Ed.* **2012**, *51*, 6452.
(368) Regner, N.; Herzog, T. T.; Haiser, K.; Hoppmann, C.; Beyermann, M.; Sauermann, J.; Engelhard, M.; Cordes, T.; Rück-Braun, K.; Zinth, W. *J. Phys. Chem. B* **2012**, *116*, 4181.
(369) Stein, M.; Middendorp, S. J.; Carta, V.; Pejo, E.; Raines, D. E.; Forman, S. A.; Sigel, E.; Trauner, D. *Angew. Chem., Int. Ed.* **2012**, *51*, 10500.

(370) Stawski, P.; Sumser, M.; Trauner, D. *Angew. Chem., Int. Ed.* **2012**, *51*, 5748.
(371) Mourot, A.; Fehrentz, T.; Le Feuvre, Y.; Smith, C. B.; Herold, C.; Dalkara, D.; Nagy, F.; Trauner, D.; Kramer, R. H. *Nat. Methods* **2012**, *9*, 396.
(372) Fehrentz, T.; Kuttruff, C. A.; Huber, F. M. E.; Kienzler, M. A.; Mayer, P.; Trauner, D. *ChemBioChem* **2012**, *13*, 1746.
(373) Polosukhina, A.; Litt, J.; Tochitsky, I.; Nemargut, J.; Sychev, Y.; De Kouchkovsky, I.; Huang, T.; Borges, K.; Trauner, D.; Van Gelder, R. N.; Kramer, R. H. *Neuron* **2012**, *75*, 271.